CHAPTER V

Results and Discussion

5.1 PHB characterization

5.1.1 IR spectroscopy

FT-IR spectra of Biomer, f-PHB1 and f-PHB2 are presented in Figure 5.1, 5.2 and 5.3, respectively. Figure 5.4 presents FT-IR spectra of PHB which was fermented and isolated at the Biochemical Engineering Laboratory, Chulalongkorn University by Dolarom [1999]. This type of PHB will be noted as "PHB-Dolarom". Figure 5.5 presents FT-IR spectra of PHB which was kindly provided by Professor Suteaki Shioya and Hiroshi Shimizu from Department of Biotechnology, Graduate school of Engineering, Osaka University, Suita, Japan. This type of PHB will be noted as "PHB-Japan". In this work, FT-IR spectra of "PHB-Dolarom" and "PHB-Japan" are used as references to compare with those of Biomer, f-PHB1 and f-PHB2. The wave numbers of the absorption peaks are summarized in Table 5.1.

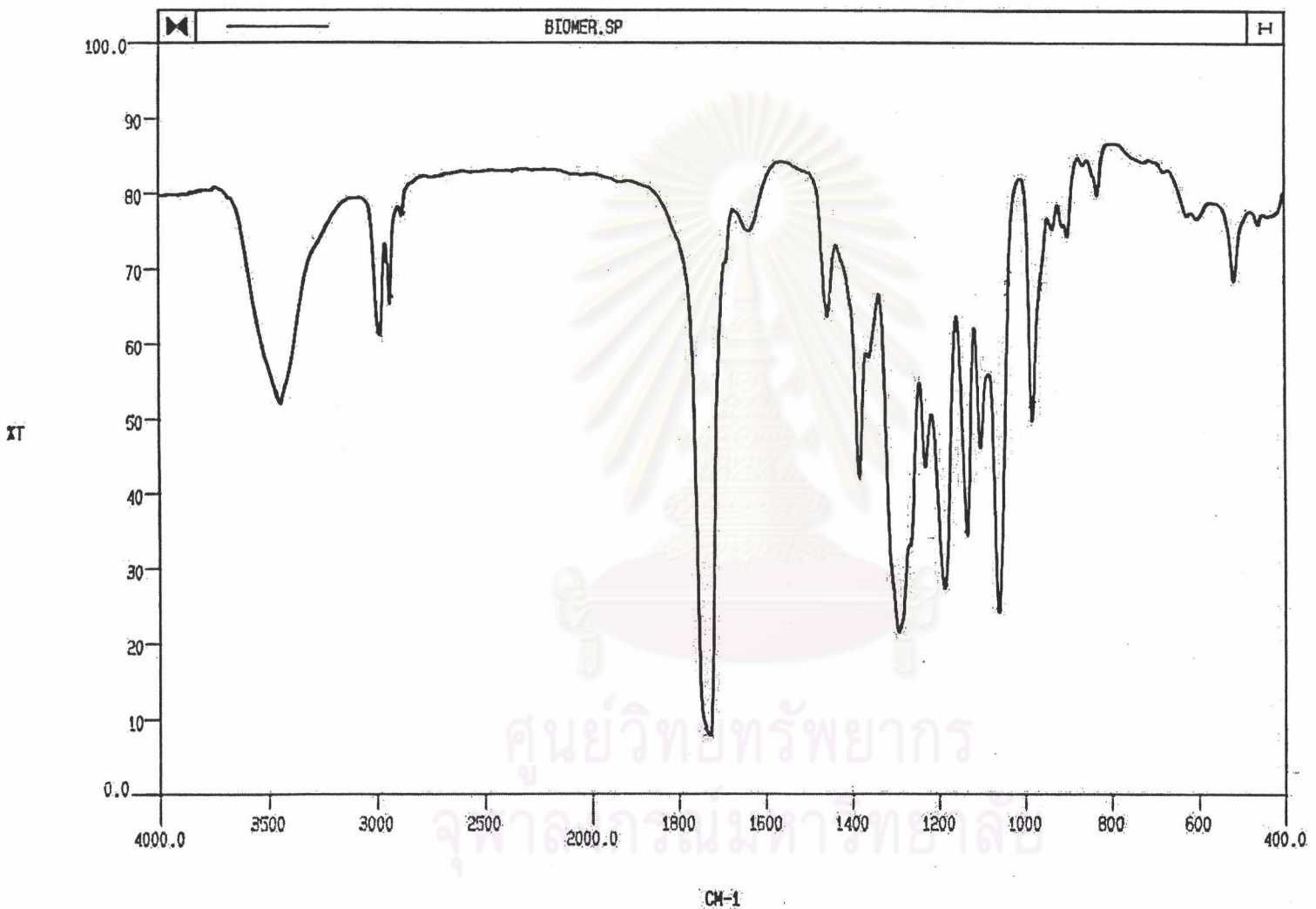

Figure 5.1 FT-IR spectra of Biomer in the wave number range of 4000-400 cm^{-1}

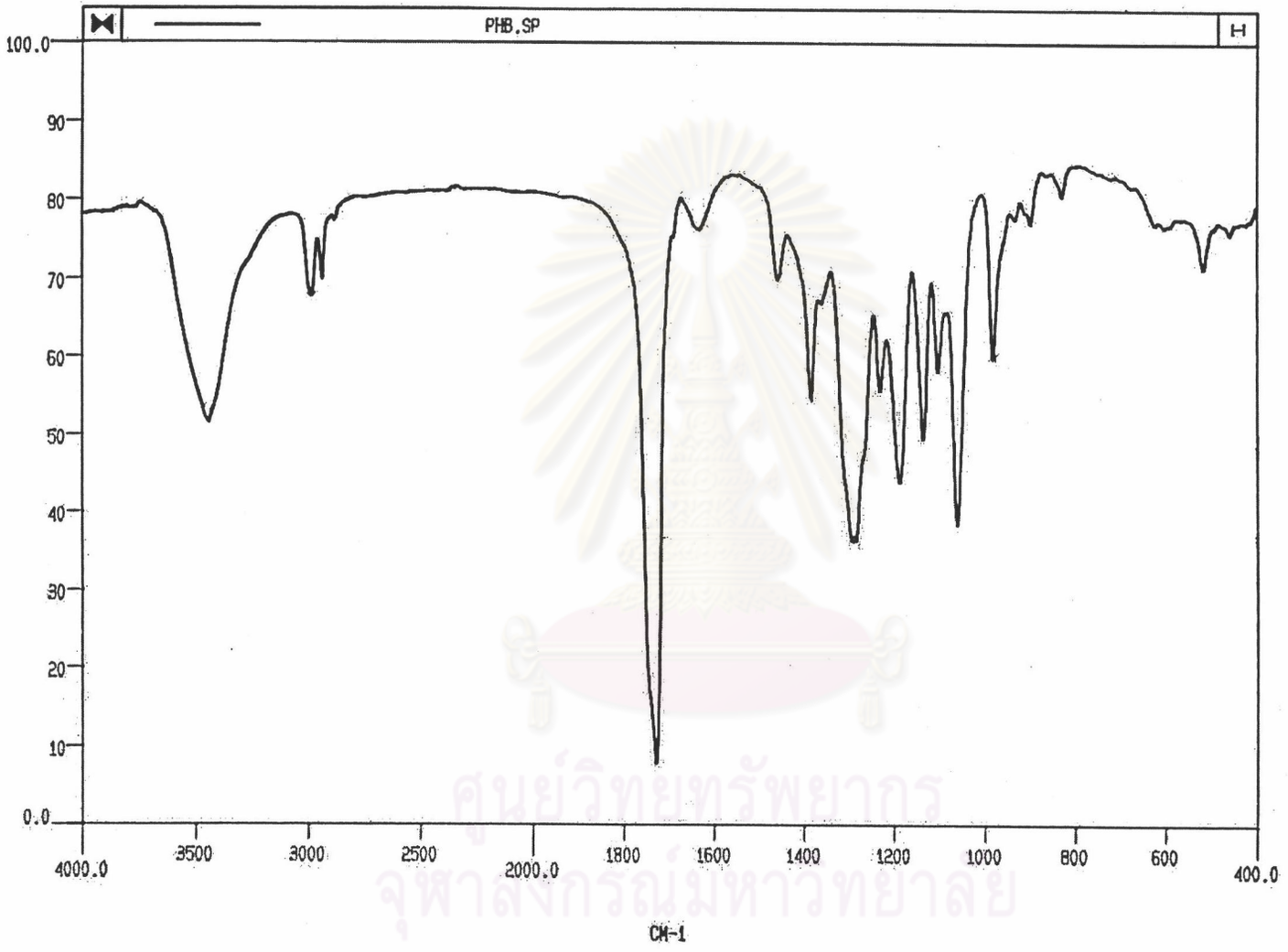

Figure 5.2 FT-IR spectra of f-PHB1 in the wave number range of 4000-400 cm^{-1}

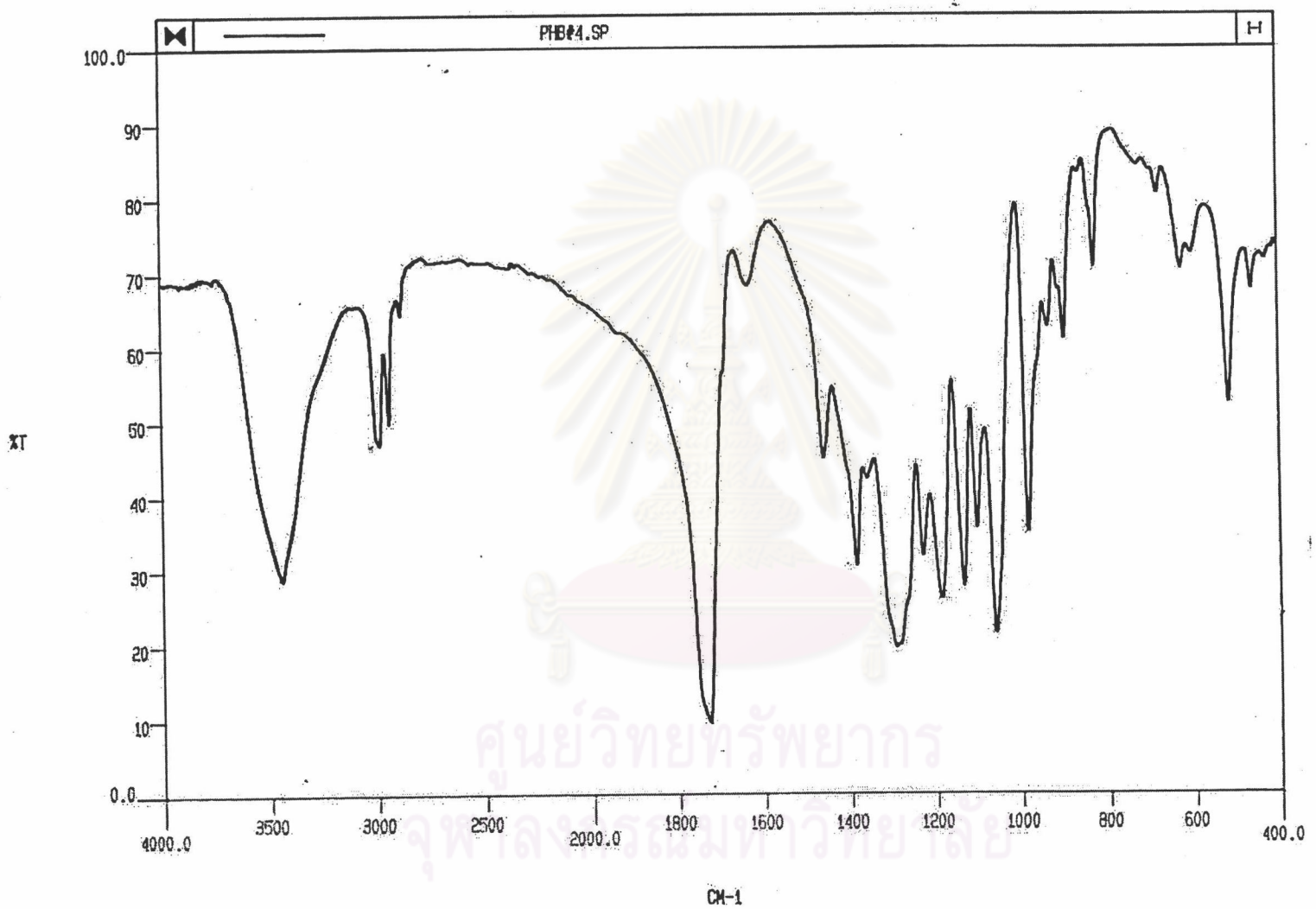

Figure 5.3 FT-IR spectra of f-PHB2 in the wave number range of 4000-400 cm^{-1}

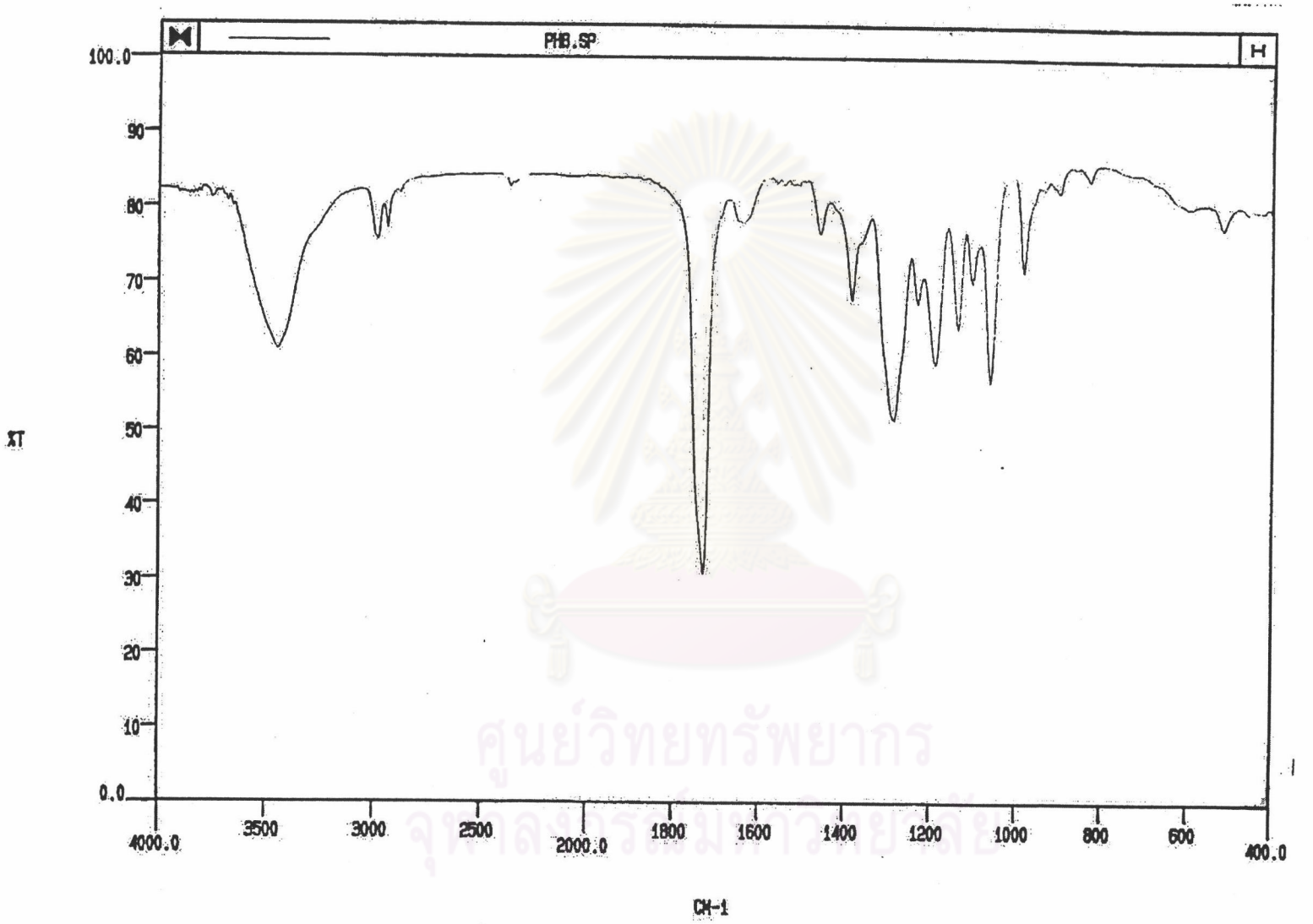

Figure 5.4 FT-IR spectra of "PHB-Dolarom" in the wave number range of 4000-400 cm^{-1}

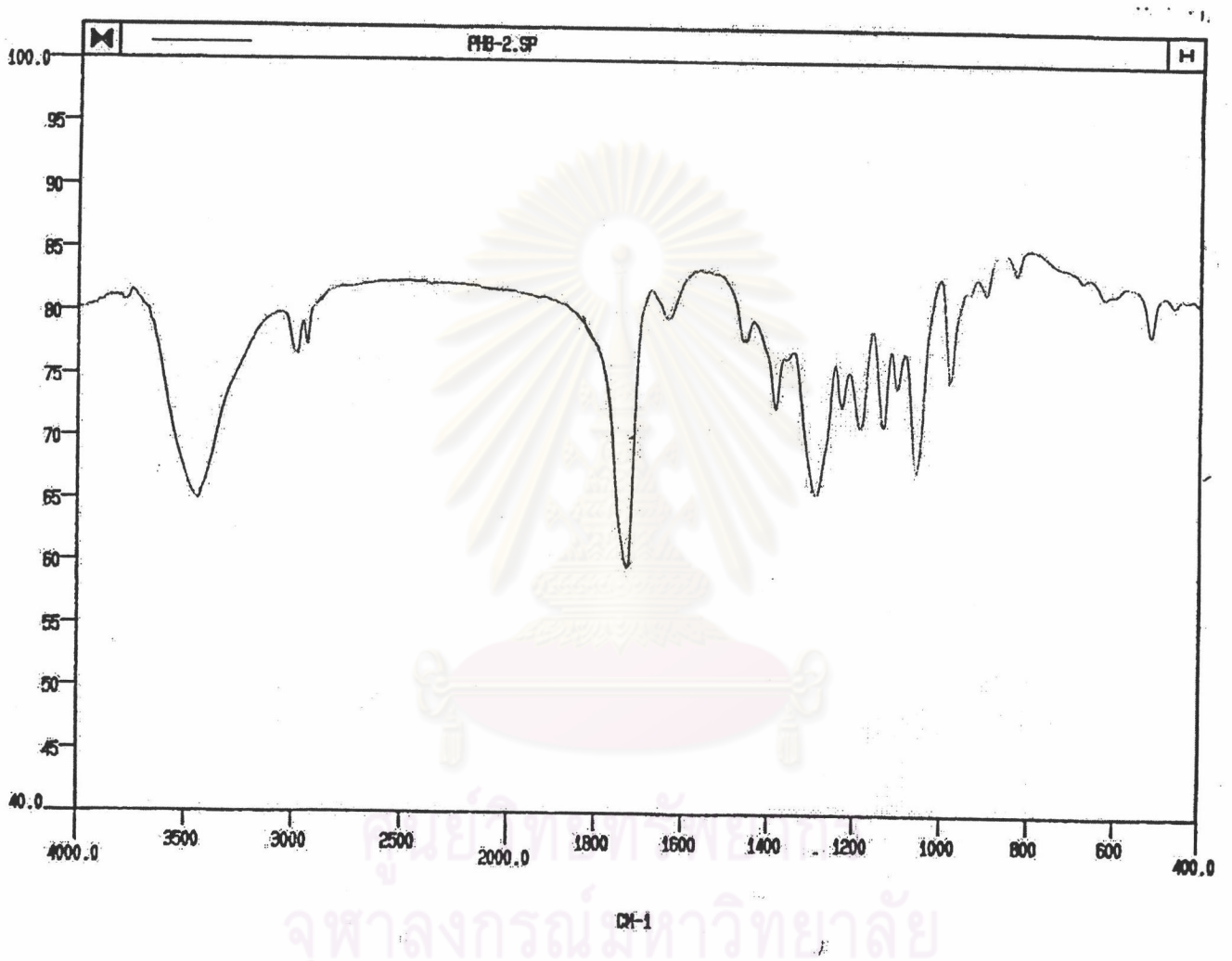

Figure 5.5 FT-IR spectra of "PHB-Japan" in the wave number range of 4000-400 cm^{-1}

Table 5.1 Wave number of absorption peaks and molecular vibration of five PHB samples

Type of PHB					Molecular vibration*
Biomer	f-PHB1	f-PHB2	PHB-Dolarom	PHB-Japan	
Wave number of the absorption peak (cm^{-1})					
-	-	-	3838	-	
-	-	-	3748	-	
3440	3439	3439	3441	3441	Adsorption of hydroxyl end groups
2982	2981	2981	2982	2983	CH_3 asymmetric stretching
2936	2936	2936	2936	2936	CH_2 asymmetric stretching
2878	-	2878	-	-	CH_3 symmetric stretching
-	-	2379	2362	-	
1727	1727	1727	1728	1728	C=O stretching
1637	1633	1632	1636	1635	
1457	1457	1459	1457	1459	CH_2 deformation, CH_3 asymmetric bending
1382	1383	1384	1382	1384	CH_3 symmetric bending
-	-	1359	-	-	
1292	1291	1292	1284	1289	
1230	1230	1229	1229	1229	Probably C-C-O asymmetric vibration
1186	1186	1186	1187	1185	C-O stretching and C-C skeletal

* From Noda *et al.* [1999], Zhang *et al.* [1997a], Zhang *et al.* [1997b], Withey and Hay [1999] and Juttner *et al.* [1975].

Table 5.1 Wave number of absorption peaks and molecular vibration of five PHB samples (cont.)

Type of PHB					Molecular vibration*
Biomer	f-PHB1	f-PHB2	PHB-Dolarom	PHB-Japan	
Wave number of the absorption peak (cm^{-1})					
1133	1134	1133	1134	1133	C-O stretching and C-C skeletal
1102	1102	1102	1102	1101	
1059	1059	1059	1059	1057	C-O stretch and others
981	981	980	981	980	CH_3 rock and C-C skeletal
935	934	934	-	-	
898	898	897	899	898	CH_3 bending
828	828	827	828	828	CH_2 bending
-	-	679	-	-	
-	-	624	-	624	
601	601	601	-	-	
516	516	516	517	516	
459	459	459	-	-	

FT-IR spectroscopy of PHB is also presented in the work of Noda *et al.* [1999], Zhang *et al.* [1997a], Zhang *et al.* [1997b], Withey and Hay [1999] and Juttner *et al.* [1975]. Noda *et al.* [1999] presented the table summarizing the wave number of the absorption peaks and type molecular vibration of PHB, as noted in Table 5.1. Zhang *et al.* [1997a] and [1997b] found that the absorption of the hydroxyl end groups of PHBwas observed at the wave number of 3436 cm^{-1}. The carboxyl regions which showed C=O stretching bands of PHB are observed at the wave number of 1723-1725 cm^{-1}. Bleombergen *et al.* [1986] found that the absorption peaks which were represented the C-H bands and C-C bands were observed at the wave number of 2900 and 977 cm^{-1}, respectively. Withey and Hay [1999] presented the FT-IR absorption peaks and its molecular vibration of PHB. PHB absorption peaks are observed at the wave number of 840 and 827 cm^{-1} which were represented the molecular assignments of CH_3 bending and CH_2 bending, respectively. Juttner *et al.* [1975] also showed the FT-IR absorption peak, which was represented to C=O band, was observed at the wave number around 1730 cm^{-1}. These absorption peaks and molecular vibration presented in the literatures are compared to the FT-IR spectrum of five PHB samples and summarized in the "molecular vibration" column in Table 5.1.

From the comparison of Table 5.1 and literatures summarized above, all of FT-IR absorption peaks mentioned in the literatures are also observed in all PHB samples except the absorption peak at the wave number of 840 cm^{-1}, which was represented to CH_3 bending band.

From Figure 5.1 to 5.5 and Table 5.1, it can be noticed that most spectra of each PHB are existed in the same range of wave number. This result preliminary assures that the polymer which was acquired by fermentation in this work is PHB.

5.1.2 Molecular weight measurement

Table 5.2 presents the results on weight average molecular weight (M_w), number average molecular weight (M_n) and molecular weight distribution (MWD) of five PHB samples randomly selected from different batches of f-PHB purification. The data of the M_w of Biomer supplied by Biomer company is also presented in the Table 5.2 (The data of the M_n and MWD of Biomer are unavailable).

Table 5.2 M_w, M_n and MWD of f-PHB and Biomer

Sample number	M_w (g/mol)	M_n (g/mol)	MWD
1	598,246	106,332	5.626
2	671,496	173,555	3.869
3	974,318	199,770	4.877
4	849,604	197,169	4.309
5	1,023,765	164,784	6.213
Biomer	327,000	-	-

The results of five f-PHB samples indicates that M_w of f-PHB varies in a wide range around 600,000 to 1,000,000 g/mol. M_n of f-PHB varies from 100,000 to 200,000 g/mol. MWD of f-PHB is about 3.8 to 6.2. The wide range of the molecular weight of f-PHB may be due to the condition of bacterial fermentation or the f-PHB extraction and purification method.

Three main factors which affect to the molecular weight of PHB are types of microorganism which accumulate PHB, growth condition of microorganisms and PHB extraction method [Lee, 1996]. f-PHB was synthesized and accumulated by fermentation the bacterial stain *Alcaligenes Eutrophus* using glucose as sole carbon source. f-PHB was isolated from the bacterial cells by solvent extraction method (using

chloroform as the solvent). The detail of the effect of PHB extraction method is presented in Appendix C. From the literatures, the molecular weights and molecular weight distributions of PHB which was synthesized and accumulated by the bacteria strain *Alcaligenes eutrophus* using various chemicals as carbon source and various isolation method are summarized in Table 5.3

M_w reported by Doi. *et al* [1988] and Kunioka *et al.* [1989] are acquired by indirect method of intrinsic viscosity measurement. These M_ws were calculated by using the correlation of the intrinsic viscosity and M_w of PHB which was presented in the work of Zhang *et al.* [1997] as follow:

$$[\eta] = 1.18 * 10^{-4} (M_w)^{0.78} \quad \text{.....(5.1)}$$

Two values of the intrinsic viscosity of PHB presented by Doi *et al.* [1998] are 4.4 and 3.3 dl/gram, which was equal to the M_w of 726,086 and 502,122 g/mol, respectively.

From Table 5.3, the M_w, M_n and MWD of PHB fermented by using glucose as carbon source varies from 500,000 to 2,000,000; from 150,000 to 1,000,000 and from 1.80 to 5.09, respectively. These data are comparable to f-PHB as glucose is used as the carbon source. It is shown that the M_w, M_n and MWD of f-PHB are in the same range as those of PHB fermented by using carbon, especially PHB fermented by Dolarom [1999] because the fermentation procedure used in this work is followed that was proposed in the work of Dolarom [1999]. The M_w, M_n of PHB presented in the work of Hahn *et al.* [1995] is higher than those of f-PHB. The MWD of PHB in the work of Hahn *et al.* [1995] is lower than that of f-PHB.

The M_w, M_n and MWD of PHB which fermented by using butyric acid as sole carbon source were reported by Abe *et al.* [1997], Kunioka et al. [1989], Noda *et al.* [1999] and Doi *et al.* [1988]. From Table 5.3, it can be concluded that the M_w of PHB which fermented by using butyric acid as sole carbon source varies around 300,000 to 600,000 g/mol. The M_n and MWD are around 250,000 g/mol and 2.2, respectively. The

M_w and M_n of PHB fermented by using butyric acid are in the same range of those of f-PHB. The MWD of PHB fermented by using butyric acid is lower than that of f-PHB.

Another group of PHB including PHB fermented by other carbon sources and PHB with unspecified the data of carbon source is also shown in Table 5.4. It is shown that the M_w, M_n of f-PHB is in the same range of those of PHB in this group.

From Table 5.3, it can be primarily concluded that f-PHB which was fermented in this work has the M_w, M_n and MWD in the same range as those of PHB reported in the literatures.

Table 5.3 M_w, M_n and MWD of PHB fermented with various types of carbon source and PHB isolation method

Carbon source	PHB isolation method	Intrinsic viscosity (dl/g)	M_w (g/mol)	M_n (g/mol)	MWD	Reference
Glucose	Sodium hypochlorite digestion and chloroform	-	771,675	151,551	5.09	Dolarom [1999]
Glucose	Solvent extraction (chloroform)	-	2,160,000	1,200,000	1.80	Hahn *et al.* [1995]
Glucose	Solvent extraction (chloroform)	4.4	726,086*	-	-	Doi *et al.* [1988]
		3.3	502,122*	-	-	
Glucose	Sodium hypochlorite digestion and chloroform	-	1,020,000	293,103	3.48	Hahn *et al.* [1994]
Glucose	Solvent extraction (chloroform)	-	1,272,000	530,000	2.4	
Glucose	Sodium hypochlorite digestion and chloroform	-	1,000,000	500,000	2.0	Hahn *et al.* [1993]
Butyric acid	-	-	646,300	281,000	2.3	Abe *et al.* [1997]
Butyric acid	Solvent extraction (chloroform)	3.3	502,122*	-	-	Doi *et al.* [1988]
		2.8	298,574*	-	-	
Butyric acid	-	-	432,000	205,714	2.1	Noda *et al.* [1999]
Butyric acid	Solvent extraction (chloroform)	3.3	502,122*	-	-	Kunioka *et al.* [1989]

Table 5.3 M_w, M_n and MWD of PHB fermented with various types of carbon source and PHB isolation method (cont.)

Carbon source	PHB isolation method	Intrinsic viscosity (dl/g)	M_w (g/mol)	M_n (g/mol)	MWD	Reference
Fructose	-	-	737,000	387,894	1.9	Noda *et al.* [1999]
Acetic acid	Solvent extraction (chloroform)	5.5	966,566*	-	-	Doi et al [1988]
		2.7	381,221*	-	-	
-	Solvent extraction (chloroform)	-	1,050,000 or 930,000	-	-	Ramsay *et al.* [1994]
-	Sodium hypochlorite	-	600,000	-	-	Ramsay *et al.* [1989]

* M_w acquired by indirect method of intrinsic viscosity measurement

5.1.3 DSC Measurement

The DSC thermograms of the first and second heating of Biomer, the first and second heating of f-PHB1 and the first and second heating of f-PHB2 are presented in Figure 5.6, 5.7,5.8, 5.9, 5.10 and 5.11, respectively. In the first heating of Biomer, f-PHB1 and f-PHB2, the melting endothermic peak is observed at the temperature 179.2°C, 178.5°C and 179.6°C, respectively. The enthalpy of fusion (ΔH_f) of the Biomer, f-PHB1 and f-PHB2 which is determined from the area under melting endothermic peak is 98.9, 98.8 and 96.7 J/g, respectively. The degree of crystallinity of Biomer, f-PHB1 and f-PHB2 which is calculated from the enthalpy of fusion is 67.7%, 67.7% and 66.2%, respectively.

After the first heating cycle and the rapid cooling (≈30°C/min), PHB may not have enough time to form a complete crystallization so that the amorphous phase can be observed. In the second heating, the glass transition temperature (T_g) of Biomer, f-PHB1 and f-PHB2 is therefore observed at 2.9°C, 2.3°C and 3.2°C, respectively. The cold crystallization temperature (T_{cc}) is only detected in f-PHB1 and f-PHB2 at 45.3°C and 45.8°C, respectively. The melting endothermic peak of Biomer, f-PHB1 and f-PHB2 is observed at 174.6°C, 175.1°C and 179.2°C, respectively. The enthalpy of fusion (ΔH_f) of the Biomer, f-PHB1 and f-PHB2 is 101.7, 104.2 and 91.2 J/g, respectively. The degree of crystallinity of Biomer, f-PHB1 and f-PHB2 is 69.6%, 71.4% and 62.5%, respectively. Thermal properties of Biomer, f-PHB1 and f-PHB2 are summarized in Table 5.4.

Considering the second heating in the Table 5.4, it is shown that the thermal properties of f-PHB1 and Biomer are similar. The thermal properties of f-PHB2 are different to those of f-PHB1 especially the degree of crystallinity. The difference may be due to the difference in the molecular weight of f-PHB1 and f-PHB2 presented in the previous section.

From Figure 5.6 to 5.11, all of the DSC thermograms show two melting peaks. The lower-temperature peak looks like the shoulder of the higher-temperature peak. This phenomenon is also observed by Yoshie *et al.* [2000], Zhang *et al.* [2000], Dubini Paglia *et al.* [1993] and Lee *et al.* [1997]. Yoshie *et al.* [2000] concluded that the two-melting peak behavior was often observed in single-polymer system in which melt/recrystallization process occurs during DSC heating run. Zhang *et al.* [2000] concluded that the two-separated endothermic peak was attributed to the occurrence of melting, recrystallzation and remelting in the melting region. The low-temperature peak is accociated with the as-formed crystals, while the high-temperature peak is associated with the melting of crystals formed from the recrystallization process during the DSC heating.

Dubini Paglia *et al.* [1993] found that the peak appearing at the lower temperature was corresponded to the melting of the original crystal of the crystallized PHB. The second endothermic peak was caused by the melting of reorganized crystal formed during the heating process

Lee *et al.* [1997] reported that the double melting behavior was frequently found in miscible blends containing PHB prepared by casting from solvent. This is consistent with the first heating of Biomer, f-PHB1 and f-PHB2 of which the samples were also prepared by solution casting method. The first heating can be assumed to be the melt-quenched process for the PHB sample in the second heating.

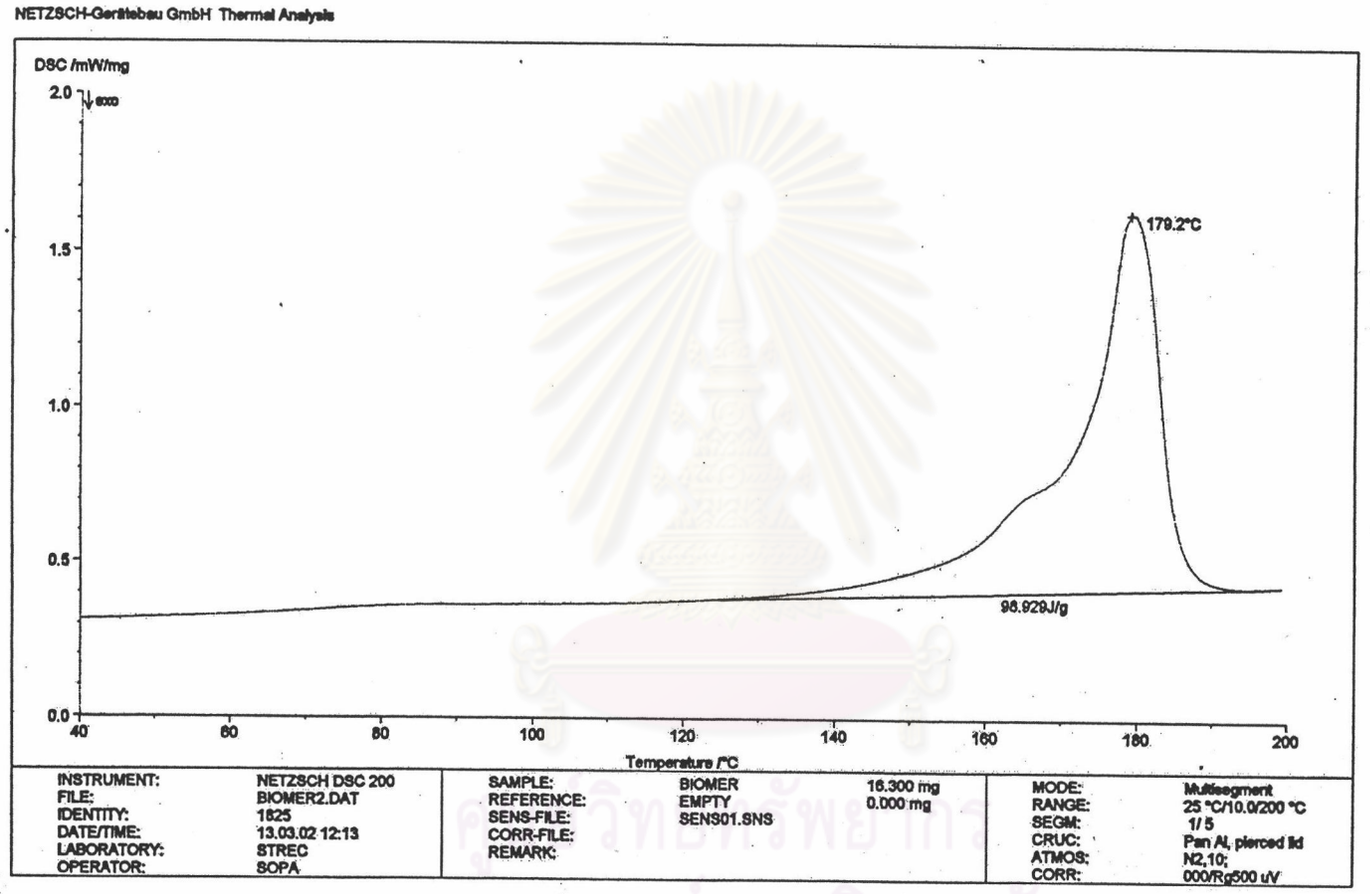

Figure 5.6 DSC thermogram of the first heating cycle of Biomer

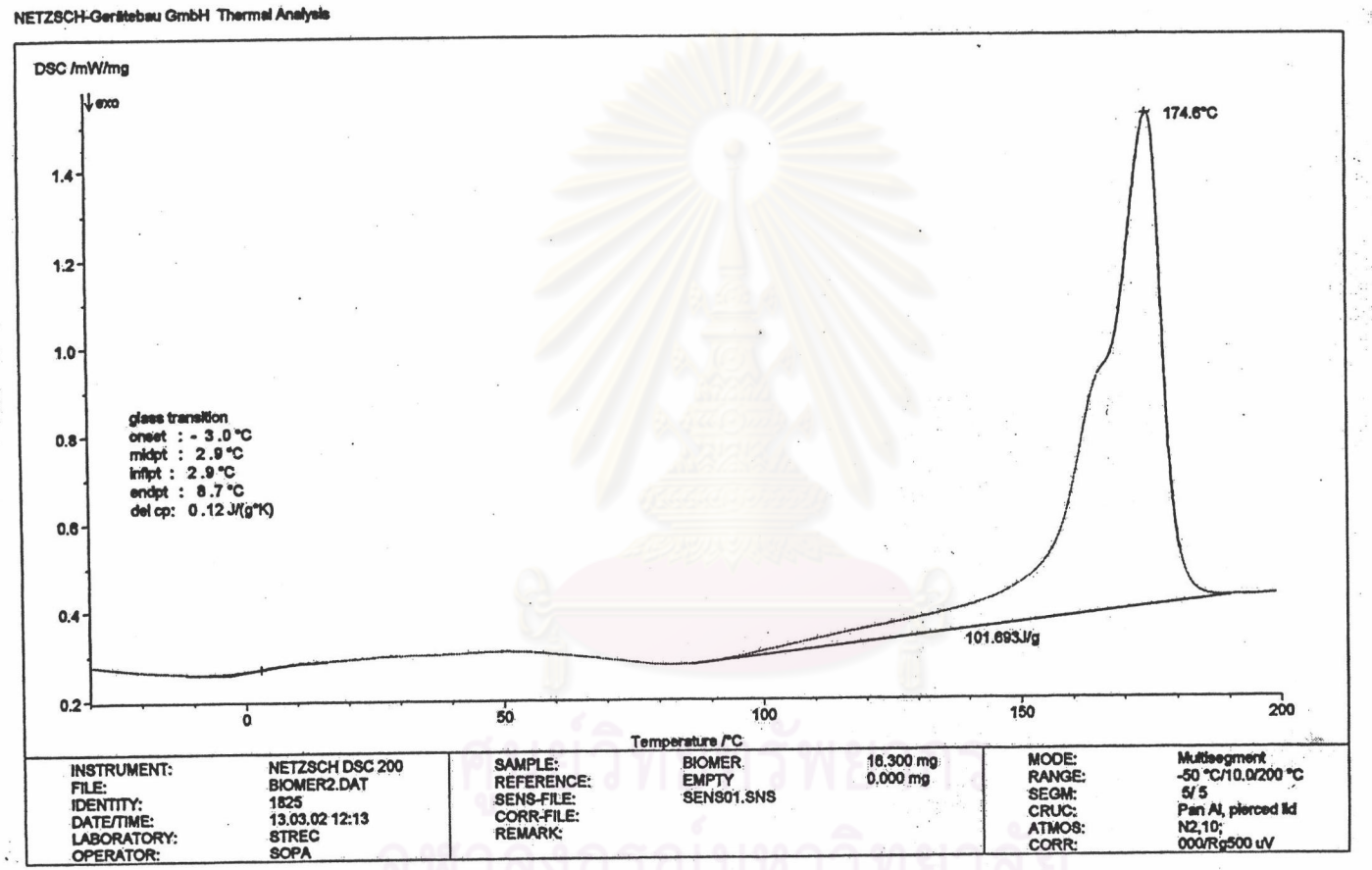

Figure 5.7 DSC thermogram of the second heating cycle of Biomer

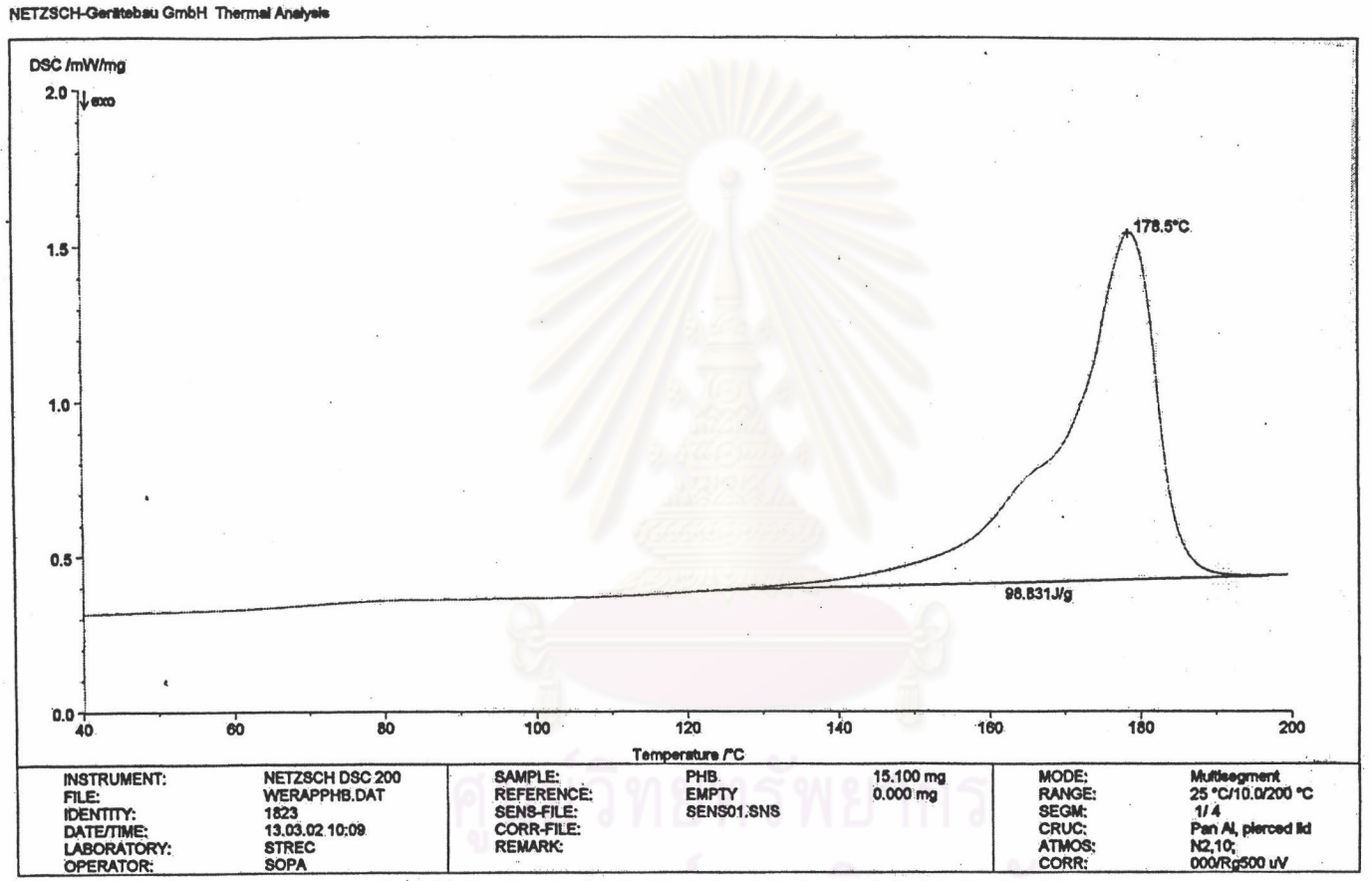

Figure 5.8 DSC thermogram of the first heating cycle of f-PHB1

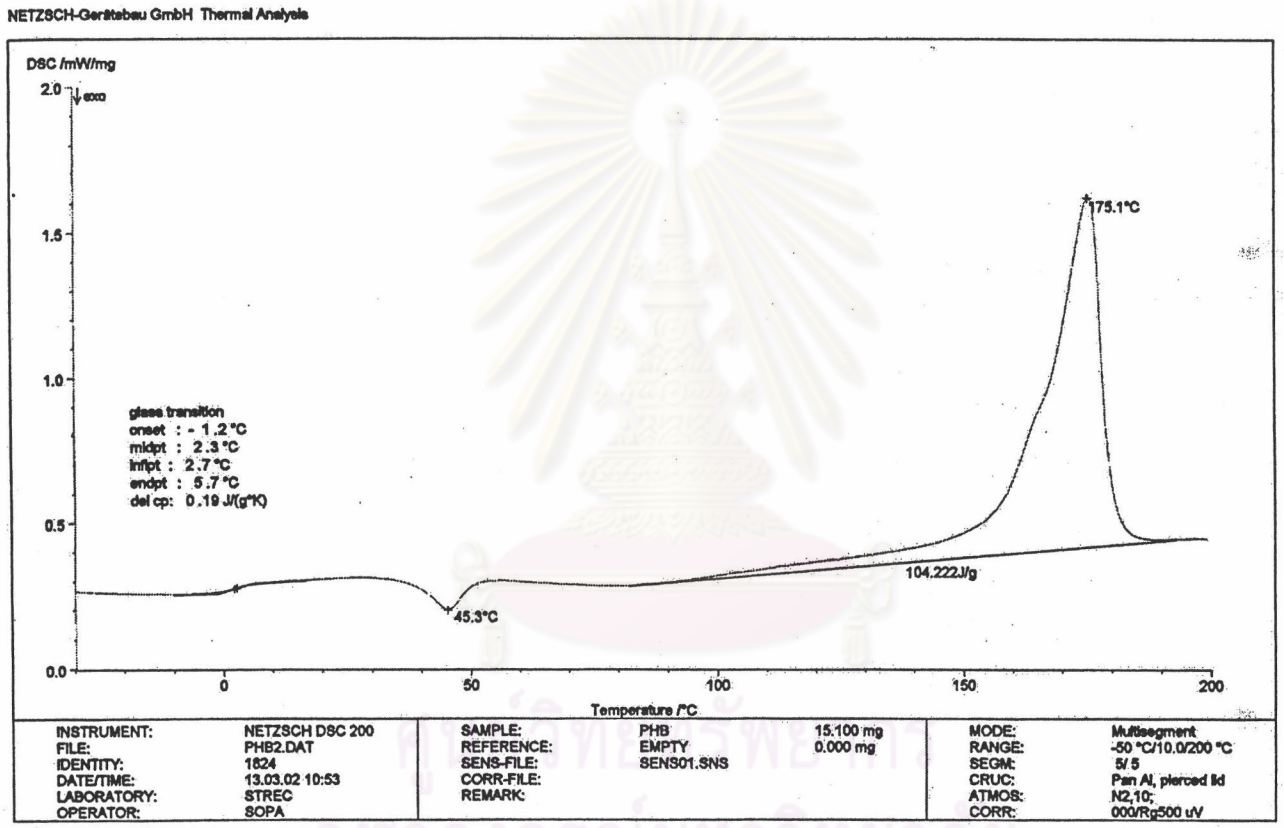

Figure 5.9 DSC thermogram of the second heating cycle of f-PHB1

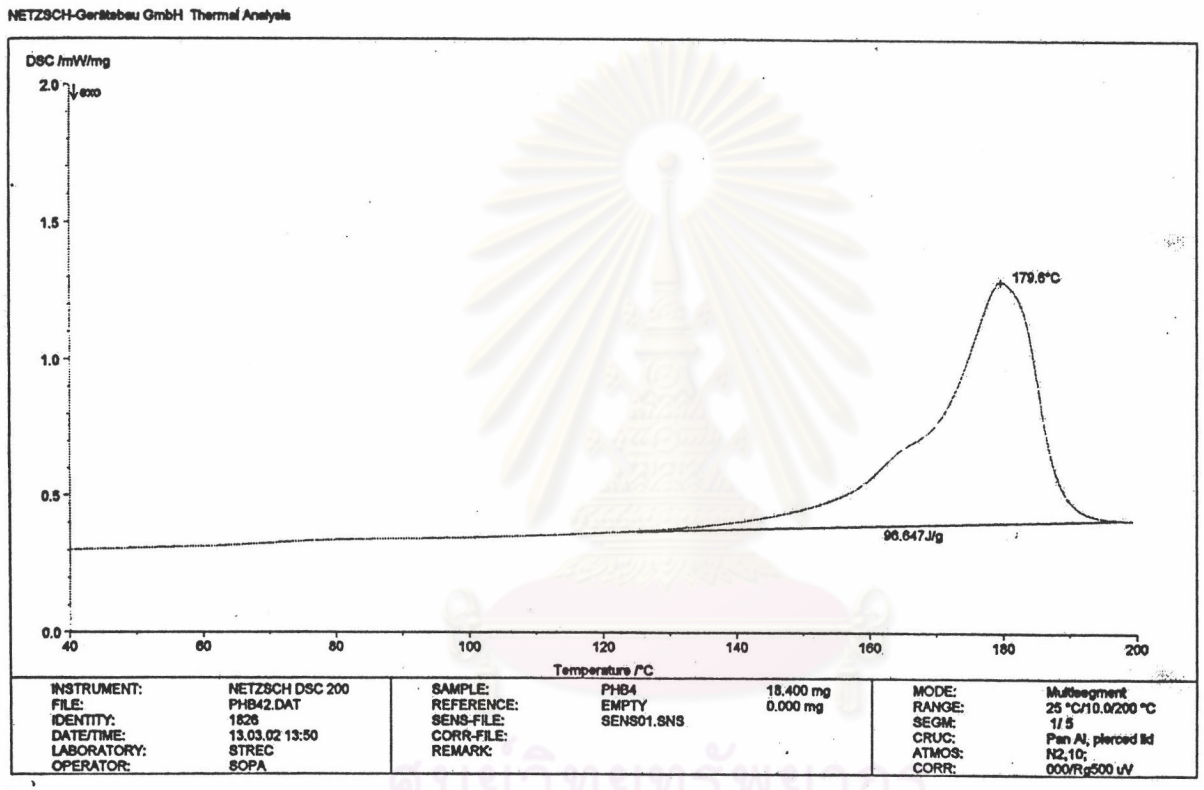

Figure 5.10 DSC thermogram of the first heating cycle of f-PHB2

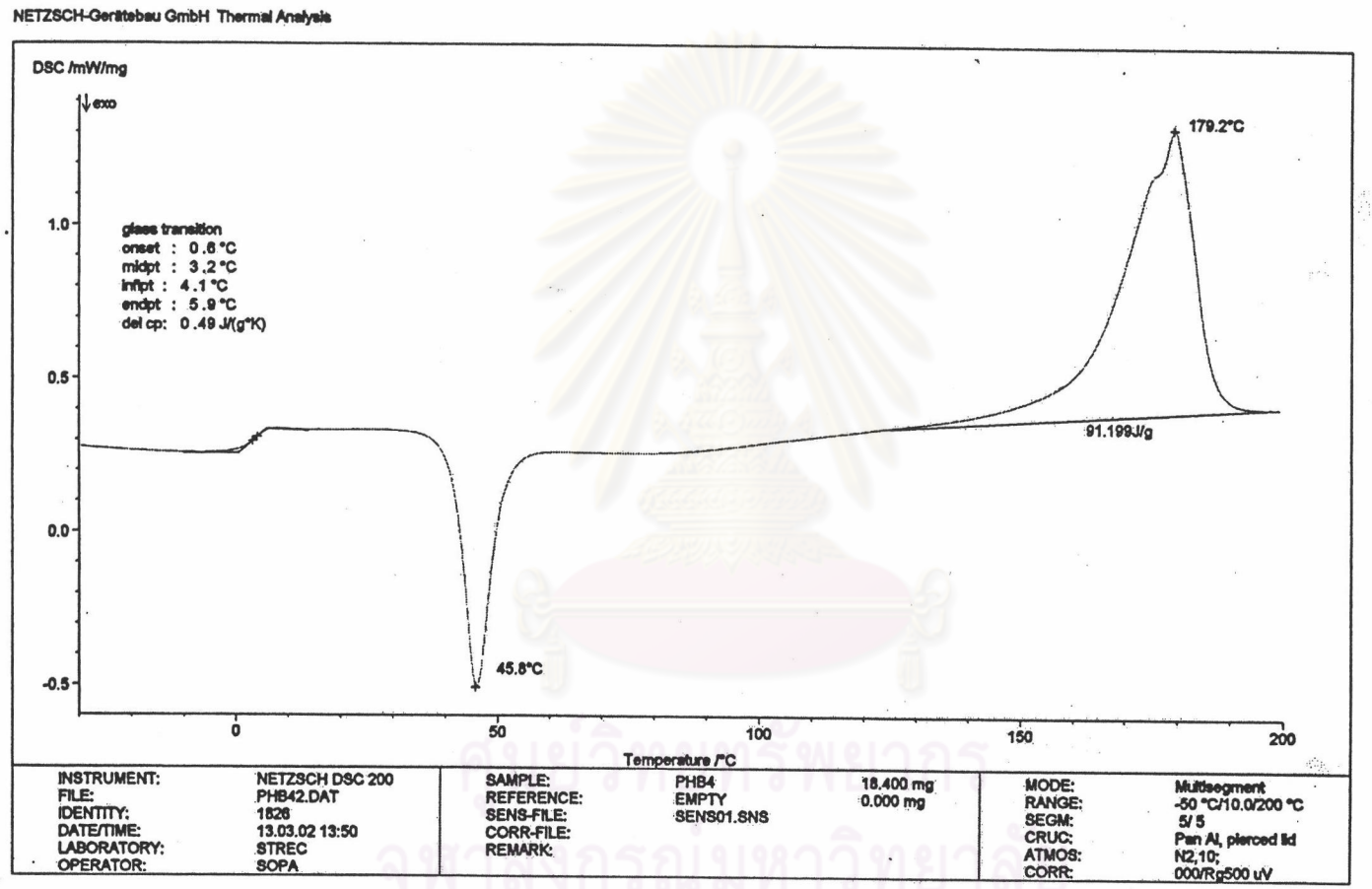

Figure 5.11 DSC thermogram of the second heating cycle of f-PHB2

Table 5.4 Thermal perperties of Biomer, f-PHB1 and f-PHB2

Sample	First heating cycle			Second heating cycle				
	T_m	ΔH_f	Degree of crystallinity	T_g	T_{cc}	T_m	ΔH_f	Degree of crystallinity
	(^oC)	(J/g)	(%)	(^oC)	(^oC)	(^oC)	(J/g)	(%)
Biomer	179.2	98.929	67.7	2.9	-	174.6	101.693	69.6
f-PHB1	178.5	98.831	67.7	2.3	45.3	175.1	104.222	71.4
f-PHB2	179.6	96.647	66.2	3.2	45.8	179.2	91.199	62.5

The thermal properties of PHB which were reported in the literatures were summarized in Table 5.5, comparing with the result of this work. It can be seen that the T_g of PHB is observed around -5°C to 5°C or 0°C to 20°C. The melting temperature (T_m) is observed around 170°C to 180°C and the degree of crystallinity of PHB is around 60-80%. It is concluded that the T_g, T_m and degree of crystallinity of Biomer, f-PHB1 and f-PHB2 are in the same range as those of PHB reported in literatures.

Table 5.5 Thermal properties of PHB presented in literatures

Group of Researchers	T_g (°C)	T_m (°C)	Degree of Crystallinity (%)
Anderson and Dawes [1990]	-5 to 5 or 0-20	174	60-80
Azuma *et al.* [1992]	-	174.3	58
Orts *et al.* [1992]	-	179	59
Pearce *et al.* [1992]	4	177	-
Scandola *et al.* [1992]	4.5	175	-
Pearce *et al.* [1994]	4	177	-
Avella *et al.* [1997]	-	176	60.95
Lee *et al.* [1997]	-3	173	78.83
Xiang *et al.* [1997]	-	172	-
Zhang *et al.* [1997]	5.3	175	76.8
Galego *et al.* [2000]	-	170	69
Zhang *et al.* [2000]	-	175	60.9
Bibers *et al.* [2001]	5	183	58
Mitomo *et al.* [2001]	4	176	-
This work (Biomer)	2.9	174.6	69.6
This work (f-PHB1)	2.3	175.1	71.4
This work (f-PHB2)	3.2	179.2	62.5

From the FT-IR spectroscopy, molecular weight measurement and thermal property measurement, it can be concluded that the f-PHB is truly PHB. The macromolecular substance acquired from fermentation of the bacterial strain *Alcaligenes eutrophus* and its fundamental characteristics and properties are not different from the literatures.

5.2 Effects of modifying agents on PHB properties

5.2.1 Mechanical properties

5.2.1.1 Biomer/PPG blends

The effects of the PPG composition on the mechanical properties of PHB are considered in this section. Table 5.6 presents the results of tensile properties of the Biomer/PPG blends. Figure 5.12 shows the maximum tensile strength of the Biomer/PPG blends. The maximum tensile strength of the blends containing 10%, 20%, 30%, 40% and 50% of PPG is lower than that of pure Biomer by 33.0%, 41.9%, 50.2%, 85.8% and 94.7%, respectively. It is noticed that the maximum tensile strength of Biomer/PPG blends decreases gradually with an increasing of PPG content. The result is in agreement with the work of Bibers *et al.* [1999].

Table 5.6 Tensile properties of the Biomer/PPG blends

Blend	Maximum tensile strength (MPa)	%Elongation at break (%)	Modulus of Elasticity (GPa)
Pure Biomer	16.61	1.55	1.664
Biomer/10%PPG	11.12	1.24	1.408
Biomer/20%PPG	9.65	1.39	1.249
Biomer/30%PPG	8.27	2.55	0.836
Biomer/40%PPG	2.35	6.82	0.221
Biomer/50%PPG	0.88	6.94	0.118

Figure 5.13 shows the %elongation at break of the Biomer/PPG blends. For the blend containing 0% to 20% of PPG, the % elongation at break of the Biomer/PPG blends varies in a narrow range. The %elongation at break of the blend containing 30%, 40% and 50% of PPG is higher than that of pure Biomer by 64.5%, 77.3% and 77.7%, respectively. It seems that the effective PPG composition that can improve the %

elongation at break of Biomer is around 20%-30%. Higher PPG composition than 40% seems to have no further effect on the %elongation at break of Biomer blends. The characteristic of the %elongation at break changing with various content of PPG in the Biomer/PPG blends is consistent with that of the %elongation at break changing at various content of plasticizer in the PHB/plasticizer blends which were studdied by Bibers *et al.* [1999]. They found that at small plasticizer concentrations, the %elongation at break varied rather moderately, whereas at the plasticizer concentration of 10% the value increased several times. A further increase in the plasticizer content leaded to a sharp increase in the %elongation at break. At the plasticizer concentration more than 30%, an insignificant increase in the %elongation at break was observed.

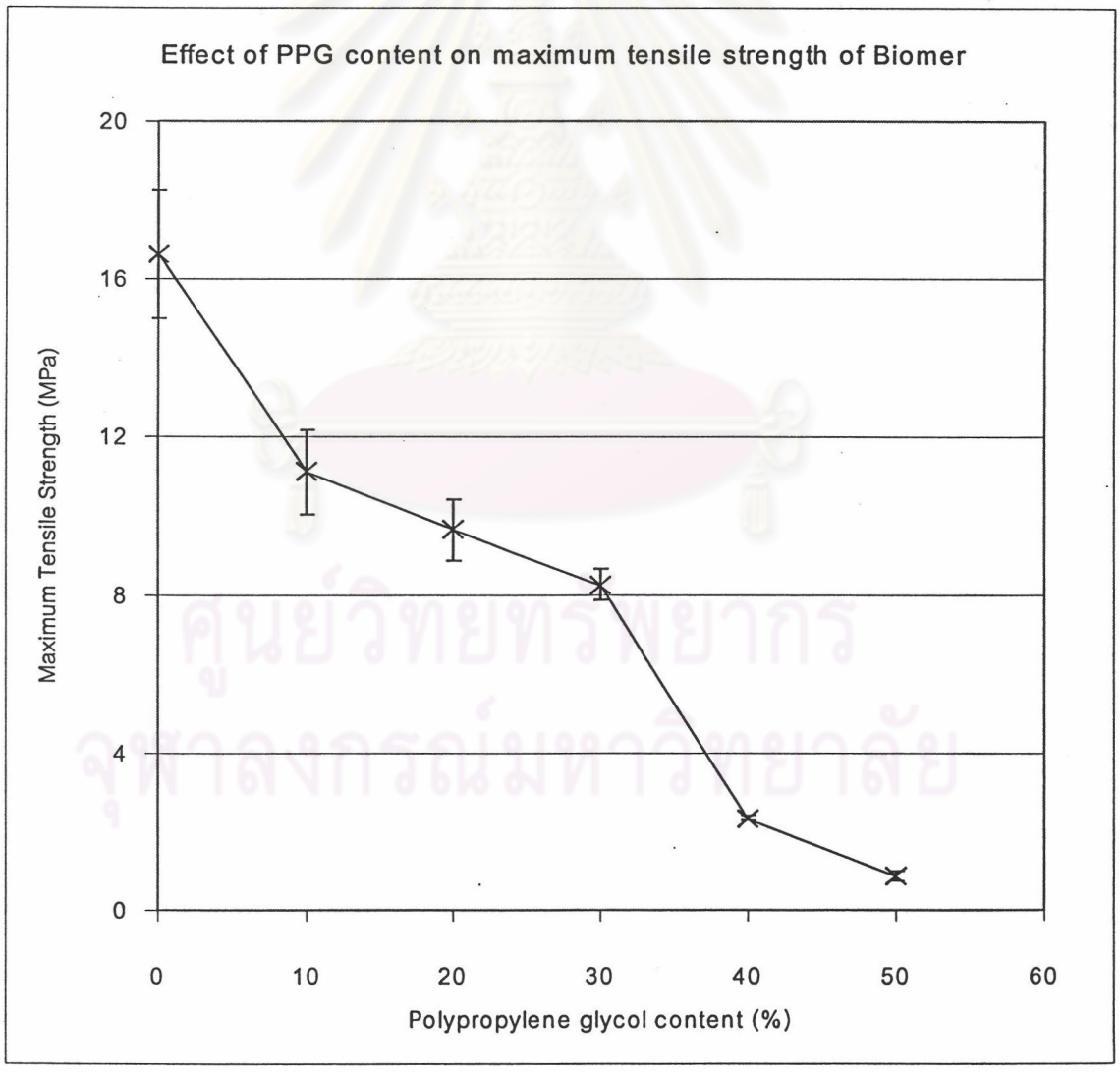

Figure 5.12 Maximum tensile strength of the Biomer/PPG blends

Figure 5.14 shows the modulus of elasticity of the Biomer/PPG blends. The modulus of elasticity of the Biomer/PPG blends decreases with an increasing of the PPG content. It is clear that the stiffness of the Biomer/PPG blends decreases when PPG is added. The modulus of elasticity of the blends containing 10%, 20%, 30%, 40% and 50% of PPG is lower than that of pure Biomer by 15.6%, 25.2%, 50.4%, 87.8% and 94.0%, respectively.

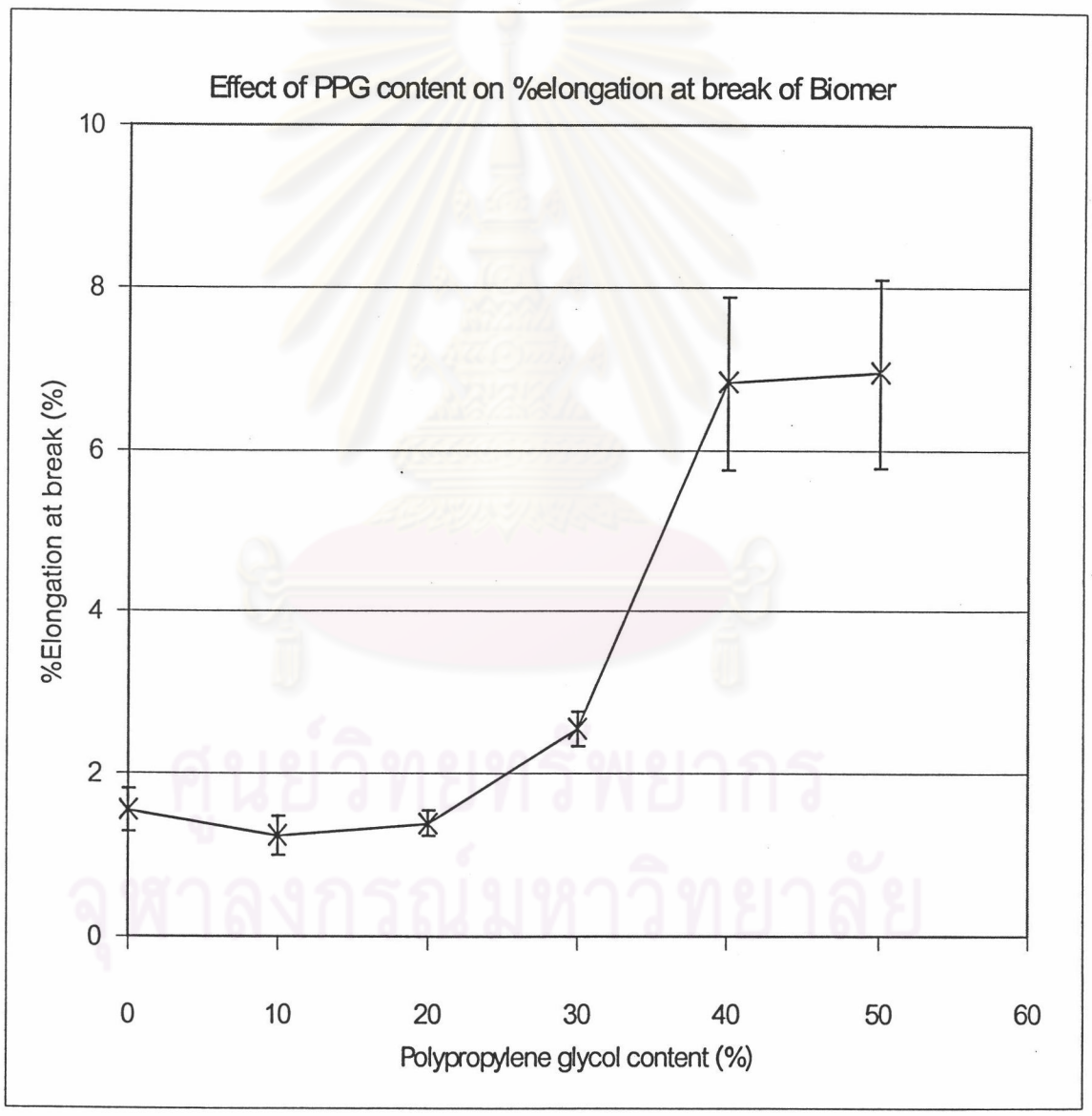

Figure 5.13 %Elongation at break of the Biomer/PPG blends

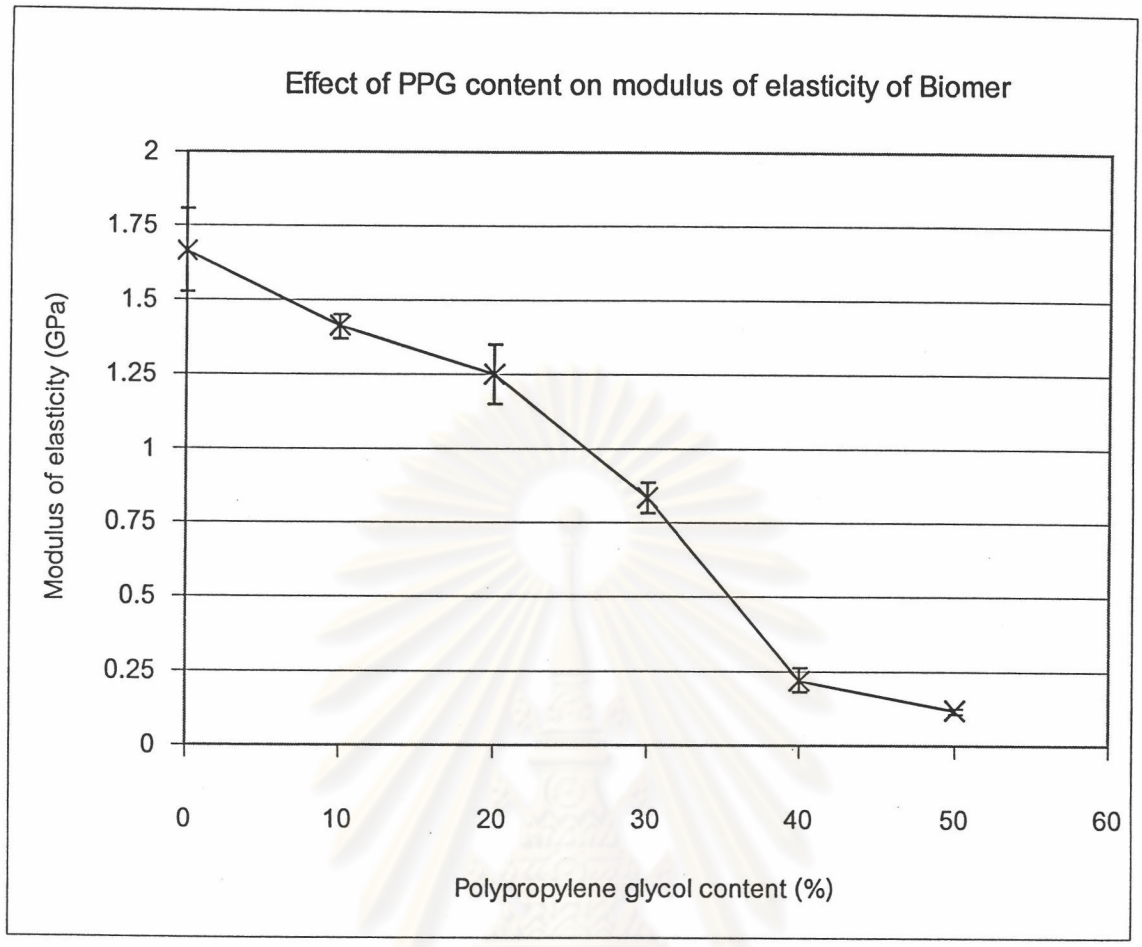

Figure 5.14 Modulus of Elasticity of the Biomer/PPG blends

Figure 5.15 present the extension-load curve of the Biomer/PPG blends at various PPG concentrations. The area under extension-load curve can be referred to the toughness of polymers. From Figure 5.15, it is noticed that the pure Biomer is changed from a hard and brittle material to a softer and more brittle material when 10%-20% of PPG is added because the modulus of elasticity and the extension are lowered. Then the blend containing 30% of PPG is changed to be softer and tougher than the blend containing 20% of PPG as the modulus of elasticity is lowered and the extension is increased. The blend containing 40% and 50% of PPG is softer and tougher than the blend containing 30% of PPG as seen from the very low modulus of elasticity and the long extension.

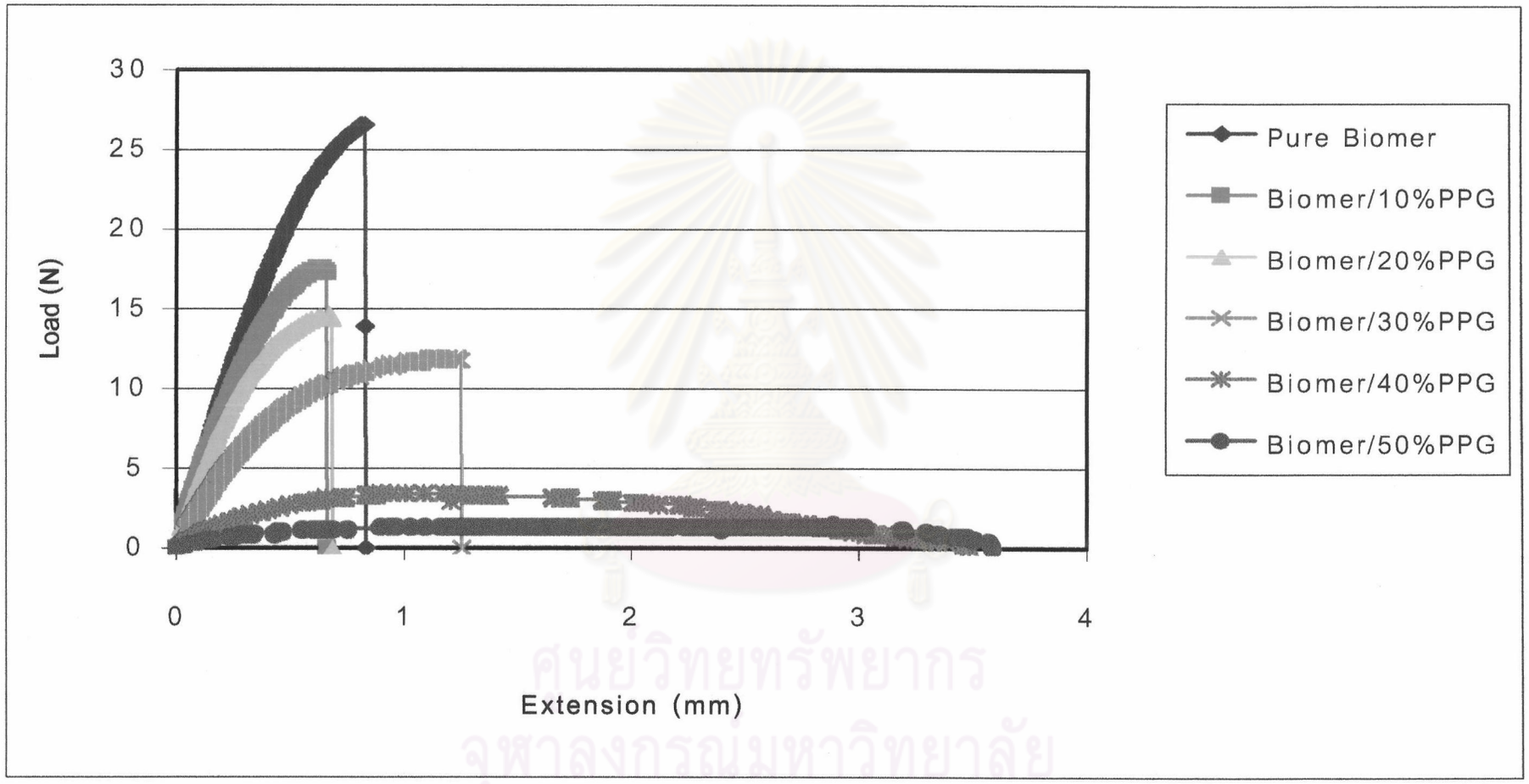

Figure 5.15 Extension-load curve of the Biomer/PPG blends at various PPG contents

5.2.1.2 Biomer/PG blends

The results of tensile properties of the Biomer/PG blends are presented in Table 5.7. Figure 5.16 shows the maximum tensile strength of the Biomer/PG blends. The maximum tensile strength of the Biomer/PG blends decreases with an increasing of the PG composition. The maximum tensile strength of the blends containing 10%, 20%, 30%, 40% and 50% of PG decreases from that of pure Biomer by 9.0%, 26.8%, 60.5%, 77.2% and 83.7%, respectively.

Table 5.7 Tensile properties of the Biomer/PG blends

Blend	Maximum tensile strength (MPa)	%Elongation at break (%)	Modulus of Elasticity (GPa)
Pure Biomer	16.61	1.55	1.664
Biomer/10%PG	15.11	1.33	1.707
Biomer/20%PG	12.16	1.72	1.238
Biomer/30%PG	6.57	4.55	0.714
Biomer/40%PG	3.78	8.35	0.371
Biomer/50%PG	2.70	2.42	0.386

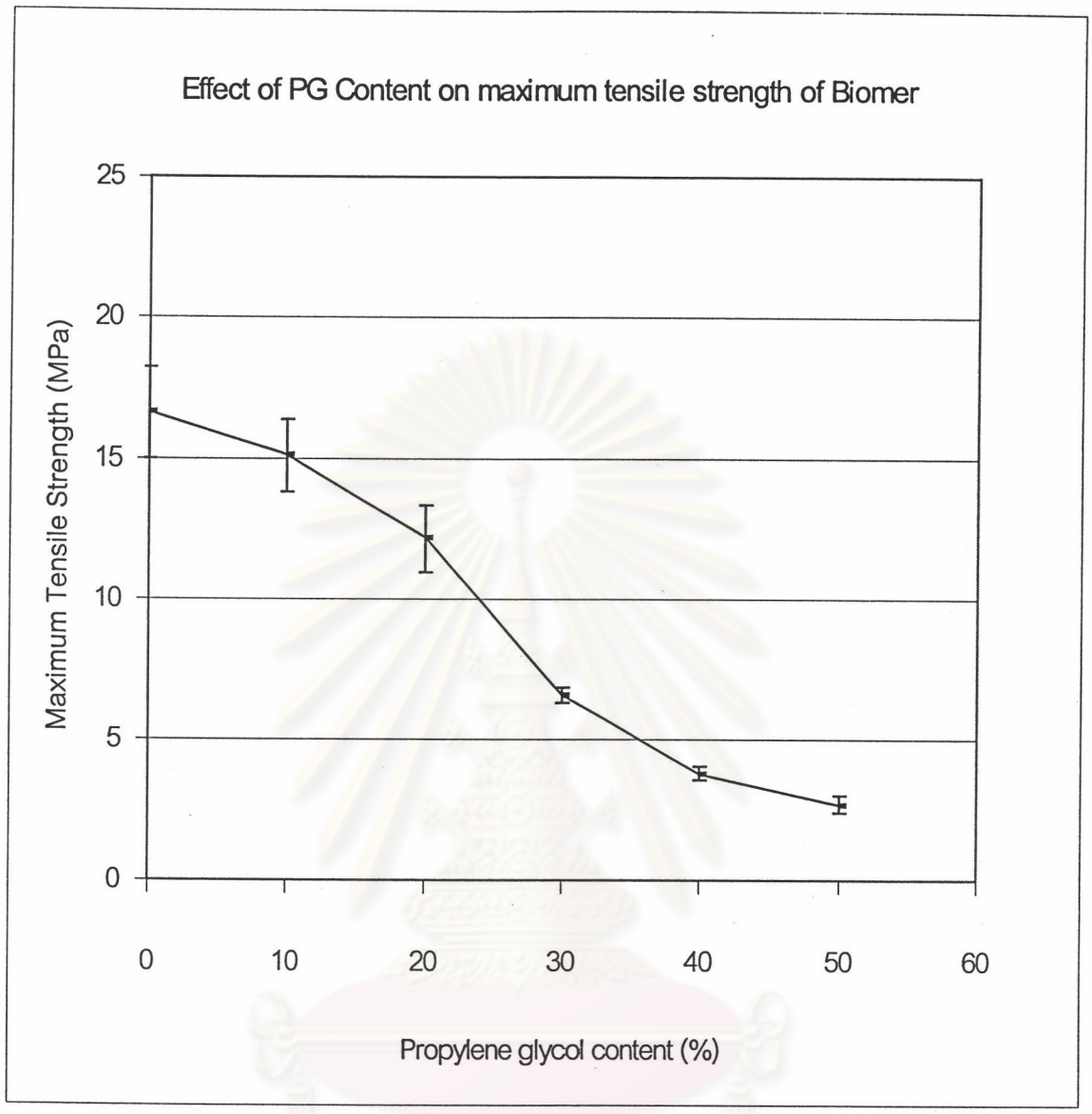

Figure 5.16 Maximum tensile strength of the Biomer/PG blends

Figure 5.17 shows the %elongation at break of the Biomer/PG blends. From 0% to 20% of PG, the %elongation at break of the Biomer/PG blends varies in a narrow range. The %elongation at break increases sharply for the blend containing 30% of PG. The %elongation at break of the blend containing 30% of PG is higher than that of pure Biomer by 193.5%. The %elongation at break of the blend containing 40% reaches the highest value with 438.7% higher than that of pure Biomer. The %elongation at break of the blend containing 50% of PG decreases from the maximum but still higher than that of pure Biomer by 56.1%.

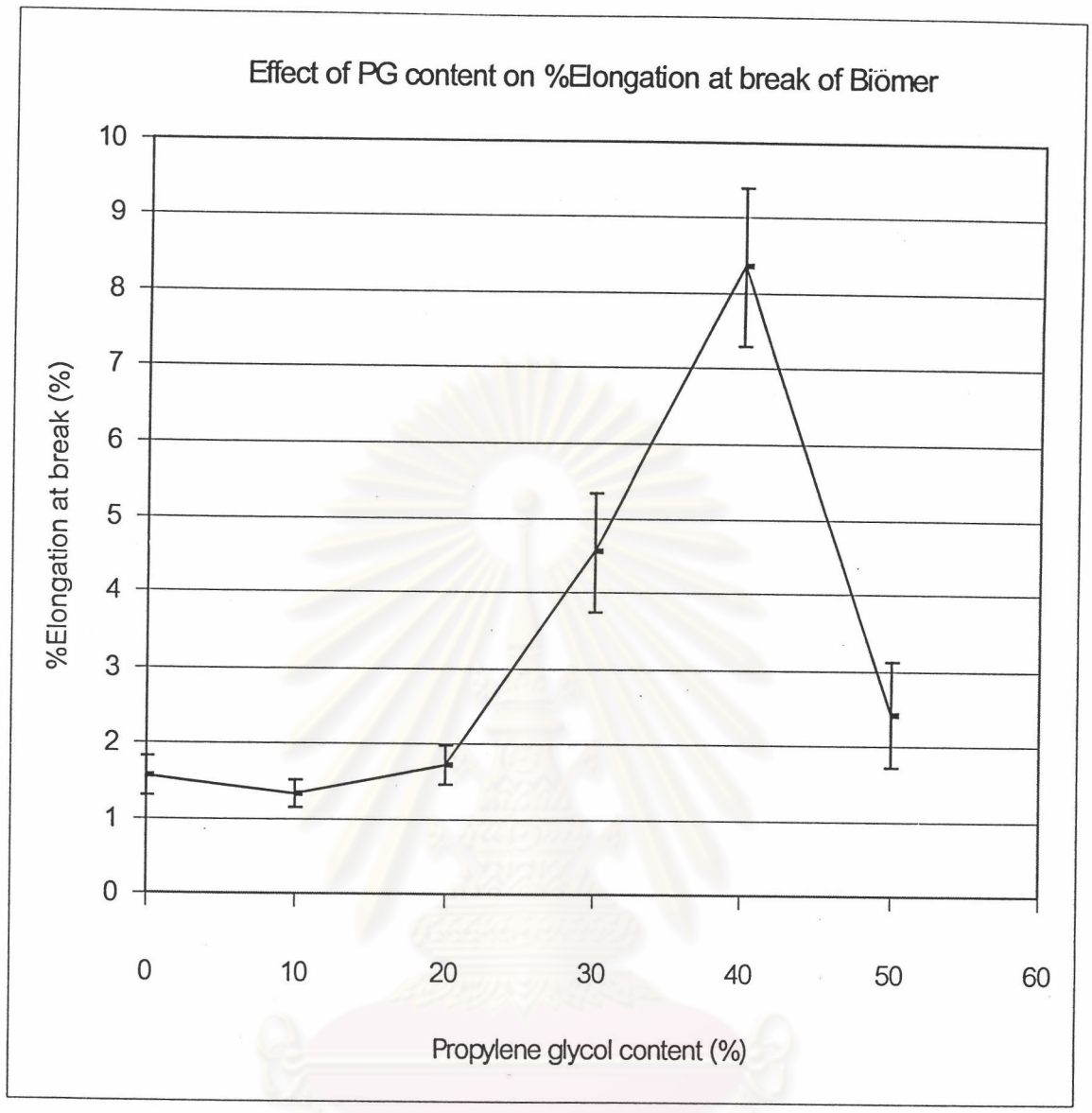

Figure 5.17 %Elongation at break of the Biomer/PG blends

Figure 5.18 shows the modulus of elasticity of the Biomer/PG blends. The modulus of elasticity of the blend containing 10% of PG is about the same as that of pure Biomer. The modulus of elasticity of the blends containing 20%, 30%, 40% and 50% of PG is lower than that of pure Biomer by 25.6%, 57.1%, 77.7% and 76.8%, respectively.

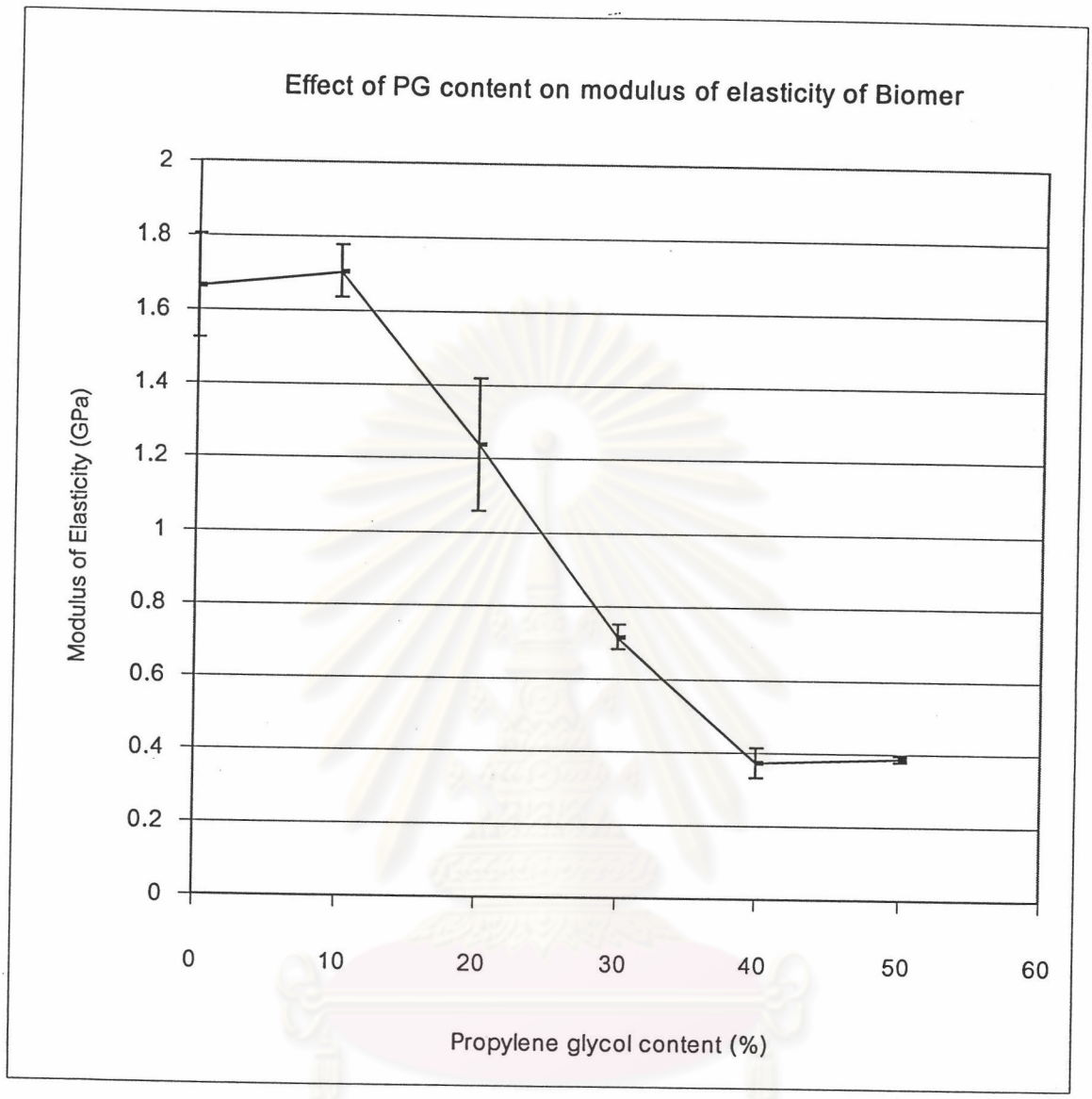

Figure 5.18 Modulus of elasticity of the Biomer/PG blends

Figure 5.19 presents the extension-load curve of the Biomer/PG blends at various PG composition. It can be seen that the Biomer begins to change from a hard and brittle material to a softer and more brittle material when 30% of PG is added. The extension-load curve of the Biomer/PG blends with 0%to 20% of PG is changed from a high modulus of elasticity and low extension pattern to a lower modulus of elasticity and higher extension for the blends containing 30% -50% of PG.

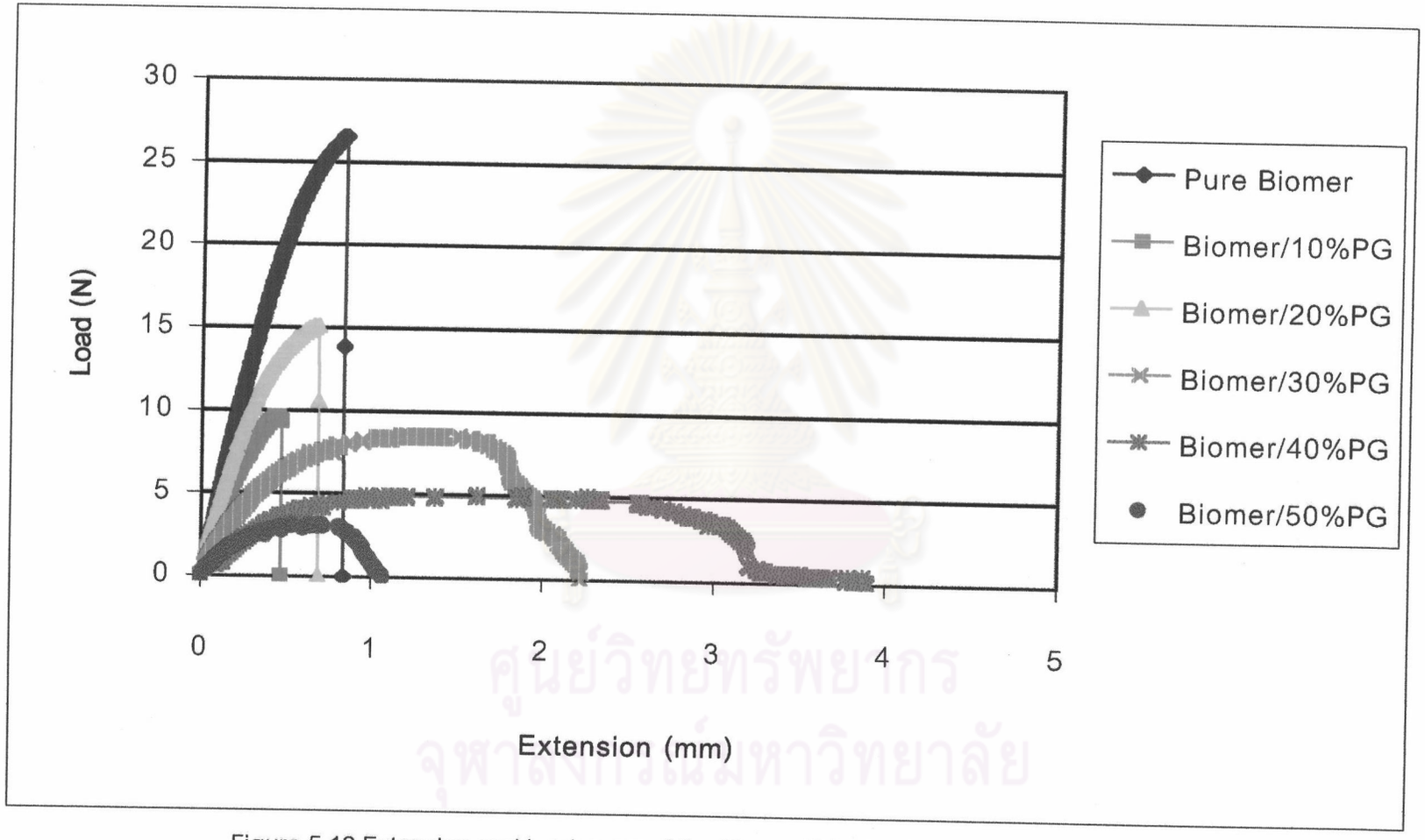

Figure 5.19 Extension and load curve of the Biomer/PG blend at various PG contents

5.2.1.3 Biomer/ESO blends

The tensile properties of the Biomer/ESO blends are presented in Table 5.8. The maximum tensile strength of Biomer/ESO blends is shown in Figure 5.20. The maximum tensile strength of Biomer/ESO blend decreases with an increasing of ESO composition. The result is consistent with that of Biomer/PPG and Biomer/PG blends. The maximum tensile strength of the blends containing 10%, 20%, 30%, 40% and 50% of ESO is lower than that of pure Biomer by 22.7%, 44%, 36.9%, 60.1% and 73.1%, respectively.

Figure 5.21 shows the %elongation at break of the Biomer/ESO blends. The %elongation at break of the system containing 10% of ESO is not different from that of pure Biomer. The %elongation at break linearly increases for the blends containing 20% and 30% of ESO and reaches the maximum value at the blend containing 30% of ESO. The % elongation at break of the blend containing 30% of ESO is higher than that of pure Biomer by 242.6%. The %elongation at break of the blends containing 40% and 50% of ESO decreases from that of the blend with 30% of ESO but they are still higher than that of pure Biomer by 124.5% and 74.2%, respectively.

Table 5.8 Tensile properties of the Biomer/ESO blends

Blend	Maximum tensile strength (MPa)	%Elongation at break (%)	Modulus of Elasticity (GPa)
Pure Biomer	16.61	1.55	1.664
Biomer/10%ESO	12.83	1.54	1.508
Biomer/20%ESO	9.30	3.49	1.017
Biomer/30%ESO	10.19	5.31	1.037
Biomer/40%ESO	6.62	3.48	0.638
Biomer/50%ESO	4.46	2.70	0.473

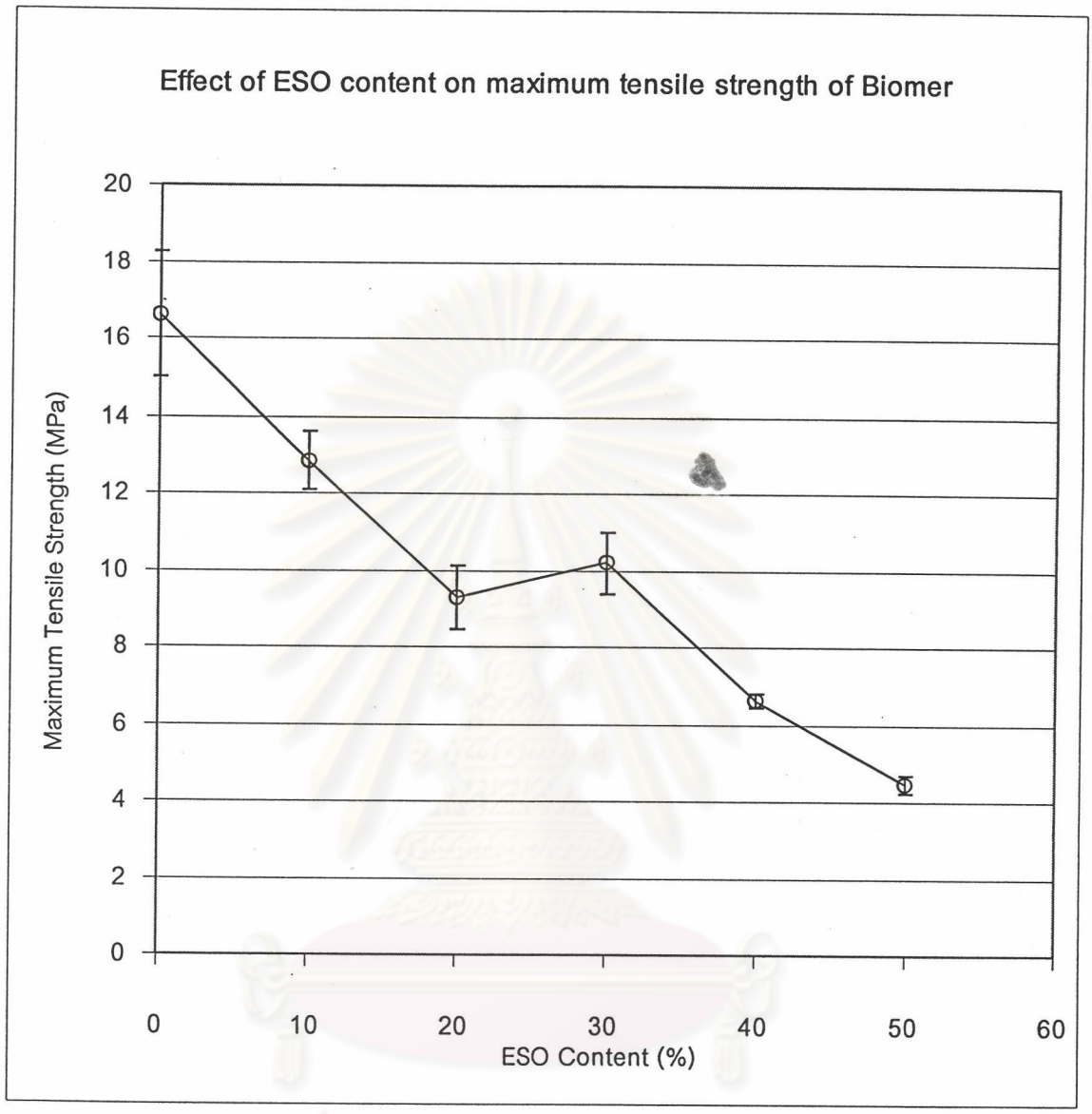

Figure 5.20 Maximum tensile strength of the Biomer/ESO blends

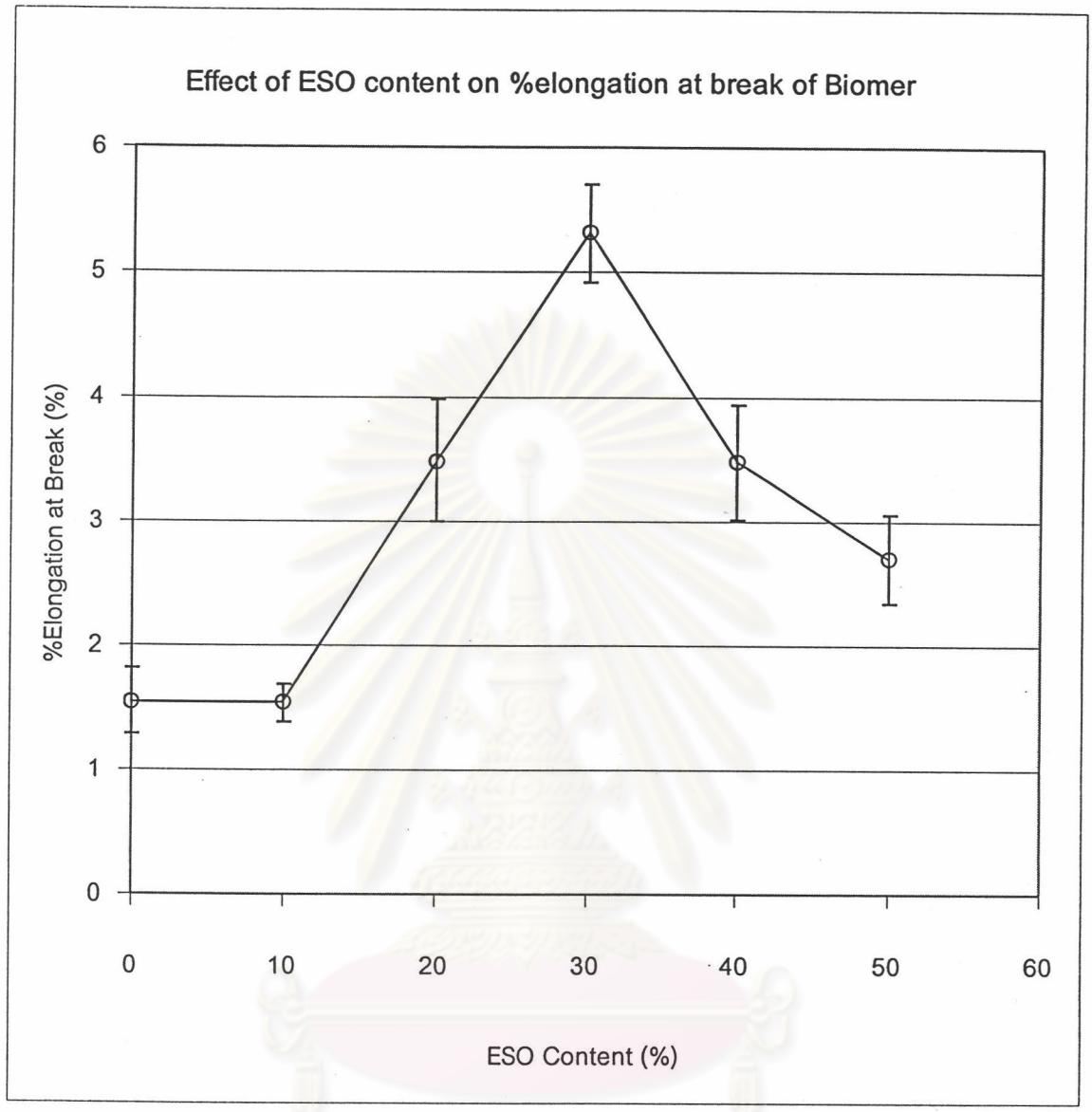

Figure 5.21 %Elongation at break of the Biomer/ESO blends

Figure 5.22 shows the modulus of elasticity of the Biomer/ESO blends. The modulus of elasticity tends to gradually decrease with an increasing of ESO content. The modulus of elasticity of the blends containing 10%, 20%, 30%, 40% and 50% of ESO is lower than that of pure Biomer by 9.4%, 38.9%, 37.7%, 61.7% and 71.6%, respectively.

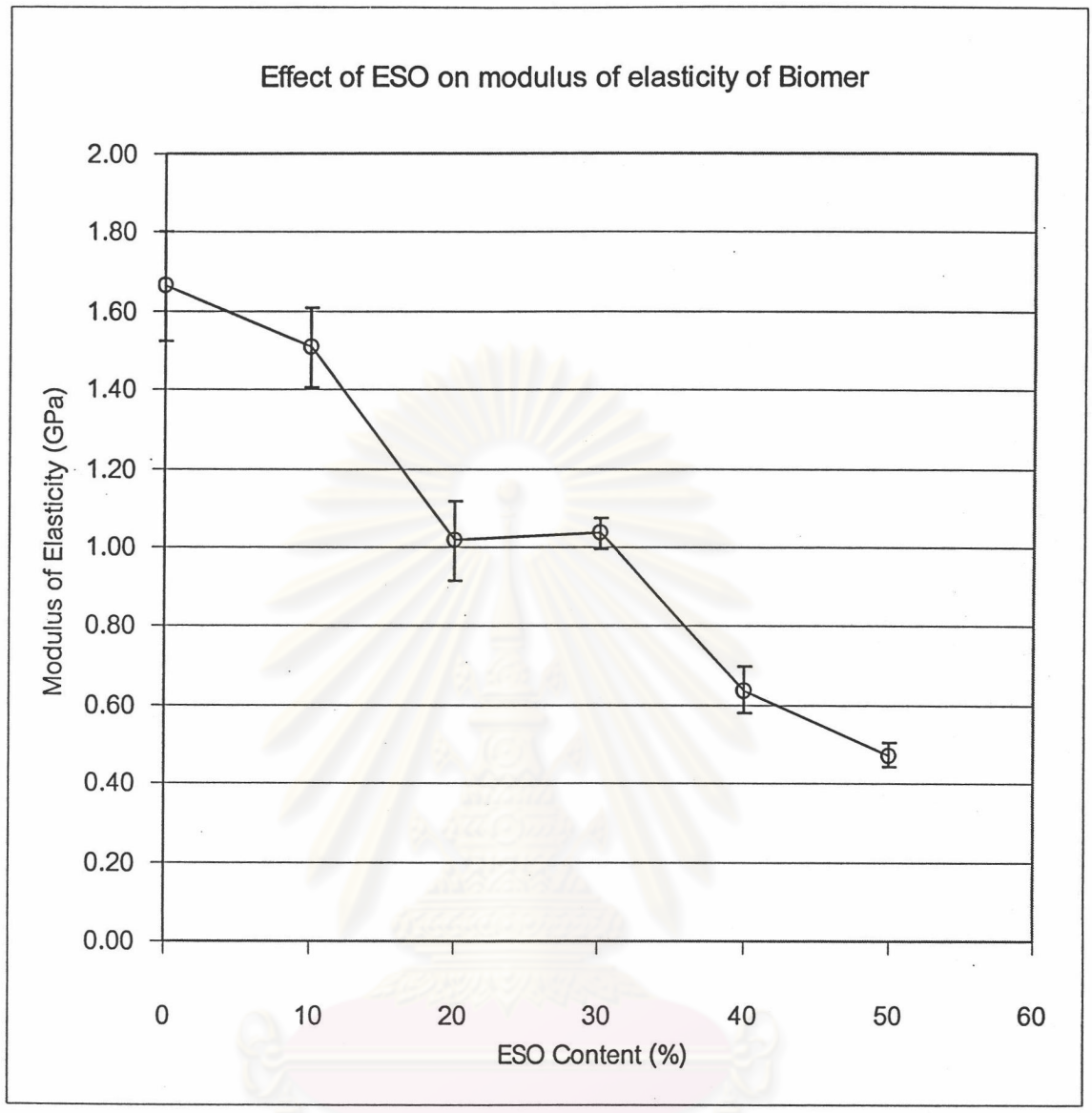

Figure 5.22 Modulus of Elasticity of the Biomer/ESO blends

Figure 5.23 presents the extension-load curve of the Biomer/ESO blends at various PG contents. It seems that pure Biomer is changed from a hard and brittle material to be softer and more brittle material for the blend containing 10% of ESO. The blend containing 20% and 30% of ESO become softer and tougher than the blend containing 10% of ESO. The softness and ductility of Biomer/ESO blend gradually decreases in the blend containing 40% and 50% of ESO.

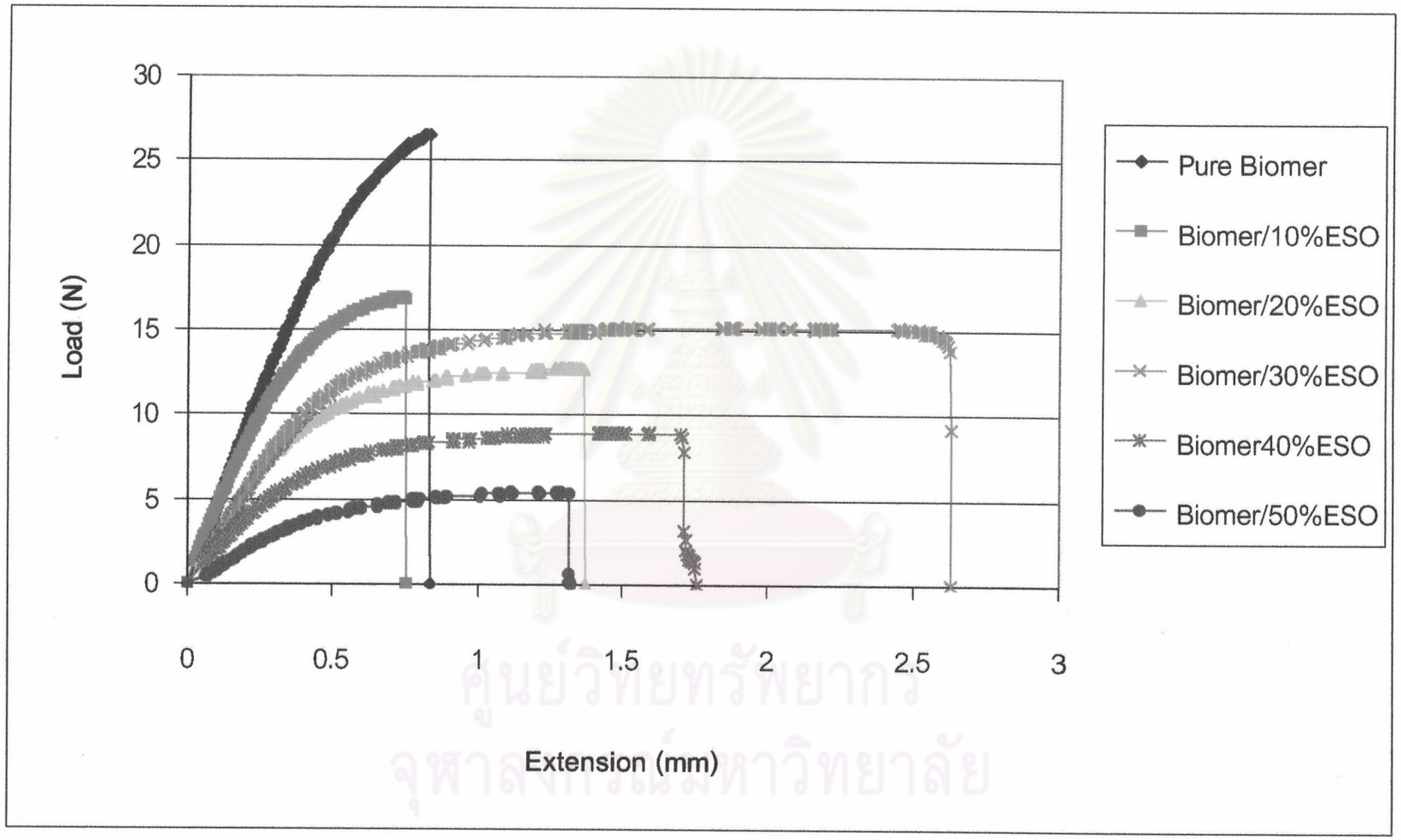

Figure 5.23 Extension-load curve of the Biomer/ESO blend at various ESO contents

5.2.1.4 f-PHB1/PPG blends

Table 5.9 presents the tensile properties of the f-PHB/PPG blends. Figure 5.24 shows the maximum tensile strength of the f-PHB1/PPG blends. The maximum tensile strength of the f-PHB1/PPG blend continuously decreases with an increasing of PPG content. The maximum tensile strength of the blend containing 10%, 20%, 30%, 40% and 50% of PPG is lower than that of pure f-PHB1 by 1.3%, 20.4%, 66.2%, 77.5% and 91%, respectively

Table 5.9 Tensile properties of the f-PHB/PPG blends

Blend	Maximum tensile strength (MPa)	%Elongation at break (%)	Modulus of Elasticity (GPa)
Pure f-PHB1	16.54	1.59	1.629
f-PHB1/10%PPG	16.33	2.01	1.618
f-PHB1/20%PPG	13.17	3.34	1.160
f-PHB1/30%PPG	5.59	8.24	0.432
f-PHB1/40%PPG	3.72	8.31	0.428
f-PHB1/50%PPG	1.49	58.82	0.153

Figure 5.25 shows the %elongation at break of the f-PHB1/PPG blends. For the blends containing 0% to 20% of PPG, the %elongation at break slightly increases from 1.59% to 3.34%. The %elongation at break of the blends containing 30% and 40% of PPG is around 8%. When 50% of PPG is added in the f-PHB1, the %elongation at break sharply increases to 58.82%.

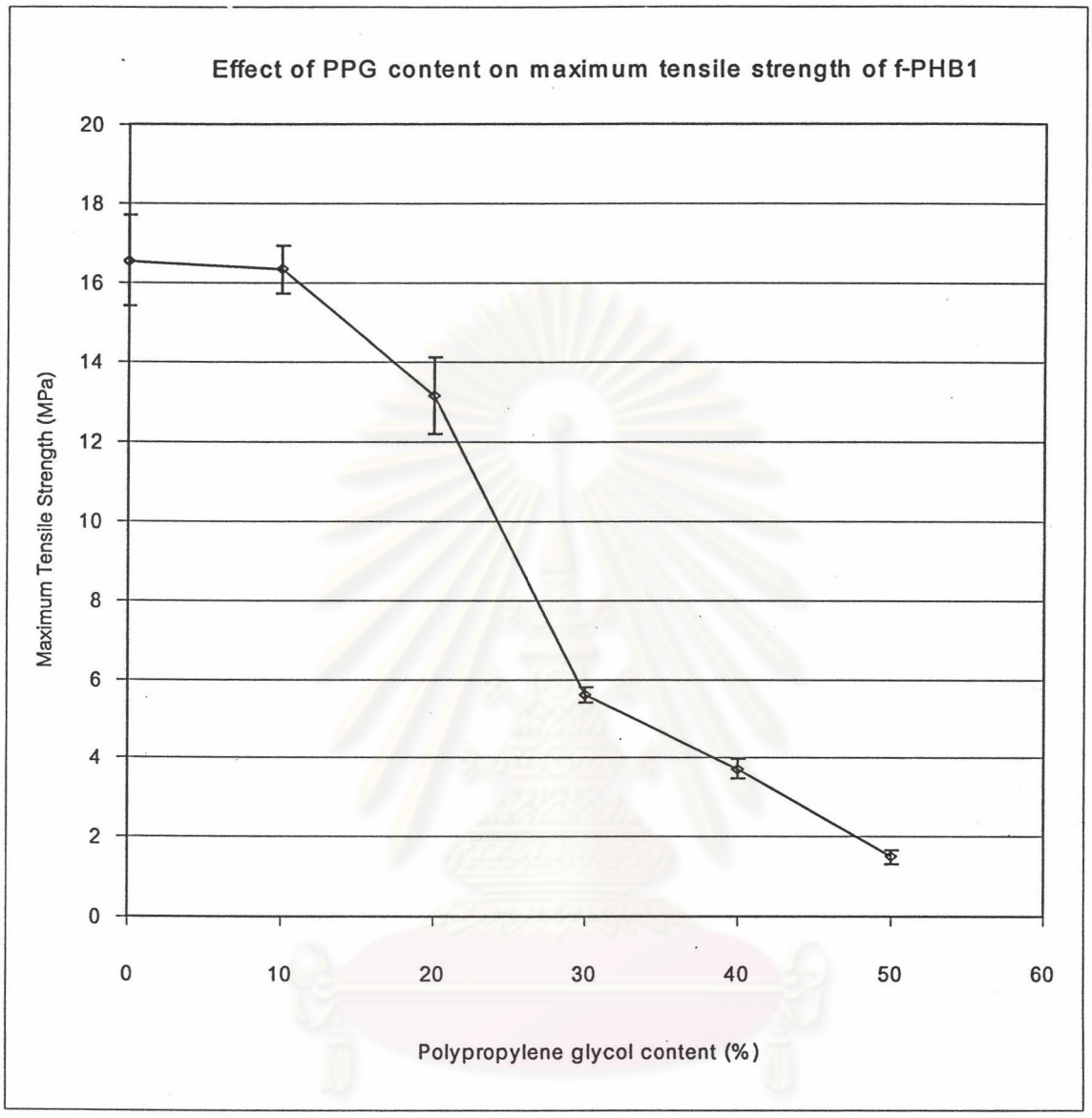

Figure 5.24 Maximum tensile strength of the f-PHB1/PPG blends

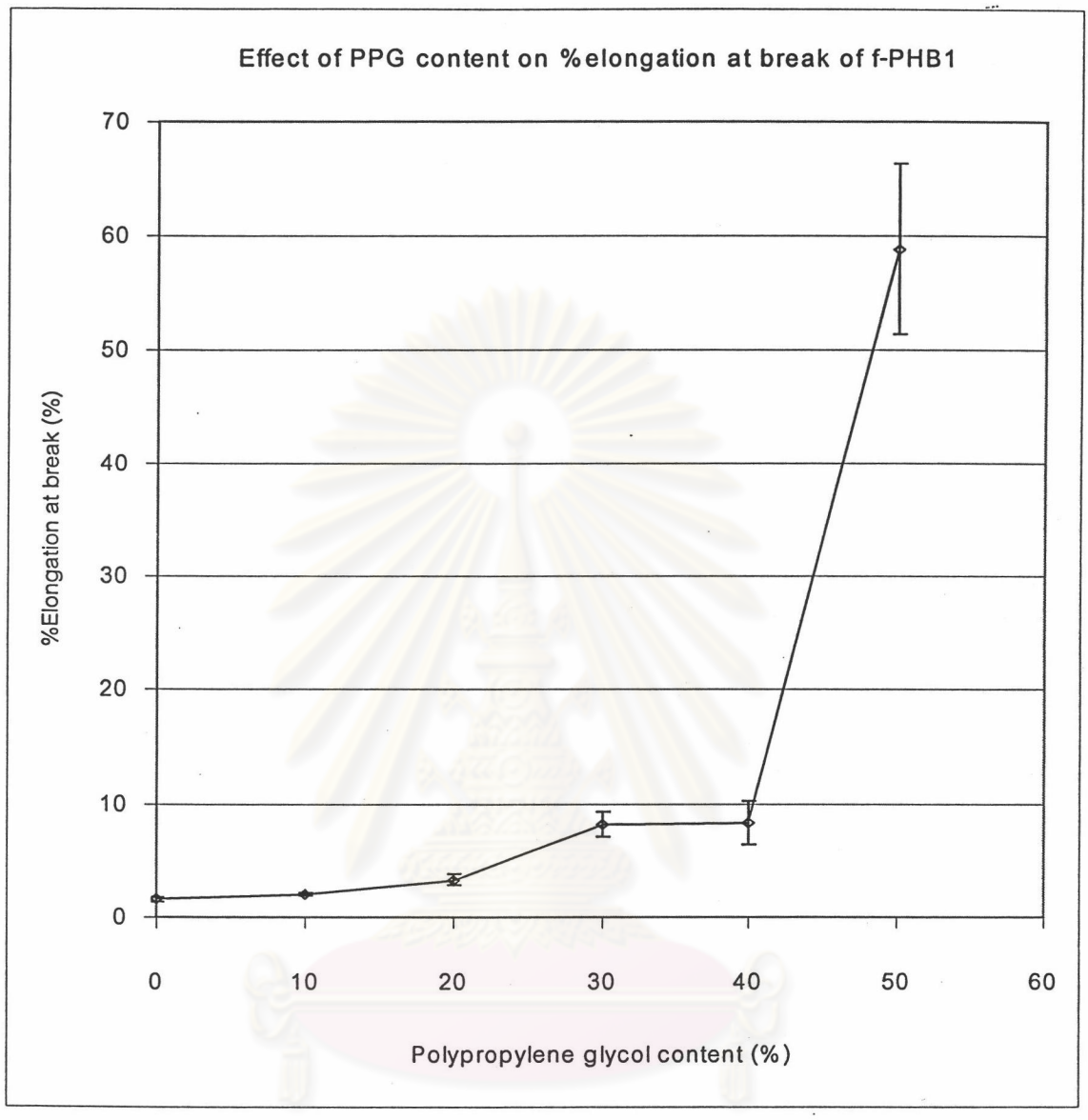

Figure 5.25 %Elongation at break of the f-PHB1/PPG blends

Figure 5.26 shows the modulus of elasticity of the f-PHB1/PPG blends. The modulus of elasticity starts to decrease with an increasing of PPG content more than 10% in the blends. The modulus of elasticity of the blends containing 20%, 30%, 40% and 50% decreases by 28.8%, 73.5%, 73.7% and 90.6%, respectively from that of pure f-PHB1.

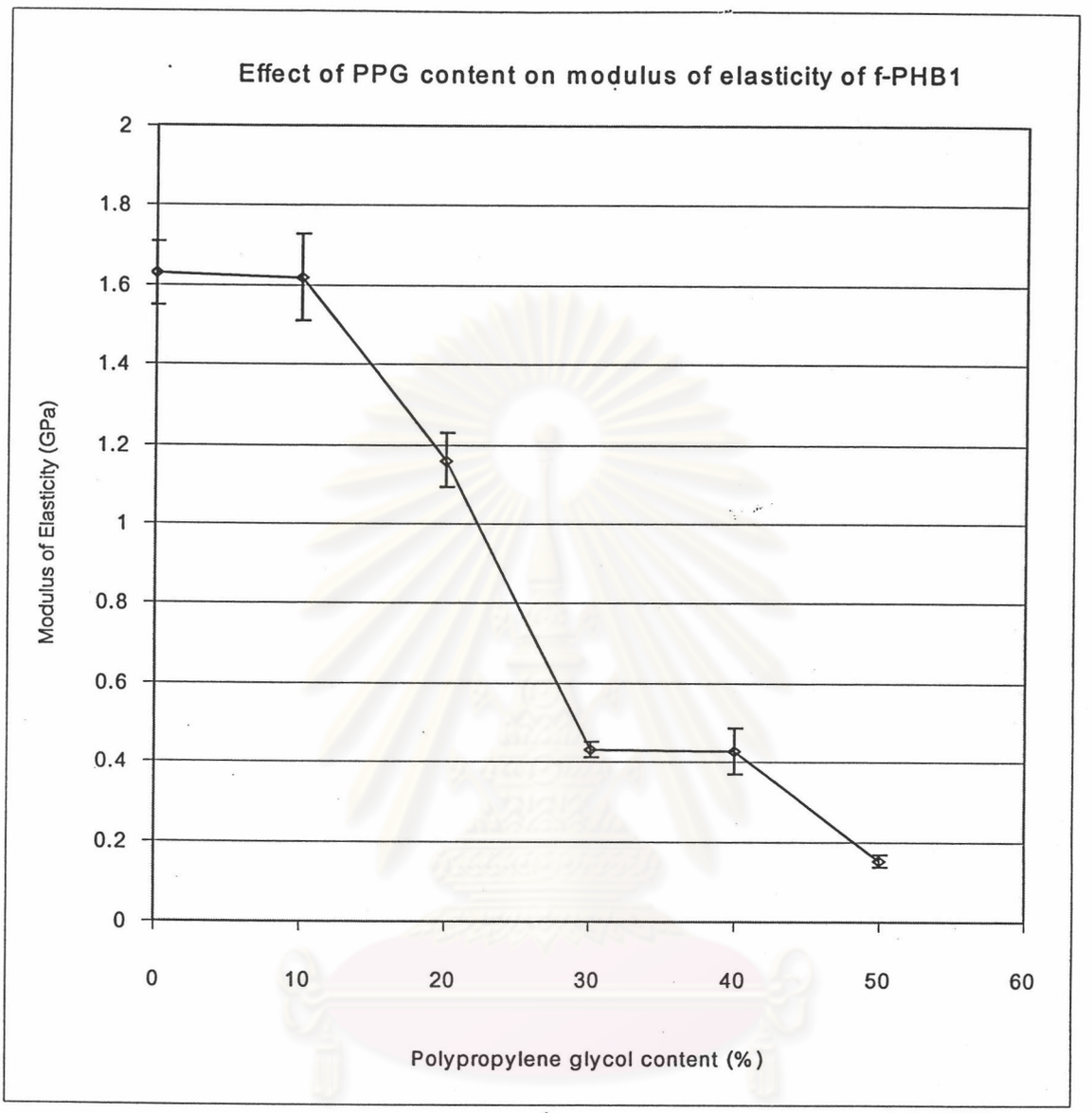

Figure 5.26 Modulus of elasticity of the f-PHB1/PPG blends

Figure 5.27 presents the extension-load curve of the f-PHB1/PPG blends at various PPG contents. The extension-load curve of the f-PHB1/PPG blend is changed from a high modulus of elasticity and low extension pattern for the blends containing 0%-20% of PPG, to a lower modulus of elasticity and higher extension for the blends containing 30% -50% of PPG.

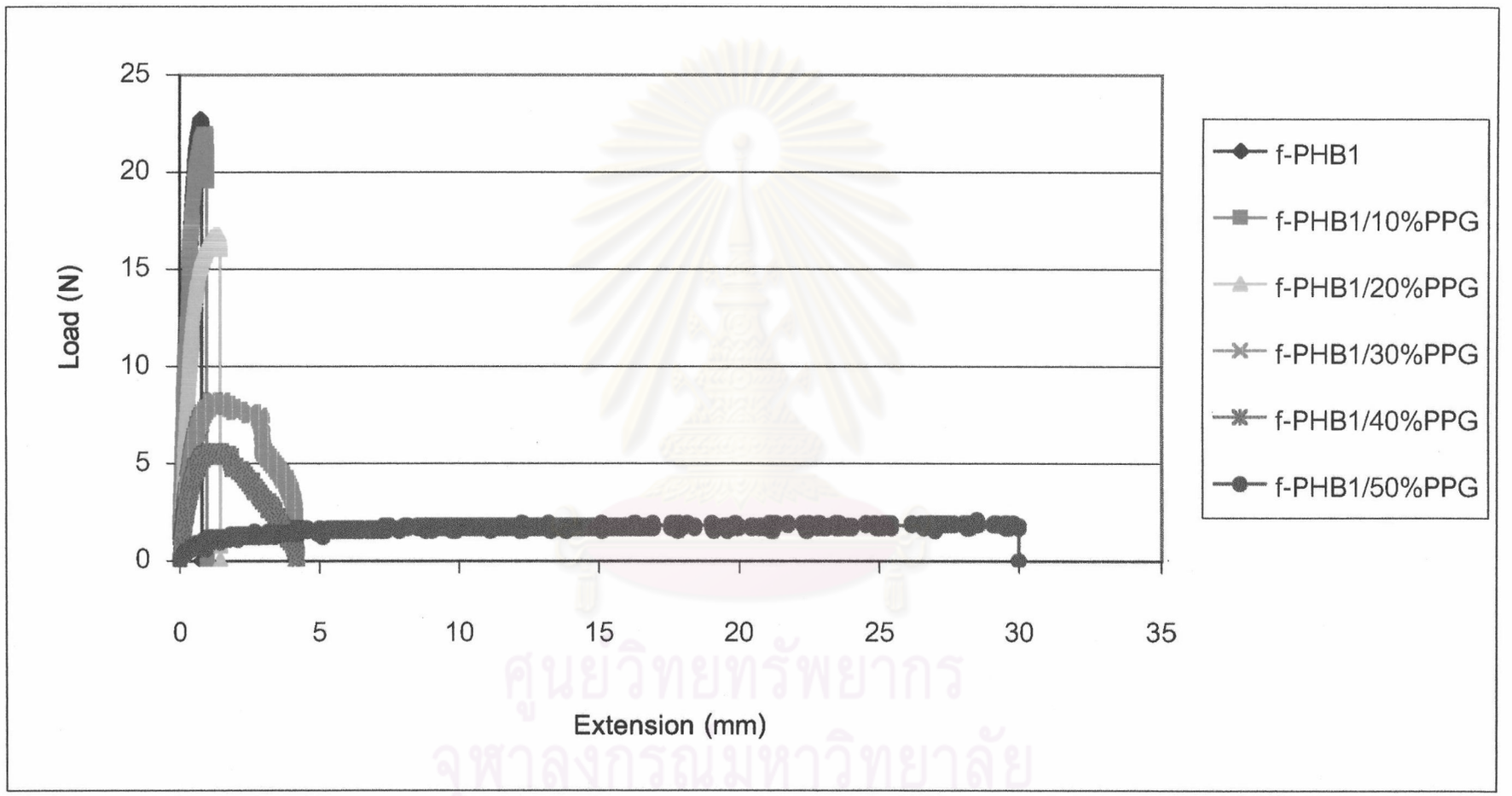

Figure 5.27 Extension-load curve of the f-PHB1/PPG blends at various PPG contents

5.2.1.5 f-PHB2/ESO blends

Table 5.10 presents tensile properties of the f-PHB2/ESO blends. Maximum tensile strength of the f-PHB2/ESO blends is shown in Figure 5.28. The maximum tensile strength of the f-PHB2/ESO blends continuously decreases with an increasing of ESO content. The maximum tensile strength of the blend containing 10%, 20%, 30%, 40% and 50% of ESO is decreased by 17.9%, 26.3%, 32.5%, 56.4% and 62.0%, respectively from that of pure f-PHB2.

Table 5.10 Tensile properties of the f-PHB2/ESO blends

System	Maximum tensile strength (MPa)	%Elongation at break (%)	Modulus of Elasticity (GPa)
Pure f-PHB2	19.92	3.28	1.710
f-PHB2/10%ESO	16.35	3.03	1.671
f-PHB2/20%ESO	14.68	6.77	1.380
f-PHB2/30%ESO	13.44	9.93	1.289
f-PHB2/40%ESO	8.68	7.02	1.293
f-PHB2/50%ESO	7.57	7.18	0.880

Figure 5.29 shows the %elongation at break of the f-PHB2/ESO blends. For the blends containing 0% and 10% of ESO, the %elongation at break varies in a narrow range. The %elongation at break of the blend containing 10% of ESO is about the same is that of pure Biomer. The %elongation at break linearly increases for the blends containing 20% and 30% of ESO and reaches the maximum value at the blend containing 30% of ESO. The %elongation at break of the blends containing 40% and 50% of ESO decreases from that of the blend with 30% of ESO but they are still higher than that of pure Biomer.

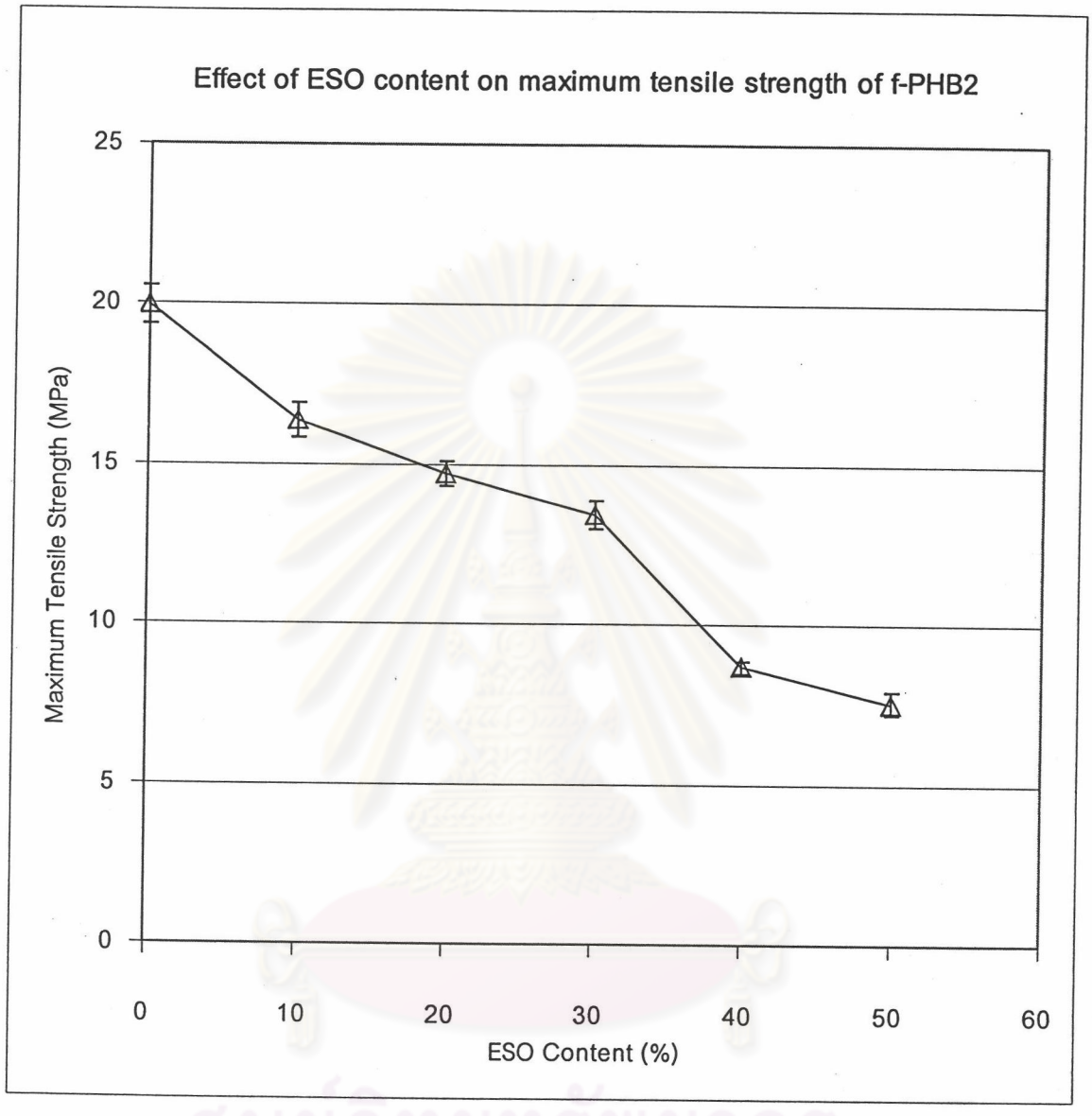

Figure 5.28 Maximum tensile strength of the f-PHB2/ESO blends.

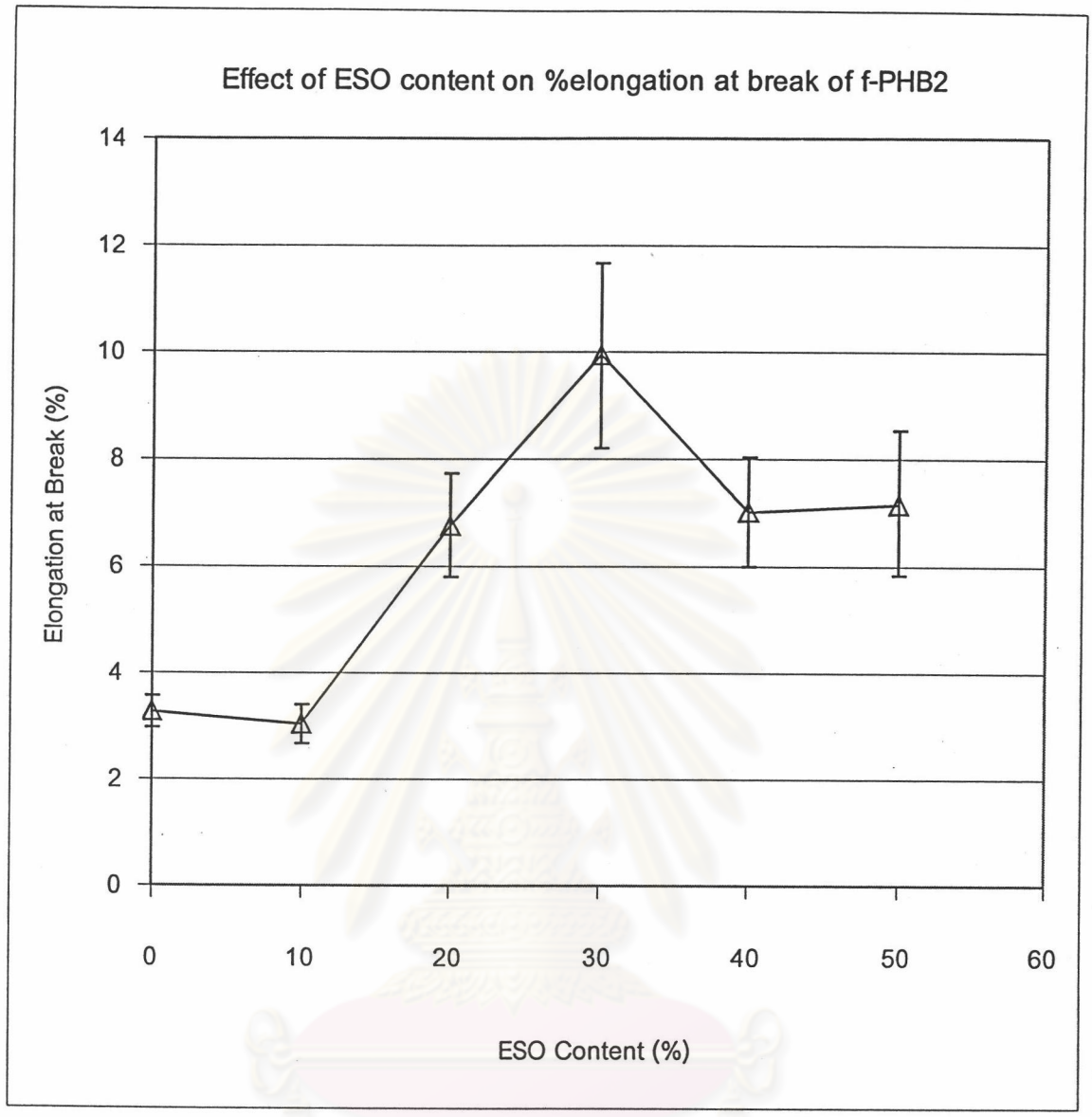

Figure 5.29 %Elongation at break if the f-PHB2/ESO blends

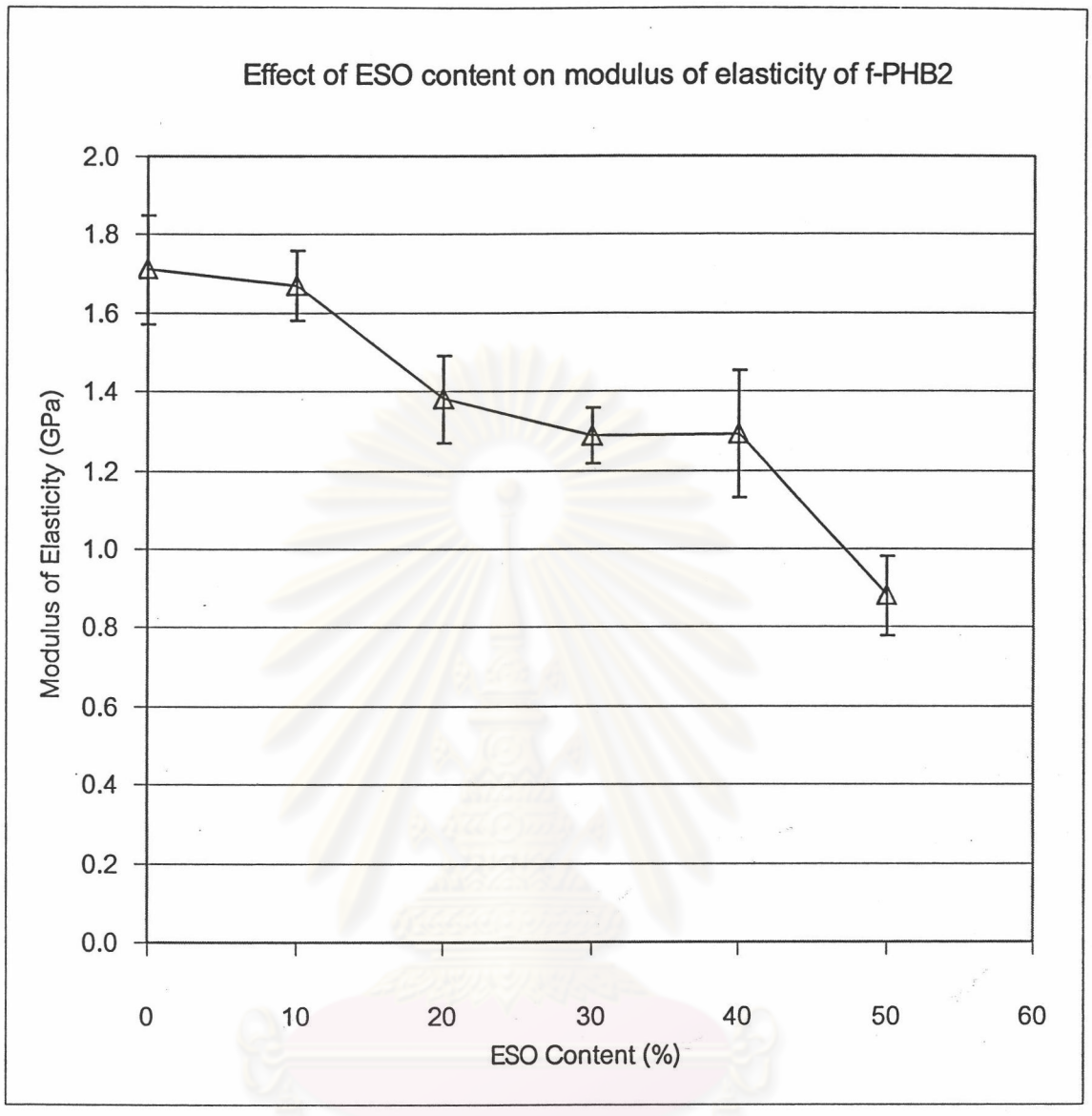

Figure 5.30 Modulus of elasticity of the f-PHB2/ESO blends

Figure 5.30 shows the modulus of elasticity of the f-PHB2/ESO blends. The modulus of elasticity of the f-PHB2/ESO blends decreases with an increasing of the ESO content. The modulus of elasticity of the blends containing 10%, 20%, 30%, 40% and 50% is decreased by 2.28%, 19.3%, 24.6%, 24.4% and 48.5%, respectively.

5.2.2 Effect of modifying agent types on the mechanical properties of Biomer

Figure 5.31 presents the effects of modifying agents on the maximum tensile strength of Biomer/modifying agent blends. It can be noticed that the maximum tensile strength of all Biomer blends continuously decreases with an increasing of the modifying agent content. This result is consistent with that of Bibers *et al.* [2001] and Bibers *et al.* [1999]. Bibers *et al.* [1999] studied the effect of plasticizers such as dioctyl sebacate, dibutyl sebacate, polyethylene glycol, Laprol 503, Laprol 5003 on the mechanical properties of PHB. The results showed that the maximum tensile strength values of all PHB/plasticizers systems were gradually decreased with an increasing of plasticizer content.

Figure 5.32 presents the effects of modifying agents on the %elongation at break of Biomer/modifying agent blends. Each modifying agent has similar influence on the %elongation at break of Biomer when 10%-30% of modifying agent is added. The %elongation at break Biomer blends with 10% of modifying agent does not much differ from that of the pure Biomer. At 20% of each modifying agent, the %elongation at break of the blends starts to increase from that of pure Biomer. At this composition, ESO seems to have strongest effect on the %elongation at break, comparing to PPG and PG. At 30% of each modifying agent, the %elongation at break of the blends continuously increases from that of the blends with 20% of modifying agent. At higher composition than 30% of modifying agent, the effects of each modifying agent on the %elongation at break tends to be changed. The %elongation at break of Biomer/ESO blends with 40% and 50% of ESO decreases gradually while the %elongation at break of Biomer/PPG and Biomer/PG blends still increases as an increasing of modifying agent composition to 40%. Increasing modifying agent composition up to 50% suddenly reduced the %elongation of Biomer/PPG blends. On the other words, the maximum %elongation at break of Biomer/PPG, Biomer/PG and Biomer/ESO blends is occurred in the blend containing 50% of PPG, 40% of PG and 30% of ESO, respectively. Generally, one can see that the change in the %elongation at break depends on the composition of the modifying agent in the blends. The most effective composition that can improve the

%elongation at break of Biomer is different for each modifying agent. This might be due to the uniform dispersion of the modifying agents in the blends and maybe the effects of the modifying agent in the crystal characteristics of Biomer.

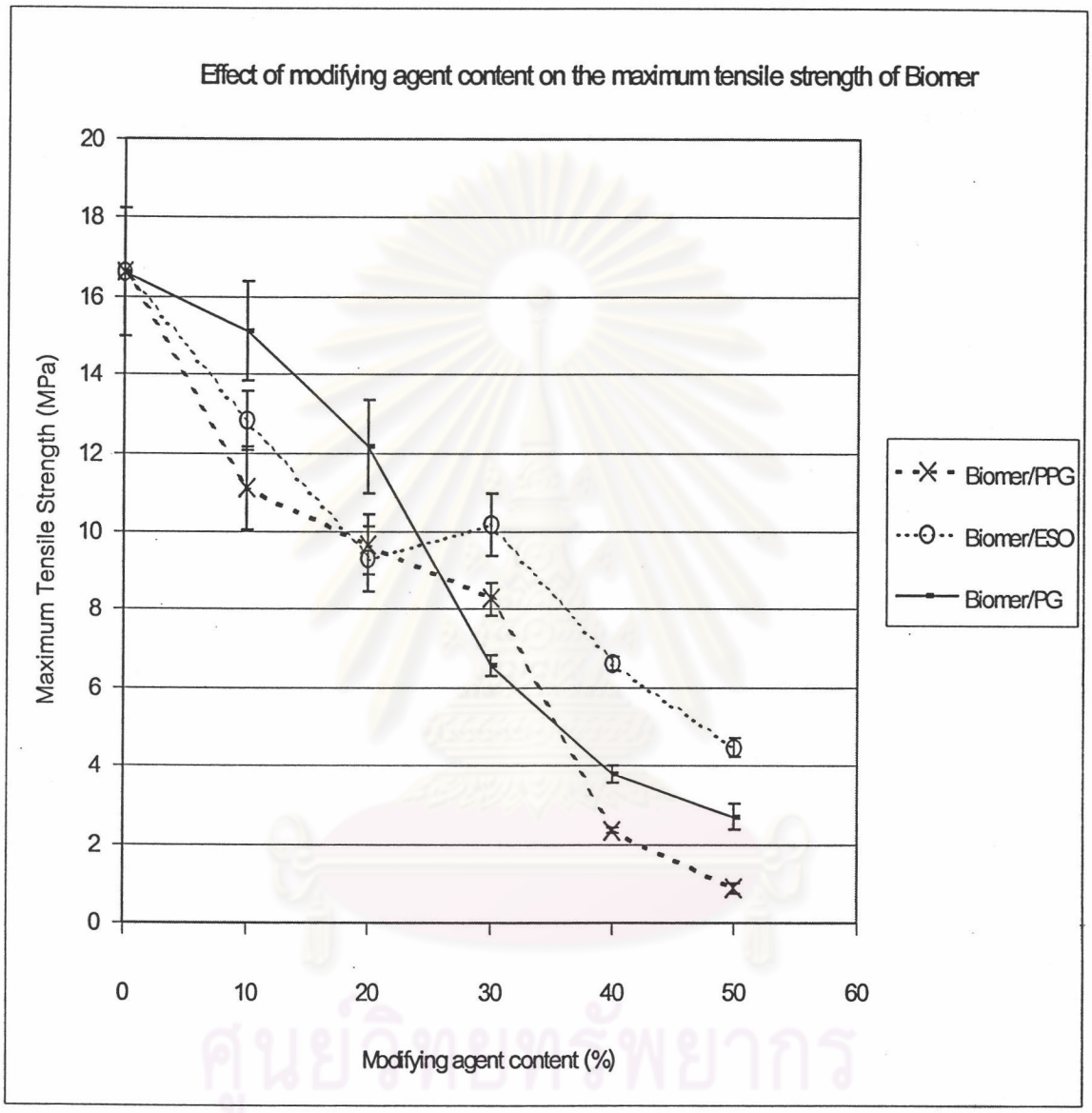

Figure 5.31 Effects of modifying agent on the maximum tensile strength of Biomer/modifying agent blends

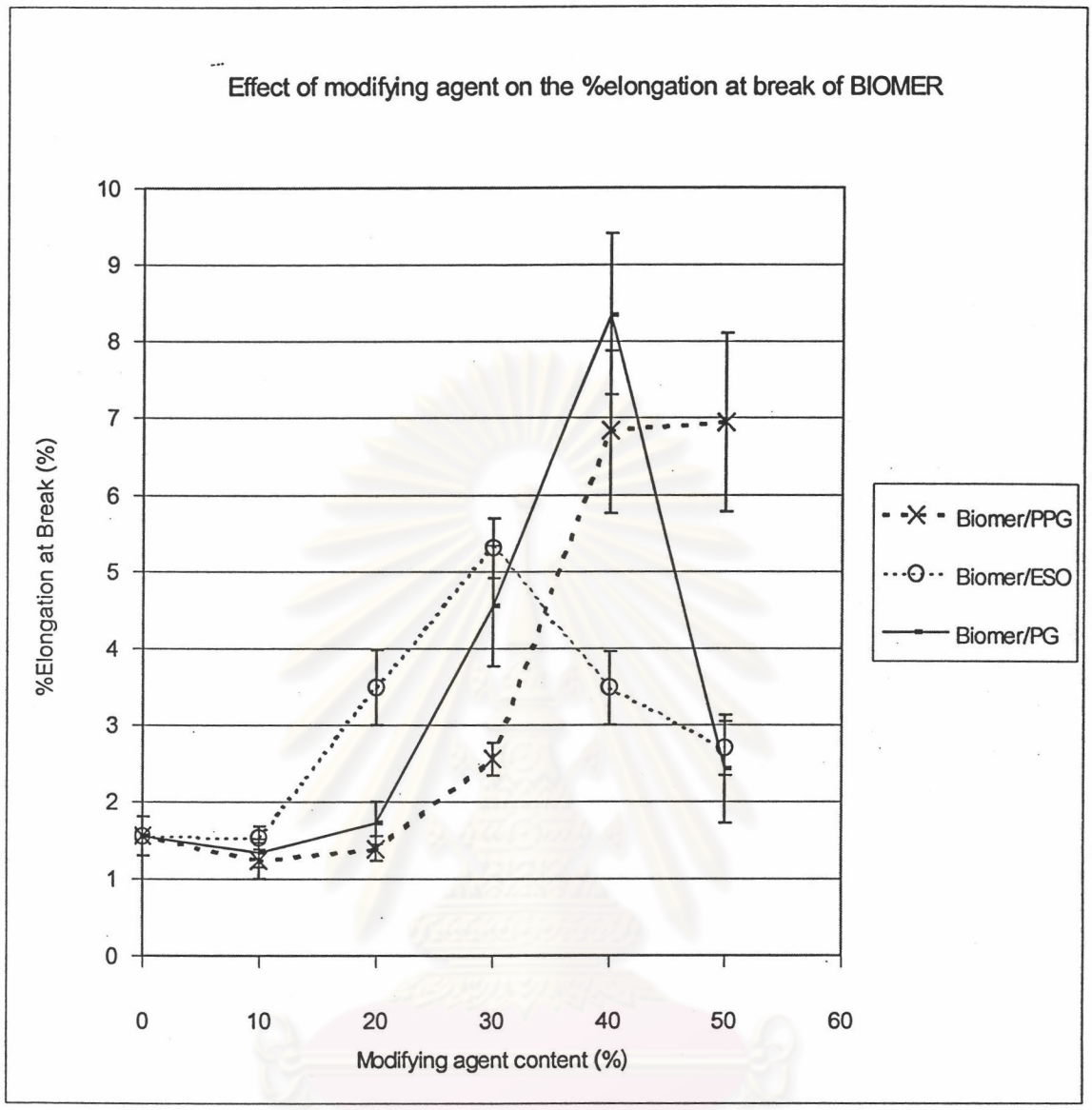

Figure 5.32 Effects of modifying agent on the %elongation at break of Biomer/modifying agent blends

Figure 5.33 presents the effects of the modifying agents on the modulus of elasticity of Biomer. It can be noticed that the modulus of elasticity of the Biomer/modifying agent decreases with an increasing of the modifying agent content. It implies that Biomer is changed from a hard to soft material when the content of modifying agent is increased.

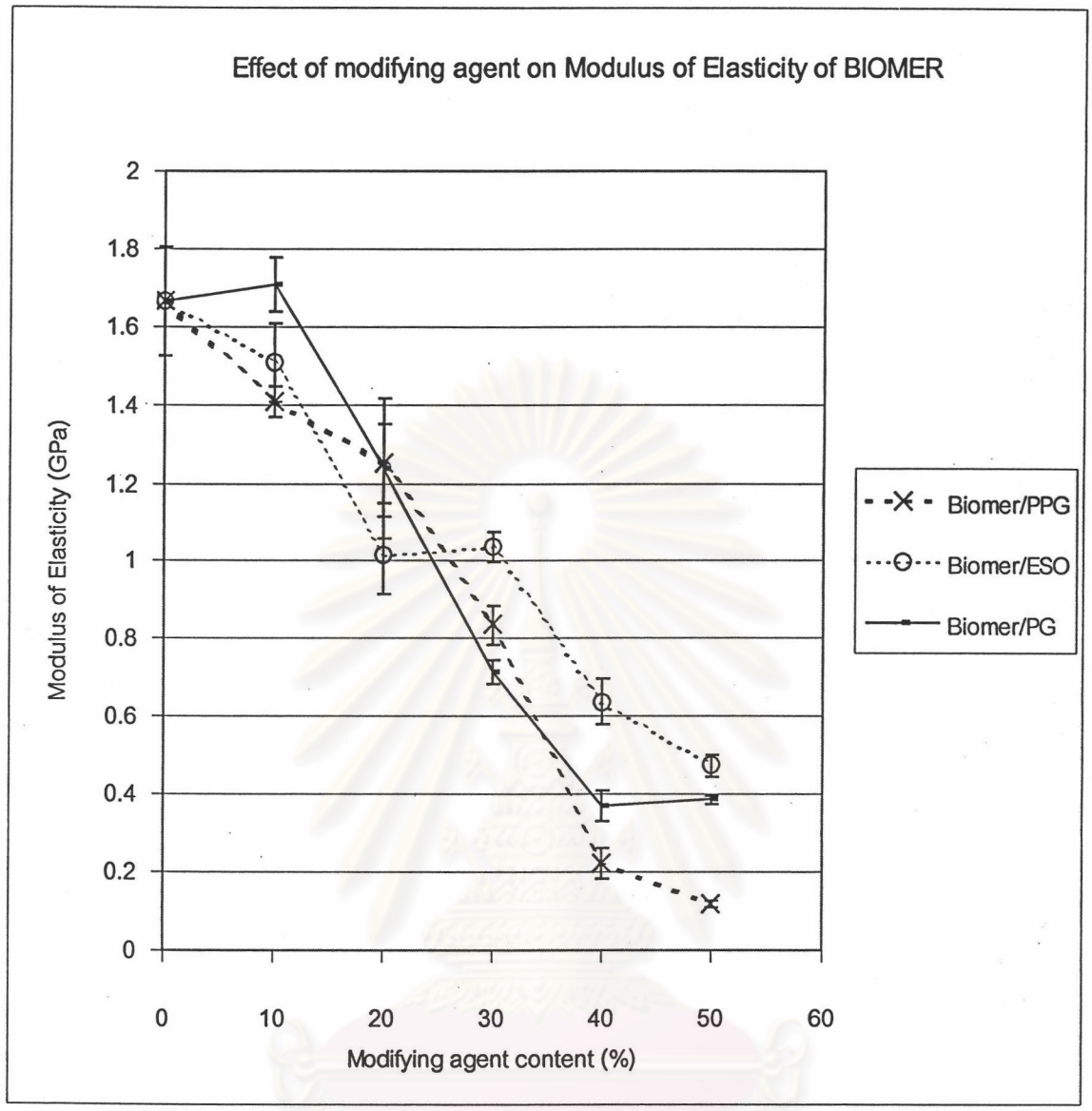

Figure 5.33 Effects of modifying agent on the modulus of elasticity of Biomer/modifying agent blends

Considering the area under extension-load curve in Figure 5.15, 5.19 and 5.23, it is shown that the area under extension-load curve of Biomer/ESO blends is higher than that of Biomer/PG and Biomer/PPG blend at every content of modifying agent studied except the blend containing 40% of ESO. This implies that the Biomer/ESO blends seem to be tougher than the Biomer/PG and Biomer/PPG blends.

5.2.3 Effect of modifying agent types on the mechanical properties of f-PHB

The effects of the two modifying agents, PPG and ESO, on the maximum tensile strength of f-PHB are presented in Figure 5.34. It can be noticed that the maximum tensile strength of f-PHB/modifying agent continuously decreases with an increasing of the content of modifying agent. This result is similar to that of the Biomer/modifying agent blends and PHB/plasticizer blends which were studied by Bibers *et al.* [1999]. From Figure 5.34, it is also shown that the maximum tensile strength of f-PHB2/ESO blends is higher than that of f-PHB1/PPG at every content of modifying agent.

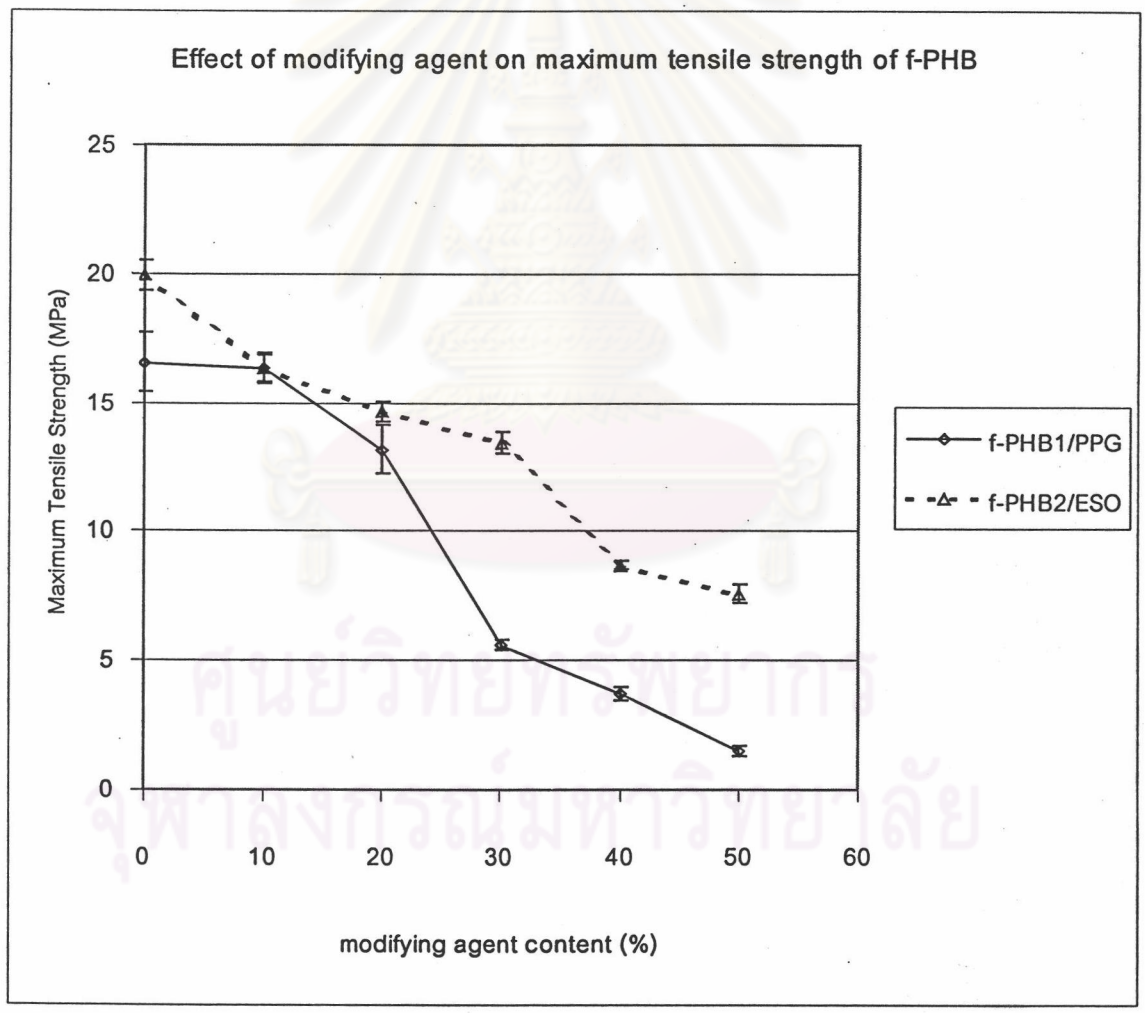

Figure 5.34 Effects of two modifying agents on the maximum tensile strength of f-PHB

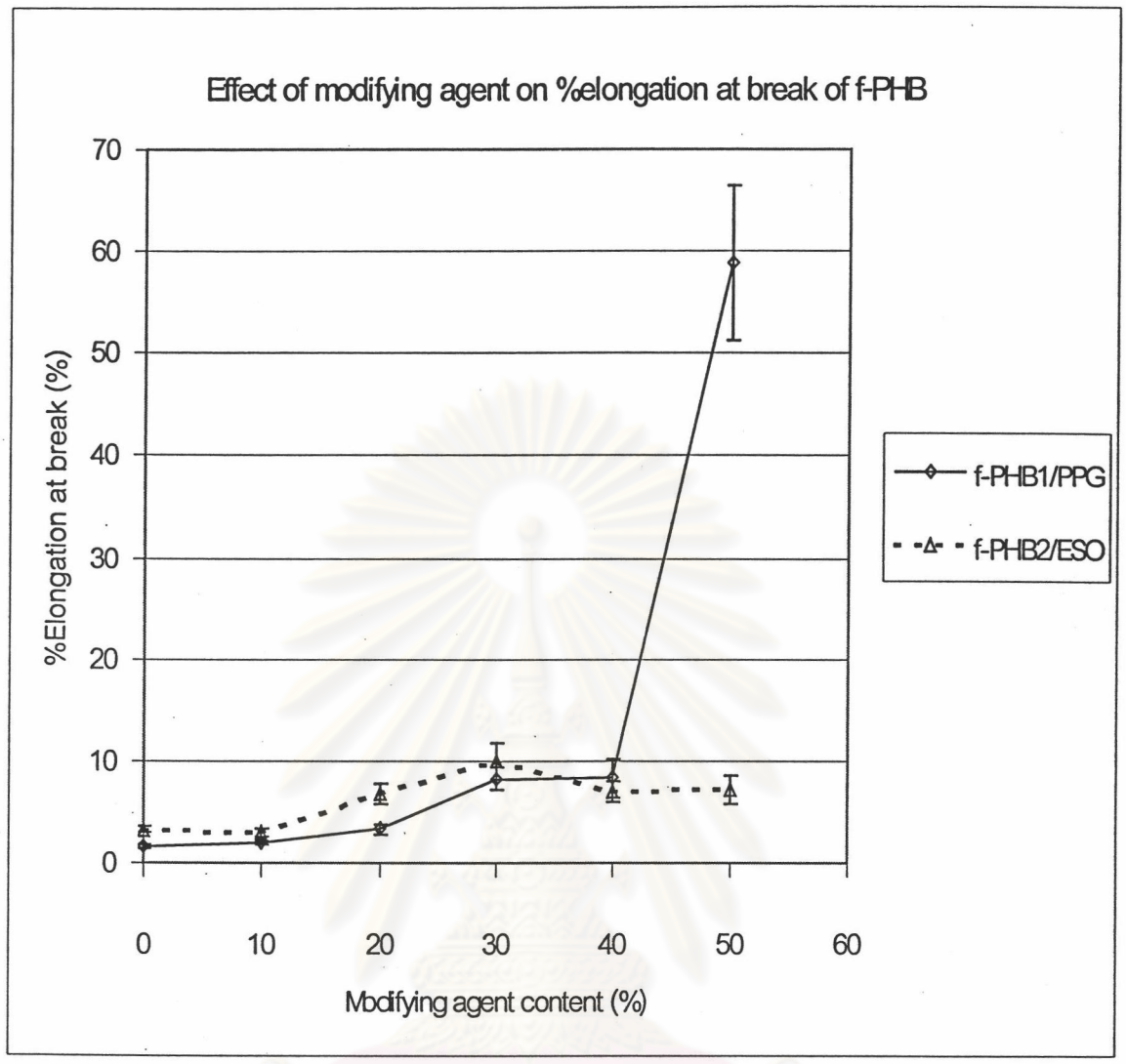

Figure 5.35 Effects of two modifying agents on the %elongation at break of f-PHB

Figure 5.35 presents the effects of two modifying agents on the %elongation at break of f-PHB/modifying agent blends. Each modifying agent has different effects on the %elongation at break of f-PHB. The %elongation at break of f-PHB2 is improved by adding ESO but in a small range of less than 10%. The f-PHB1/PPG blends give a good result in the elongation improvement. The %elongation at break of the f-PHB1/PPG blends varies around 0% to 10% for the blend containing 0% to 40% of PPG but it is greatly improved to 58.82% for the blend containing 50% of PPG.

Figure 5.36 presents the effects of two modifying agent on the modulus of elasticity of f-PHB. It can be seen that the modifying agents have a similar effect on the modulus of elasticity of f-PHB. Both f-PHB1/PPG and f-PHB2/ESO blends exhibit a continuously decrease of the modulus of elasticity when the content of the modifying agent is increased. The decreasing rate of the modulus of elasticity of f-PHB1/PPG blends is higher than that of f-PHB2/ESO blends. The modulus of elasticity of f-PHB2/ESO blend is higher than that of f-PHB1/PPG blends at every content of the modifying agent. This result shows that, at 10%-50% of the modifying agent, the f-PHB2/ESO blends are harder or more rigid than the f-PHB1/PPG blends.

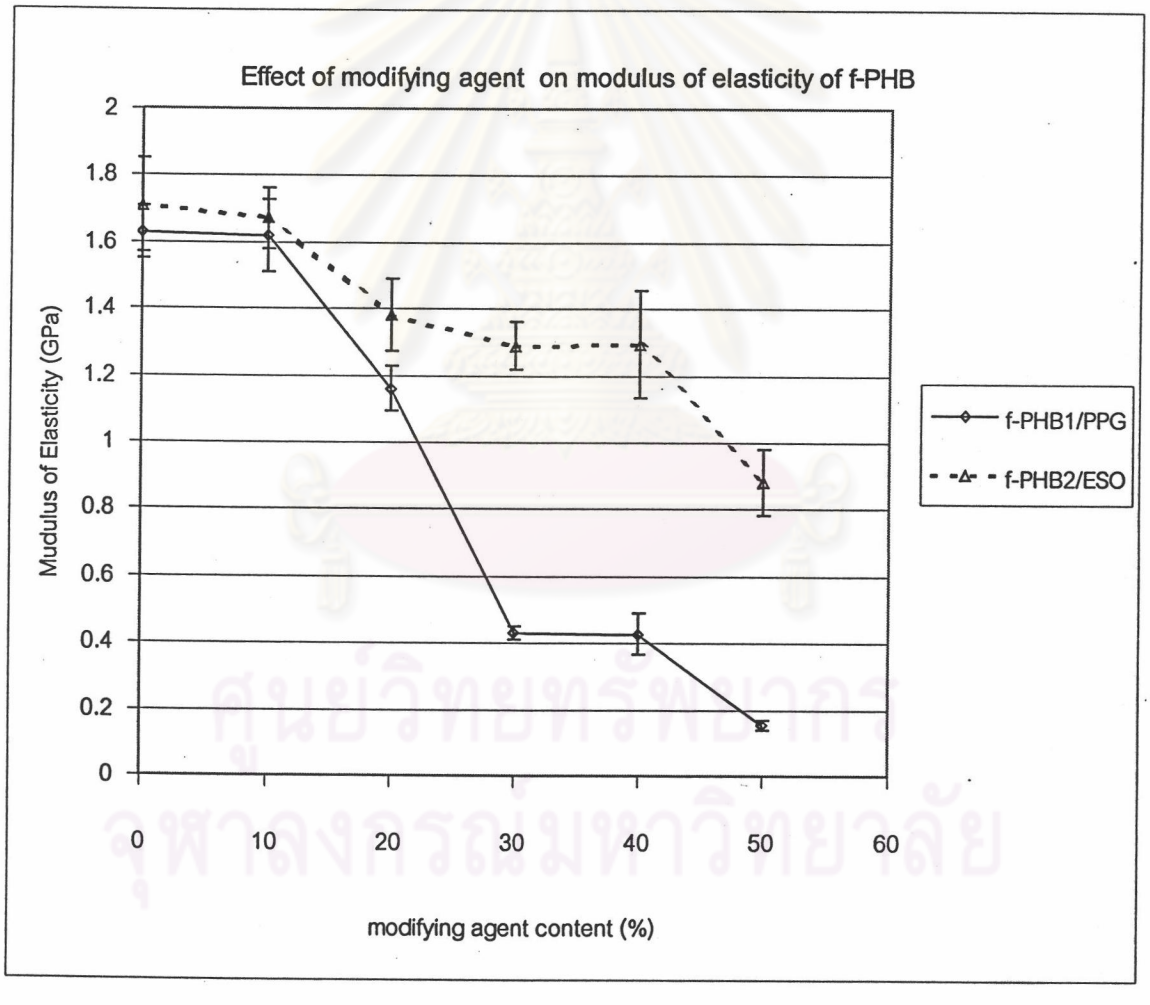

Figure 5.36 Effects of the modifying agents on the modulus of elasticity of f-PHB

5.2.4 Effects of PHB source on the mechanical properties of PHB/ESO blends

Figure 5.37 presents the effects of the PHB sources, Biomer and f-PHB2, on the maximum tensile strength of the PHB/ESO blends. At every blend composition, the maximum tensile strength of f-PHB2/ESO blends is higher than that of Biomer/ESO blends. This means that the f-PHB2/ESO blends tend to sustain more loads than the Biomer/ESO blends.

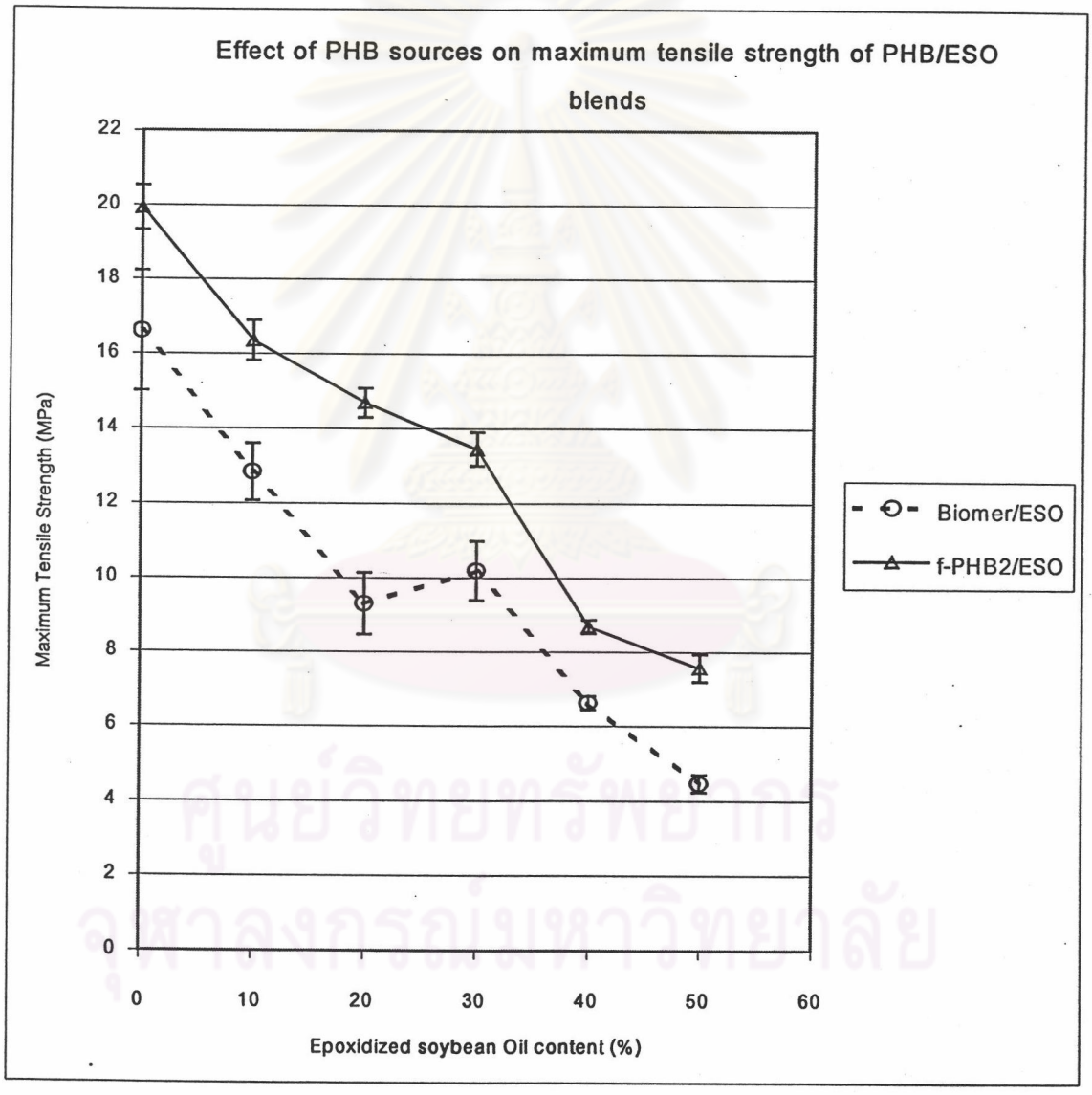

Figure 5.37 Effect of PHB sources on the maximum tensile strength of the PHB/ESO blends

Figure 5.38 presents the effects of the PHB sources on the %elongation at break of the PHB/ESO blends. The %elongation at break of both blends is changed in the same manner. The %elongation at break of both blends containing 0% and 10% of ESO varies in a narrow range. The %elongation at break of both blends increases linearly for the blend containing 10%-30% of ESO and reaches the maximum values for the blend containing 30% of ESO. At higher ESO composition (40%-50%), the %elongation at break of both blends decreases. From Figure 5.38, it can be seen that the %elongation at break of the f-PHB2/ESO blends is higher than that of Biomer/ESO blend in all blends compositions.

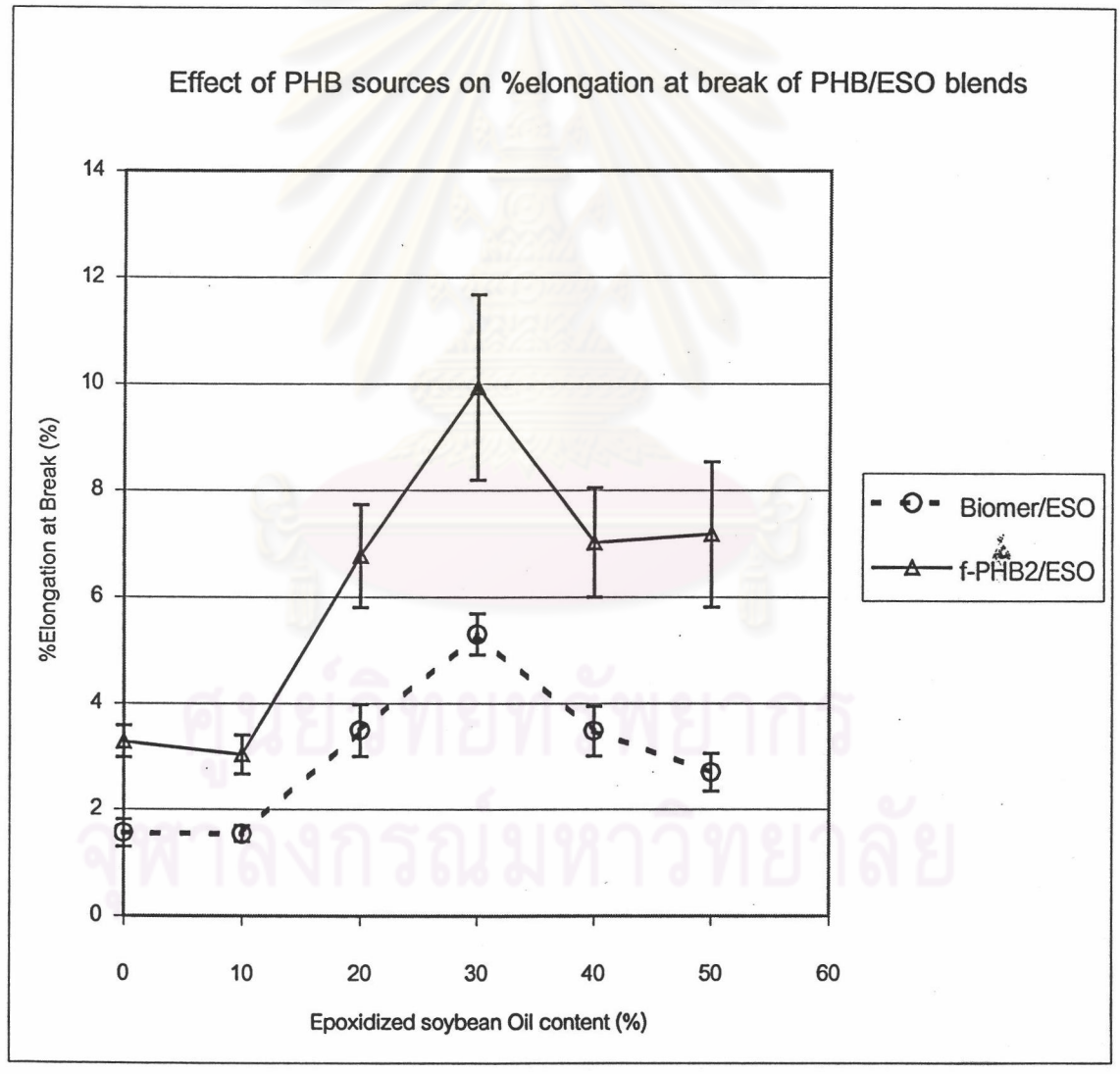

Figure 5.38 Effects of PHB sources on the %elongation at break of the PHB/ESO blends

Figure 5.39 presents the effects of PHB sources on the modulus of elasticity of the PHB/ESO blends. At all blend compositions, the modulus of elasticity of the f-PHB2/ESO blends is higher than that of Biomer/ESO blends. This result shows that the f-PHB2/ESO blends have more rigidity than the Biomer/ESO blends.

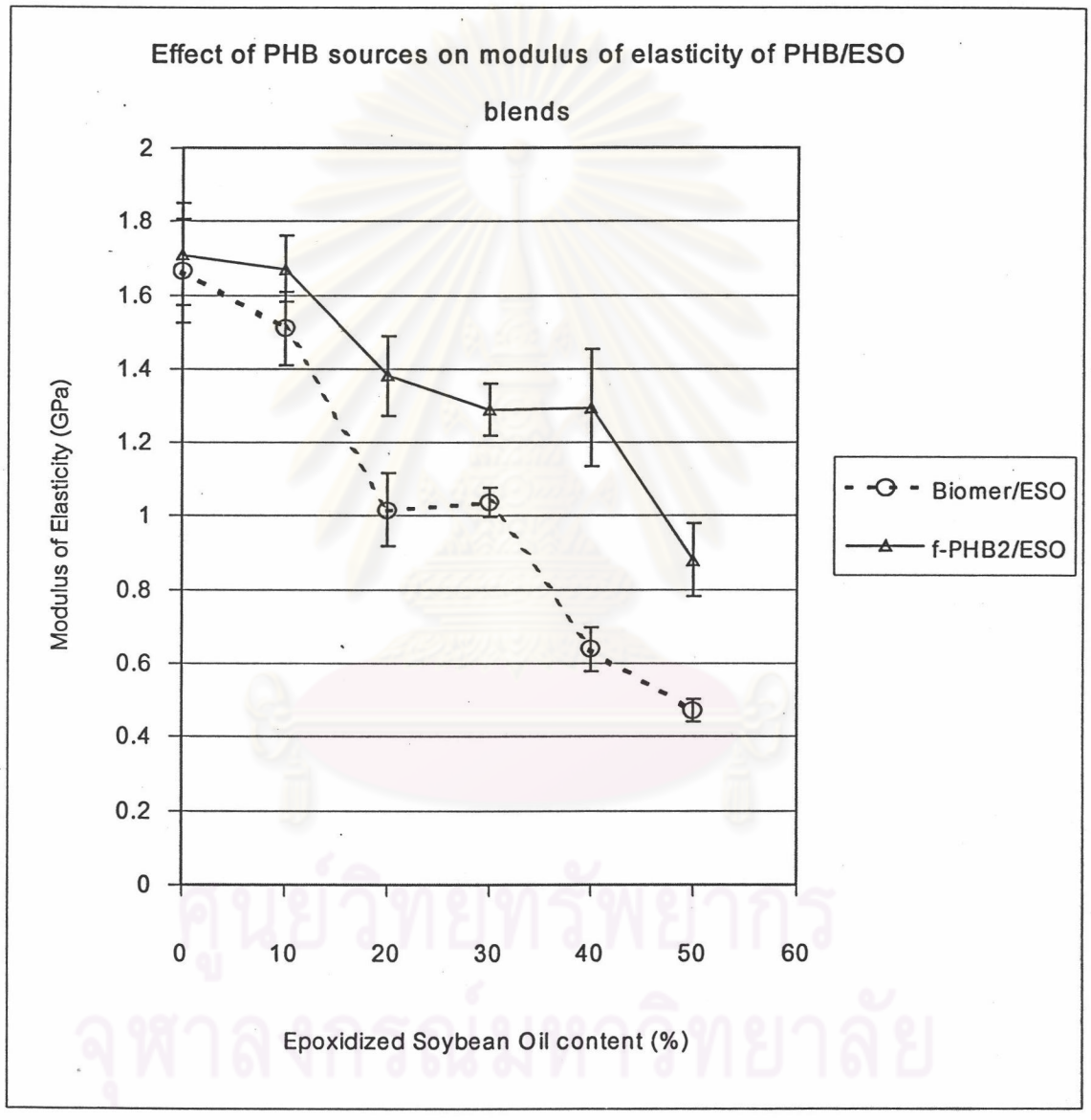

Figure 5.39 Effects of PHB sources on the %elongation at break of the PHB/ESO blend

Considering the graph of the maximum tensile strength, the %elongation at break and the modulus of elasticity of Biomer/ESO and f-PHB2/ESO blends in Figure 5.37 to 5.39, if the results of the mechanical properties of Biomer/ESO blends is shifted up to overlap with those of f-PHB2/ESO blends, it can be seen that the changes in the tensile properties of both Biomer and f-PHB2 with the composition of ESO are very similar. This implies that ESO has a similar effect on the tensile properties of two sources of PHB, Biomer and f-PHB2. The differences in the tensile properties can only be noticed in the pure Biomer and f-PHB2, i.e. the tensile properties of pure f-PHB2 are slightly higher than those of pure Biomer. This is attributed to the difference in the characteristics and the properties of PHB.

5.2.5 Effects of PHB sources on the mechanical properties of PHB/PPG blends

Considering the mechanical properties of pure Biomer and pure f-PHB1 in the Figure 5.40, 5.41 and 5.42, It can be noticed that the mechanical properties are very similar. The thermal properties, i.e., glass transition temperature, melting temperature and degree of crystallinity, of Biomer and f-PHB1 shown in Section 5.1.2 are also very similar. The similarity in the mechanical properties of pure Biomer and pure f-PHB1 can be supported by the similarity in the thermal properties of Biomer and f-PHB1.

Figure 5.40 presents the effects of PHB sources on the maximum tensile strength of the PHB/PPG blends. Both blends exhibit a decrease in the maximum tensile strength when the content of PPG is increased. It is also noticed that the trend of the changes in maximum tensile strength is not much different.

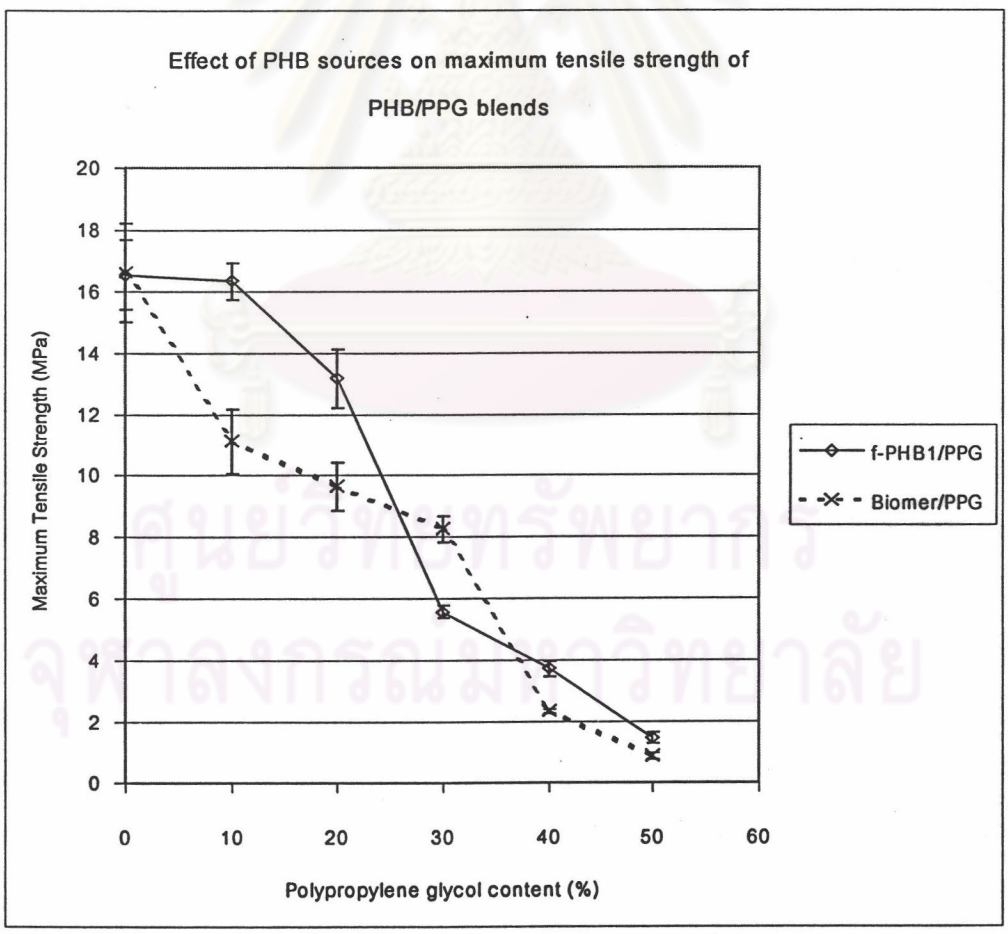

Figure 5.40 Effect of PHB sources on the maximum tensile strength of PHB/PPG blends

Figure 5.40 presents the effects of PHB sources on the %elongation at break of the PHB/PPG blends. It is observed that at the range of 10% to40% of PPG composition, the %elongation at break of f-PHB1/PPG blends is slightly higher than that of the Biomer/PPG blends. A significant difference in the %elongation at break is observed in the blend containing 50% of PPG. For the blend with 50% of PPG, the %elongation at break of f-PHB/PPG increases up to 58.82% while that of Biomer/PPG blend does not change. On the other words, 50% of PPG has a much stronger effect on improvement of %elongation at break of f-PHB1 than Biomer. This could be due to a difference in the PHB sources or characteristics of PHB, PHB purification process and morphology of Biomer/PPG and f-PHB1/PPG blend. Weight average molecular weight of PHB is one of the important characteristics that can affect its property. The molecular weight of f-PHB1 and Biomer is about 800,000 and 327,000 g/mol, respectively. This is consistent with the work of Bibers *et al.* [1999]. Bibers *et al.* [1999] studied the effect of degradable plasticizers, i.e. dioctyl sebacate (DOS), dibutyl sebacate (DBS), polyethylene glycol (PEG), Laprol 503 (L503), Laprol 5003 (L5003), on the mechanical properties of PHB which has the average molecular weight around 1,900,000 g/mol. They found that, at 0%-10%, the % elongation at break of the PHB/plasticizer blends was not much different from that of pure PHB. At 20% of each plasticizer, the %elongation at break of the blends starts to increase from that of pure PHB. At this composition, L503 seems to have strongest effect on the %elongation at break comparing to DOS, DBS, PEG and L5003. At 30% of each plasticizer, the %elongation at break of the blends continuously increases from that of the blends with 20% of plasticizers. At higher composition than 30% of plasticizer, the %elongation at break of the blends reaches the maximum value. PHB/L503 blends exhibit the most value of %elongation at break around 300%, comparing to other blends. The manner of the change of %elongation at break of the f-PHB1/PPG blends reported in this work is similar to that of PHB/plasticizer blends reported by Bibers *et al.* [1999] but the content of the plasticizers that can significantly improve the %elongation at break of PHB is different to the content of PPG that effectively improves the %elongation at break of f-PHB1.

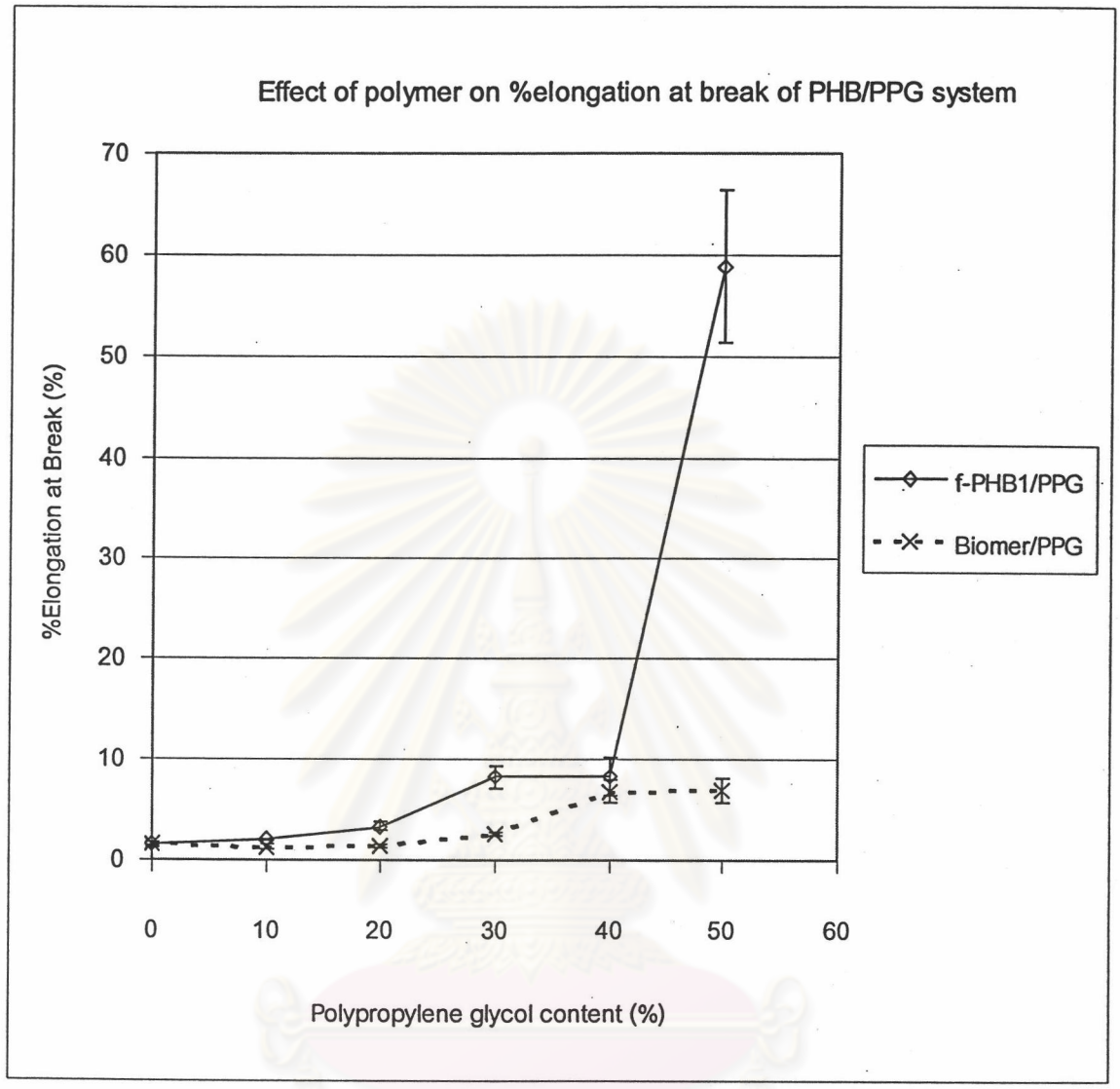

Figure 5.41 Effect of PHB sources on the %elongation at break of PHB/PPG blends

Figure 5.42 presents the effects of PHB sources on the modulus of elasticity of the PHB/PPG blends. The modulus of elasticity of both blends decreases in a similar manner with an increasing in PPG content. The modulus of elasticity of both blends is not much different.

From Figure 5.15 and 5.27, the area under extension-load curve of the Biomer/PPG and f-PHB1/PPG blends is considered. It is shown that the area under the extension-load curve of f-PHB1/PPG blends is higher than that of the Biomer/PPG blends at ever blend composition. It can imply that the f-PHB1/PPG blends are tougher than the Biomer/PPG blends. The rigidity of both blends which can be implied by the modulus of elasticity is not different.

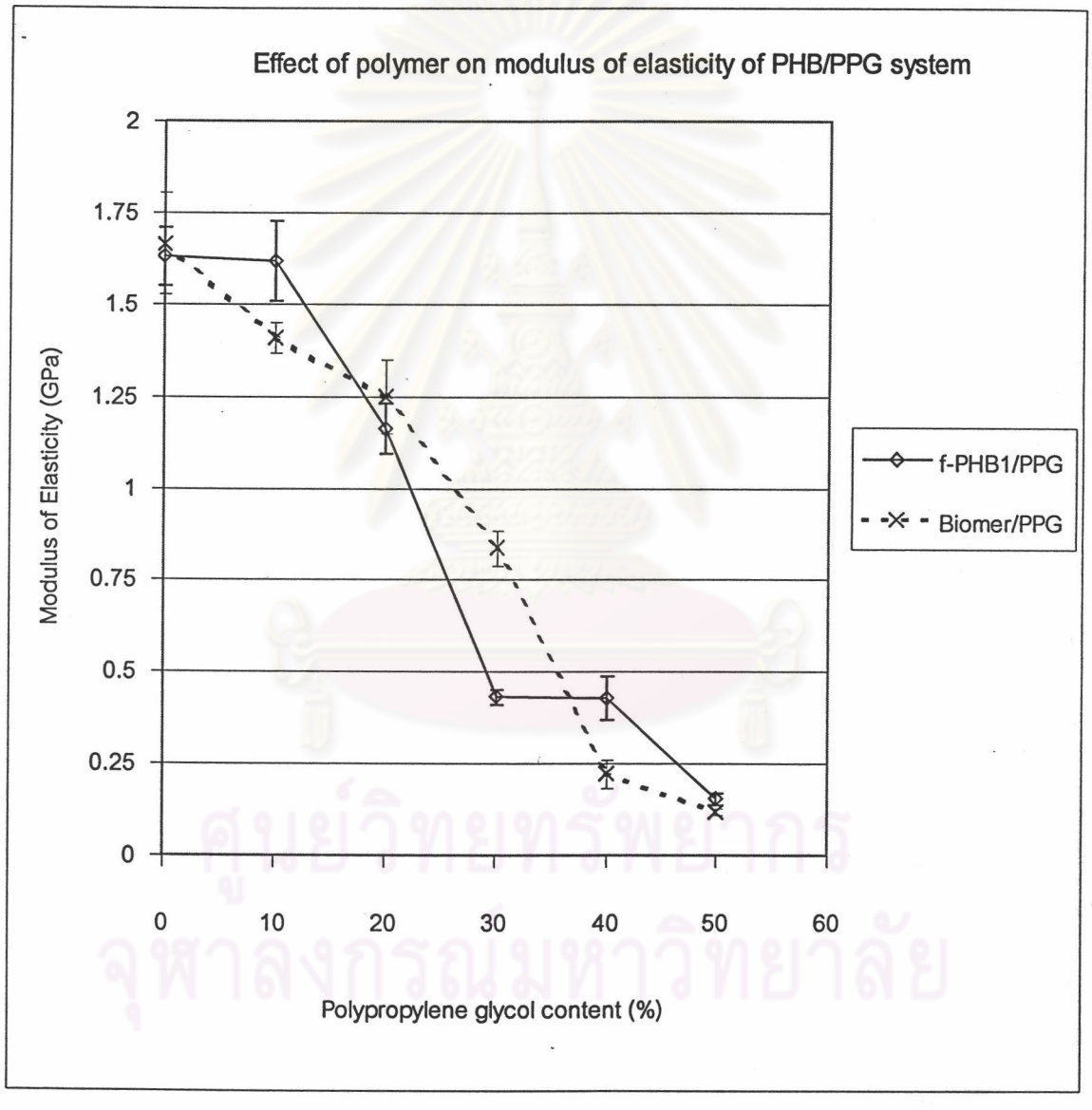

Figure 5.42 Effect of PHB sources on the modulus of elasticity of PHB/PPG blends

From the results of the biodegradable modifying agents such as Polypropylene glycol, propylene glycol and epoxidized soybean oil on the mechanical properties of two samples of PHB; Biomer (which is purchased from Biomer Company) and f-PHB (self-fermented and purified in this work), it can be summarized that in all blends the maximum tensile strength and modulus of elasticity gradually decreases when the content of the modifying agent is increased. For the same type of PHB, each modifying agent has a different effect on the %elongation at break of the blends. The %elongation at break of the each Biomer/modifying agent blend reaches the maximum value at the different content of the modifying agent. At 10-50% of modifying agent, the %elongation at break of the Biomer/modifying agent blends is improved but not exceed than 9%. This indicates that the PHB is changed from a hard and brittle material to be softer and more ductile. The %elongation at break is most improved in the f-PHB1/50%PPG blend up to 58.82%. This maybe due to many reasons such as the good dispersion of PPG with f-PHB1 and the fundamental characteristics of PHB caused from different synthesis methods.

5.3 Morphology study

In this section, the morphology of the Biomer/PPG and f-PHB1/PPG blends, containing 0%, 30% and 50% of PPG, after tensile testing is considered. The discussion is divided as follows:

5.3.1 Morphology of pure Biomer and pure f-PHB1

The morphology of the surface of the pure Biomer and pure f-PHB1 by SEM is presented in Figure 5.43 (a) and (b), respectively. It is shown that the surface of pure Biomer and pure f-PHB1 is solid. The surface of pure Biomer is slightly rougher than that of f-PHB1. The rough surface may be due to the powder of Biomer which was undissolved in the Biomer pretreating process.

The morphology of the fracture surface of pure Biomer is presented in Figure 5.44 (a) and (b) and that of pure f-PHB1 is presented in Figure 5.45 (a) and (b). It is shown that the fracture surface of pure Biomer and pure f-PHB1 is similar. From the surface and fracture surface morphology, it can be seen that the specimens of pure Biomer and pure f-PHB1 is completely solid without any voids presented.

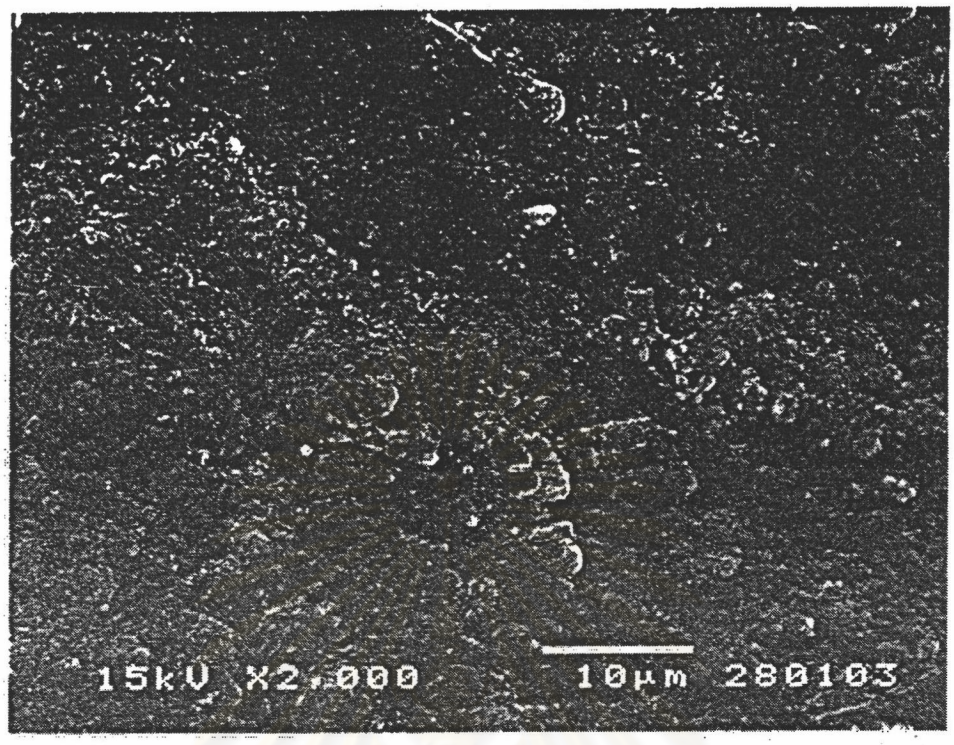

(a)

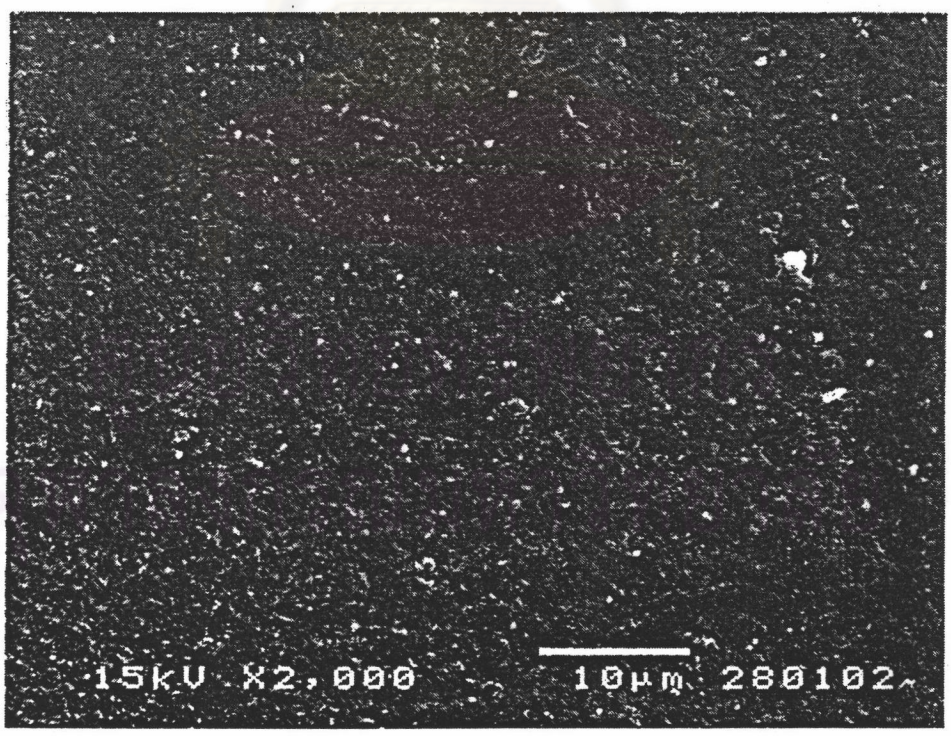

(b)

Figure 5.43 Morphology of the (a) pure Biomer and (b) pure f-PHB

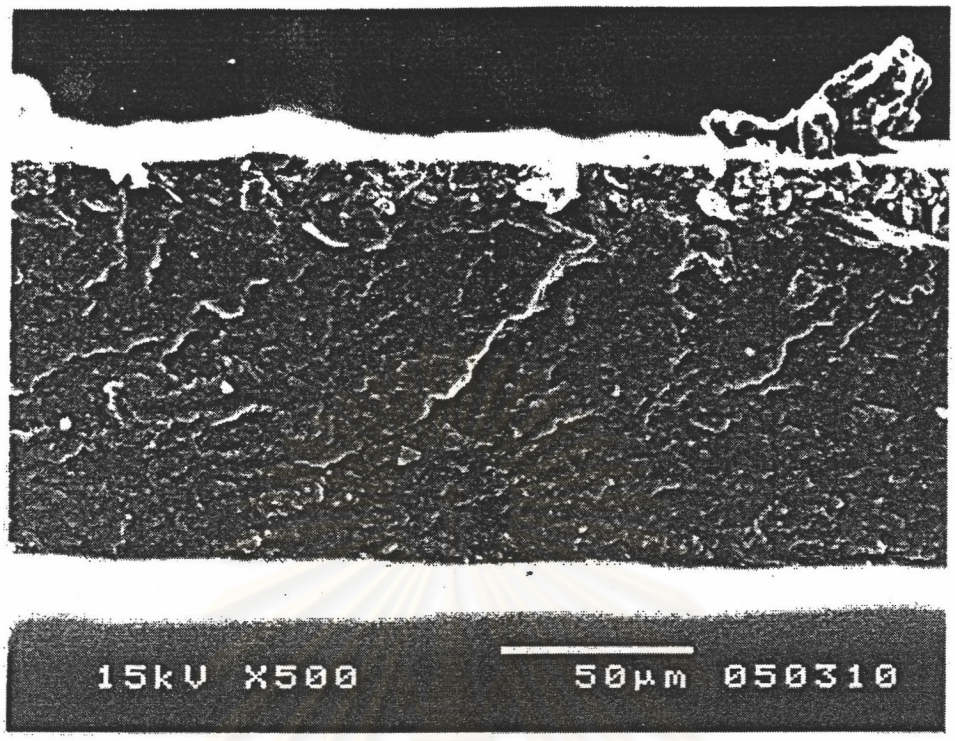

(a)

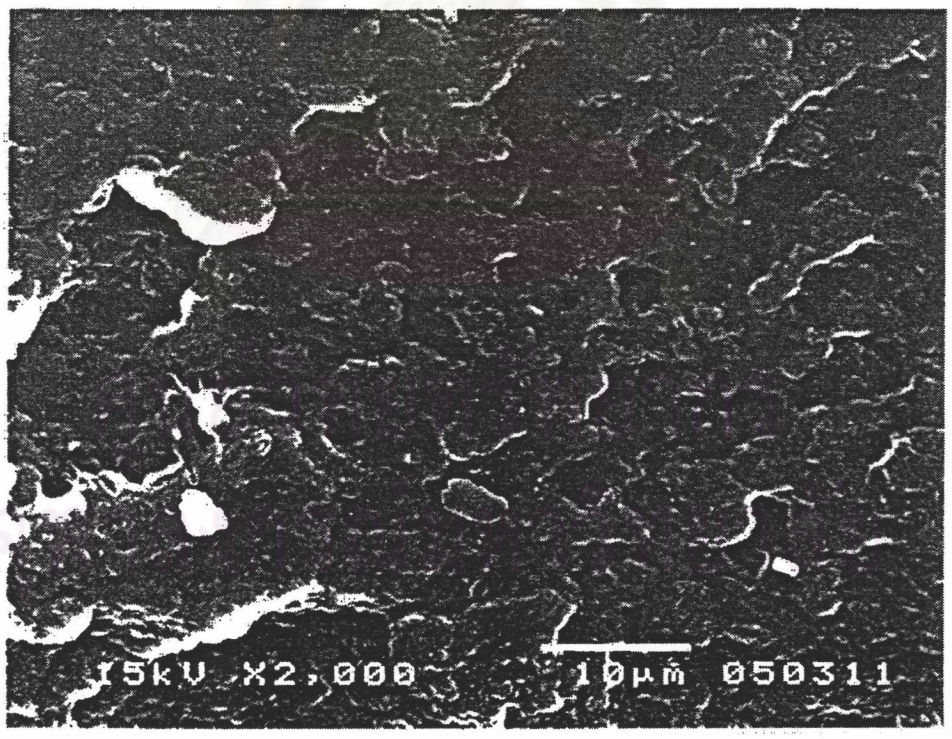

(b)

Figure 5.44 Fracture surface of pure Biomer at two magnification (a) x500 and (b) X2000

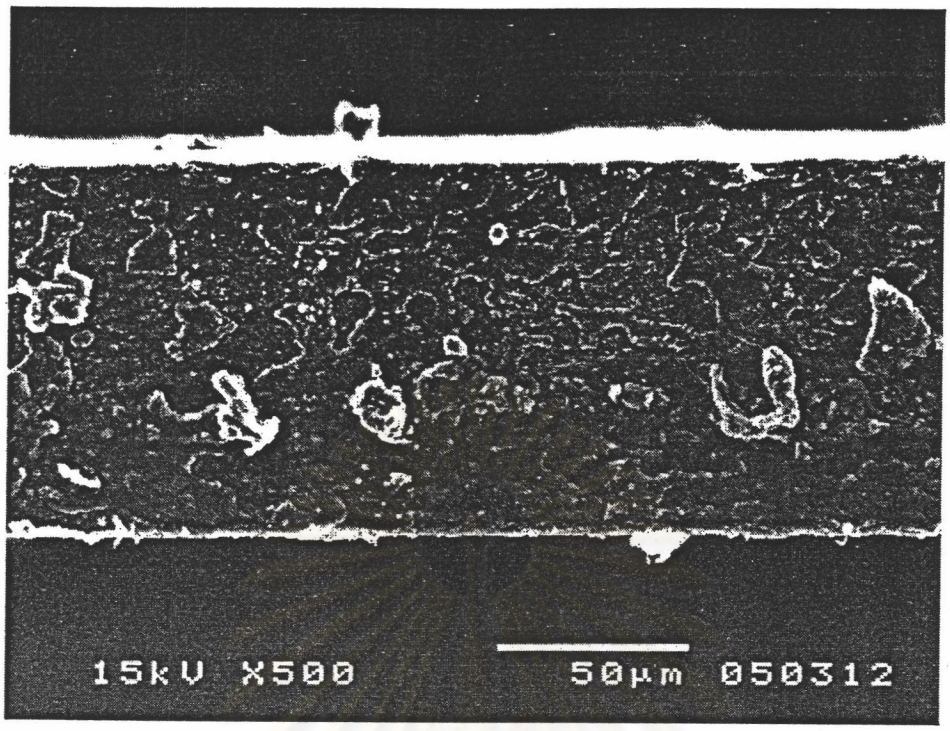

(a)

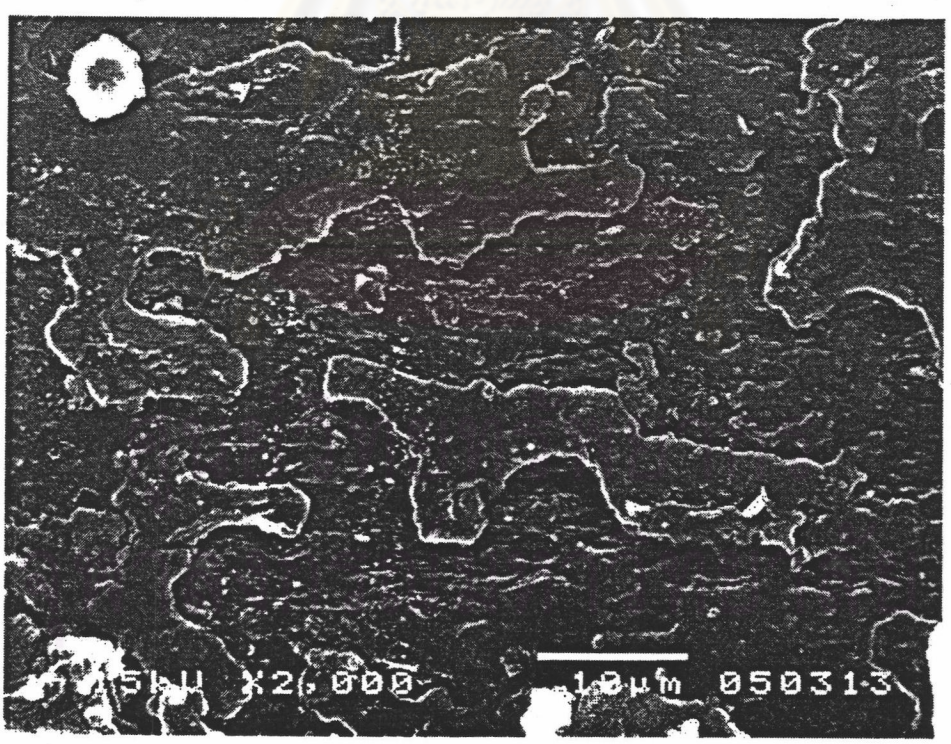

(b)

Figure 5.45 Fracture surface of pure f-PHB1 at two magnification (a) x500 and (b) X2000

5.3.2 Morphology of Biomer/30%PPG and f-PHB1/30%PPG blends

The morphology of the surface of Biomer/30%PPG and f-PHB1/30%PPG blends after tensile testing is presented in Figure 5.46. It is shown that there is a difference in the surface texture of both blends. The small hole-like morphology with a uniform distribution over the whole surface is observed at the surface of the Biomer/30%PPG blend. The diameter of the hole is less than 1 μm. In the f-PHB1/30%PPG blend, the hole-like morphology is also presented but less than those presented in the Biomer/30%PPG blend. The holes presented in the f-PHB1/30%PPG blend are bigger than those presented in Biomer/30%PPG blend. The diameter of the holes presented in the f-PHB1/30%PPG blend is about 2-4 μm. In addition, many cracking lines which are placed in vertical direction are observed on the surface of the f-PHB1/30%PPG blend. These lines may be due to the elongation of the specimen of the f-PHB1/30%PPG blend.

The morphology of the fracture surface of the Biomer/30%PPG blend is presented in Figure 5.47. It is shown that there are two distinct different morphologies, which are sponge-like morphology and completely solid morphology. High magnification (x2000) of different morphologies is presented in Figure 5.48 (a) and (b). The sponge-like morphology, which is seen in the upper bound of the fracture surface in Figure 5.47, is shown in Figure 5.48 (a). It is noticed that the sponge-like morphology is consisted of flat-shaped holes with the diameter of 3-4 μm. The completely solid morphology which seen in the lower bound of the fracture surface in Figure 5.47 is shown in Figure 5.48 (b). The completely solid morphology is similar to the morphology of the fracture surface of pure Biomer presented in Figure 5.44.

The morphology of the fracture surface of the f-PHB1/30%PPG blend is presented in Figure 5.49. It is shown that the morphology of the fracture surface of f-PHB1/30%PPG is also consisted of sponge-like morphology and completely solid morphology. The high magnification of sponge-like morphology and completely solid morphology is presented in Figure 5.50 (a) and (b), respectively. A short fibril-like structure in the sponge-like morphology can be noticed. This is in agreement with the

results on higher %elongation at break of f-PHB1/30%PPG blend than that of Biomer/30%PPG blend (see Figure 5.41)

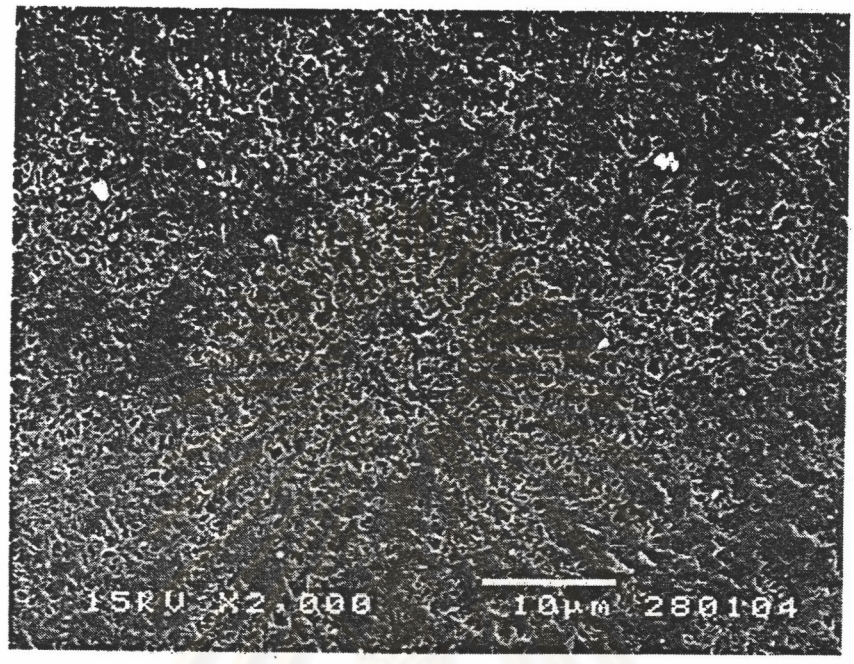

(a)

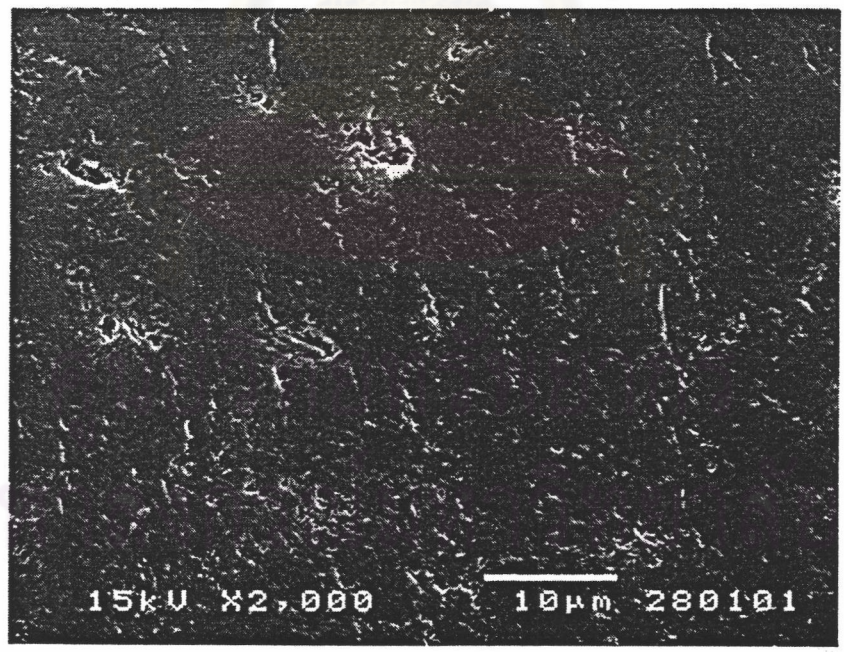

(b)

Figure 5.46 Morphology of the surface of the (a) Biomer/30%PPG blend and (b) f-PHB1/30%PPG blend

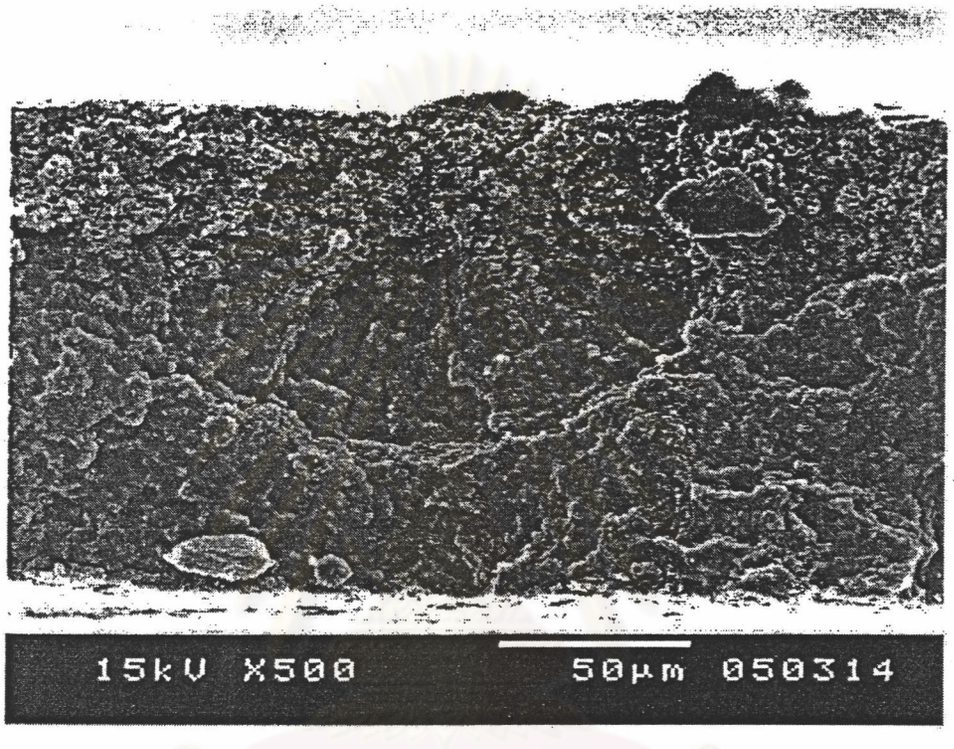

Figure 5.47 Fracture surface of Biomer/30%PPG blend

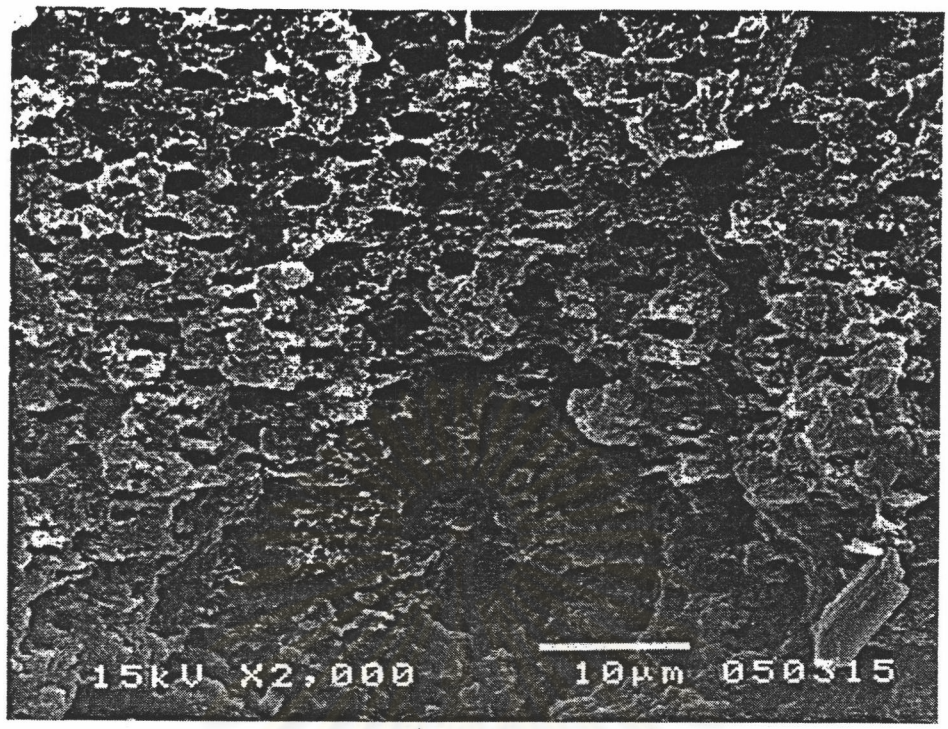

(a)

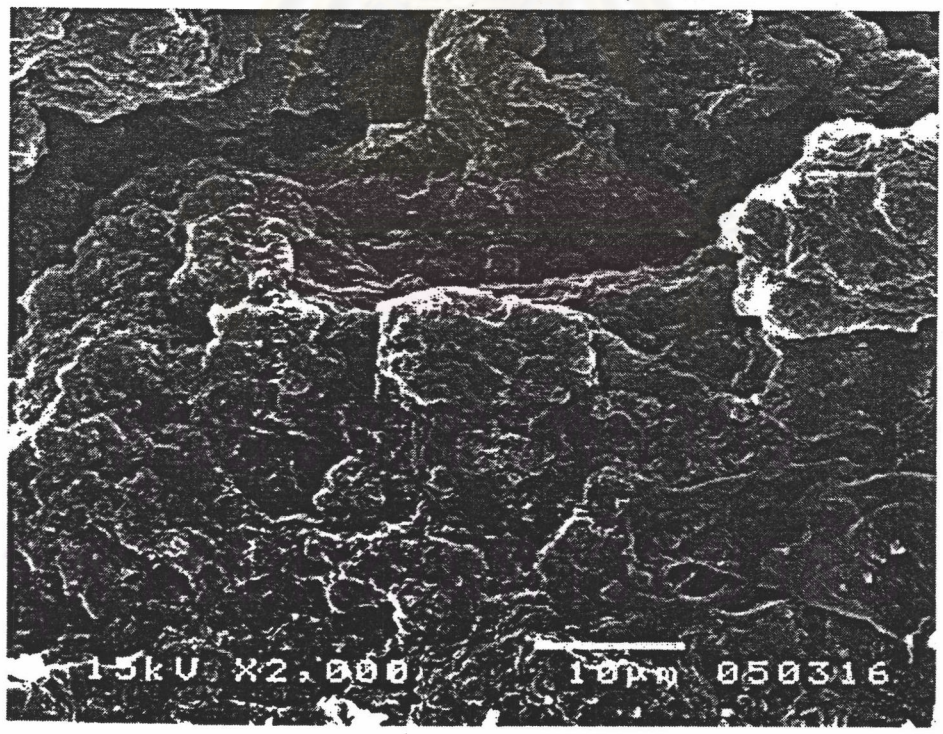

(b)

Figure 5.48 Morphology of the (a) sponge-like morphology and (b) completely solid morphology in the Biomer/30%PPG blend at high magnification (x2000)

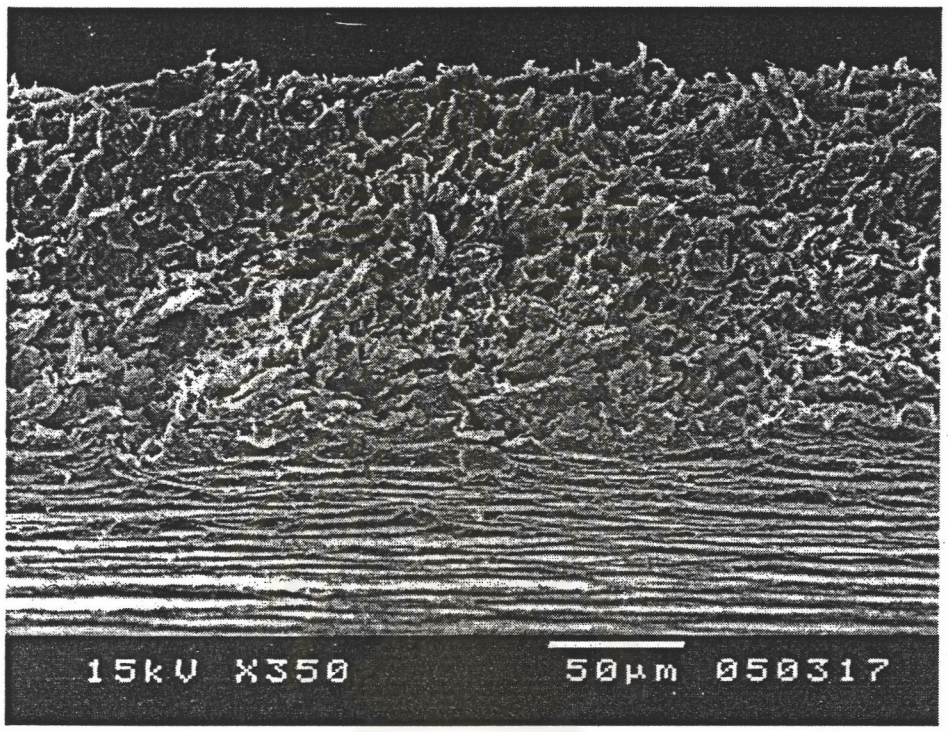

Figure 5.49 Fracture surface of the f-PHB1/30%PPG blend

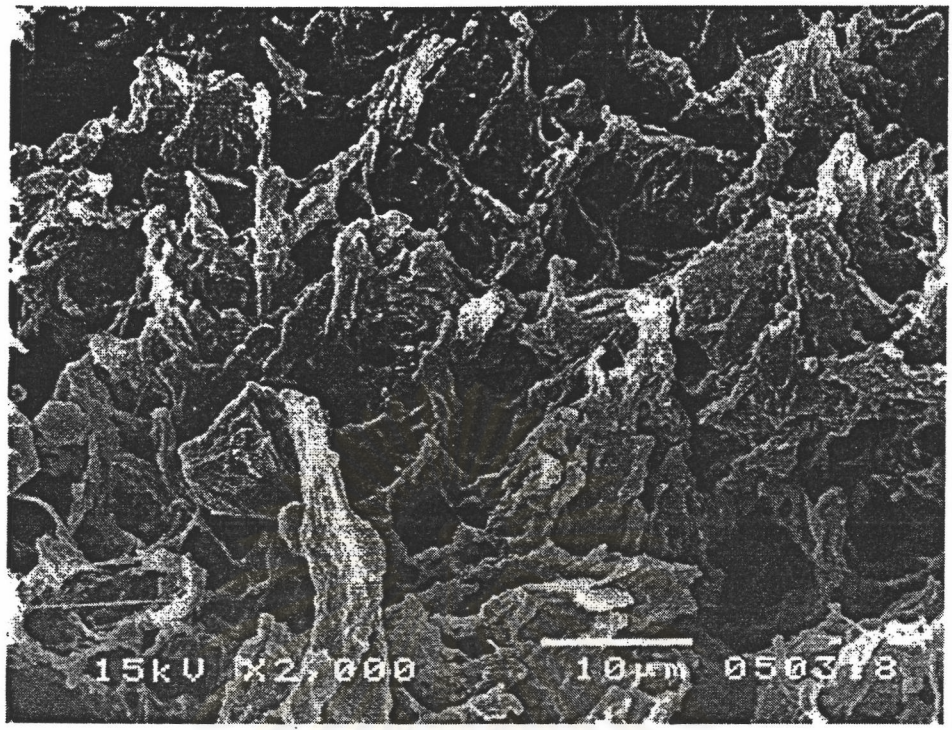

(a)

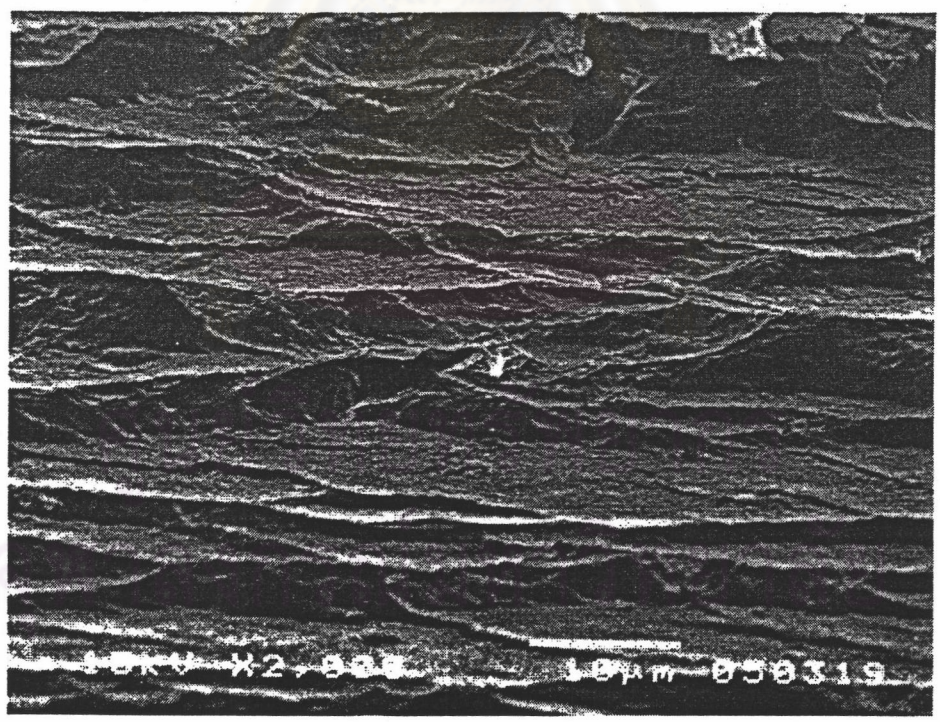

(b)

Figure 5.50 Morphology of (a) the spong-like morphology and (b) completely solid morphology in the f-PHB1/30%PPG at high magnification (x2000)

5.3.3 Morphology of the Biomer/50%PPG and f-PHB1/50%PPG blends

The morphology of the surface of the Biomer/50%PPG and f-PHB1/50%PPG blends after tensile testing is presented in Figure 5.51. It is shown that Biomer/50%PPG blend exhibits hole-like morphology on the surface of the blend. Different sizes of the holes are observed in the Biomer/50%PPG blend; large hole with the diameter of about 4-5 μm, and small hole with the diameter of about 1 μm. This hole-like morphology is similar to that of Biomer/30%PPG blend but the hole size of the Biomer/50%PPG is bigger than that of Biomer/30%PPG. Figure 5.52 presents the difference of the surface morphology at the edge of the specimen broken by tensile testing and by specimen cutting. It is shown that at the fracture front, the cracking sign caused by elongation of the specimen are observed. The cracking sign cannot be observed at the edge occurred by specimen cutting.

The morphology of the surface of the f-PHB1/50%PPG blend (Figure 5.51 (b)) is different to that of Biomer/50%PPG blend (Figure 5.51 (a)). Although the hole-like morphology is also observed on the surface of the f-PHB1/50%PPG blend, but the hole size of the f-PHB1/50%PPG blend is about 5-8 μm which is bigger than those of Biomer/50%PPG blend. The amount of holes formed on the surface of the f-PHB1/50%PPG is less than those formed on the surface of Biomer/50%PPG blend. A lot of cracking lines which can be caused by elongation of the specimen are observed on the whole surface of the specimen of f-PHB1/50%PPG blend. These cracks lie perpendicularly to the direction of the tension load. Figure 5.53 presents the cracks on the surface of the f-PHB1/50%PPG blend at two magnifications. In Figure 5.53, the high magnification (x7500) presents the elongated fraction of PHB in the cracks. This can imply the ductility of the f-PHB1/50%PPG blend.

The morphology of the fracture surface of the Biomer/50%PPG and f-PHB1/50%PPG blend is presented at two magnifications, low magnification (x500) presented in Figure 5.54 and high magnification (x2000) presented in Figure 5.55. It is shown that both blends have a sponge-like morphology over the whole cross sectional

area of the specimens. There are no differences in the morphology of the fracture surface of both blends. The sponge-like morphology at the fracture surface of both Biomer/50%PPG and f-PHB1/50%PPG blend is different to that of the Biomer/30%PPG and f-PHB1/30%PPG blend because the sponge-like morphology is occurred over the whole cross sectional area of the Biomer/50%PPG and f-PHB1/50%PPG blend, while this morphology is partially observed on the fracture surface of Biomer/30%PPG and f-PHB1/30%PPG blend.

The morphology of the Biomer/PPG blend at various content of PPG can be summarized as follows. In pure Biomer, the Biomer exhibits a complete solid morphology over the whole specimens. When 30% by weight of PPG is added to pure Biomer, the morphology is changed from a complete solid to a material having many holes on the surface like a sponge. These holes are also observed on some parts of the fracture surface of the Biomer/30%PPG blend. In Biomer/50%PPG blend, the holes become bigger than those on the surface of the Biomer/30%PPG blend. For the fracture surface of the Biomer/50%PPG, the holes are observed over the entire cross sectional area of the Biomer/50%PPG blend.

The morphology of the f-PHB1/PPG blend at various content of PPG can be summarized as follows. In pure f-PHB1, f-PHB1 is a complete solid without any holes presented. The f-PHB1/30%PPG blend exhibits the holes on the surface and on some parts of the fracture surface. Many cracking line are observed on the surface of the f-PHB1/30%PPG blend. The holes are more and bigger on the surface of the f-PHB1/50%PPG blend. The holes are observed over the entire fracture surface of the f-PHB1/50%PPG blend. The cracks observed on the f-PHB1/50%PPG blend are larger than those observed on the surface of f-PHB1/30%PPG blend.

The difference in the ductility of Biomer/PPG and f-PHB/PPG blend may be described by the morphology. Considering the value of %elongation at break and the surface morphology of the Biomer/30%PPG and f-PHB1/30%PPG blend, the Biomer/30%PPG blend has no cracks on the surface, while the f-PHB1/30%PPG blends

has many cracks. This indicates that the fracture is suddenly occurred in the Biomer/30%PPG blend but in the f-PHB1/30%PPG, the tensile load is distributed over the entire specimen and the elongation which causes the cracks on the surface is occurred. Considering Biomer/50%PPG and f-PHB1/50%PPG blend, the cracks are only observed at the fracture edge of the Biomer/50%PPG blend, while the cracks are observed over the entire surface of f-PHB1/50%PPG blend. This can imply that f-PHB1/50%PPG blend can distribute the tensile load better than the Biomer/50%PPG blend. The differences in the fracture mechanism observed in SEM photographs of Biomer/50%PPG and f-PHB1/50%PPG blends support the difference in the %elongation at break reported in section 5.2.5. This could be due to the better uniform dispersion of PPG with the f-PHB1 than with the Biomer.

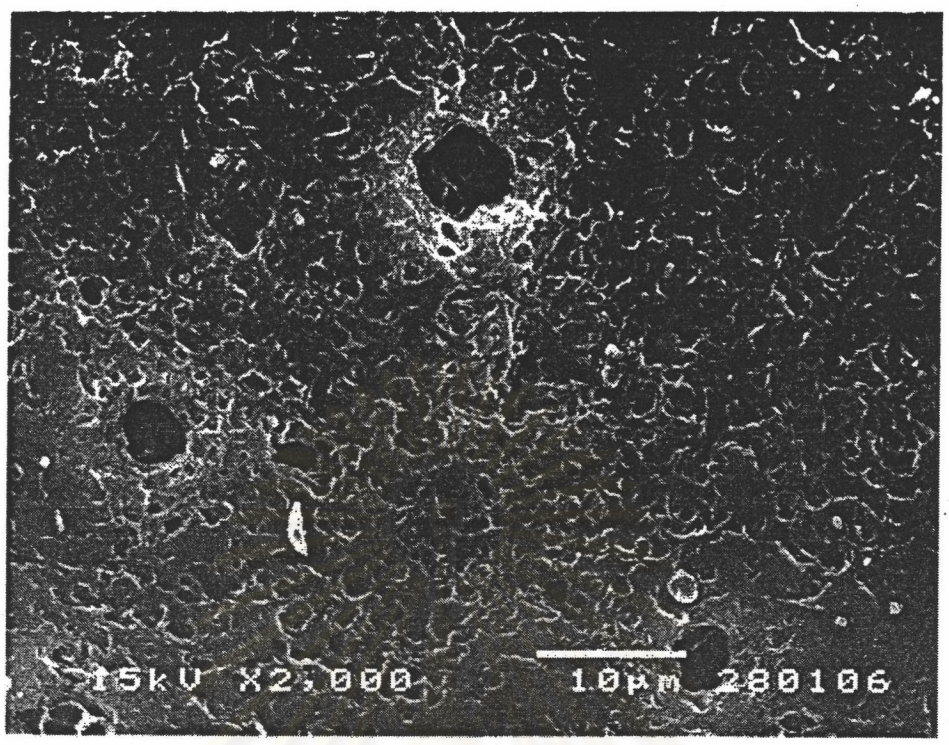

(a)

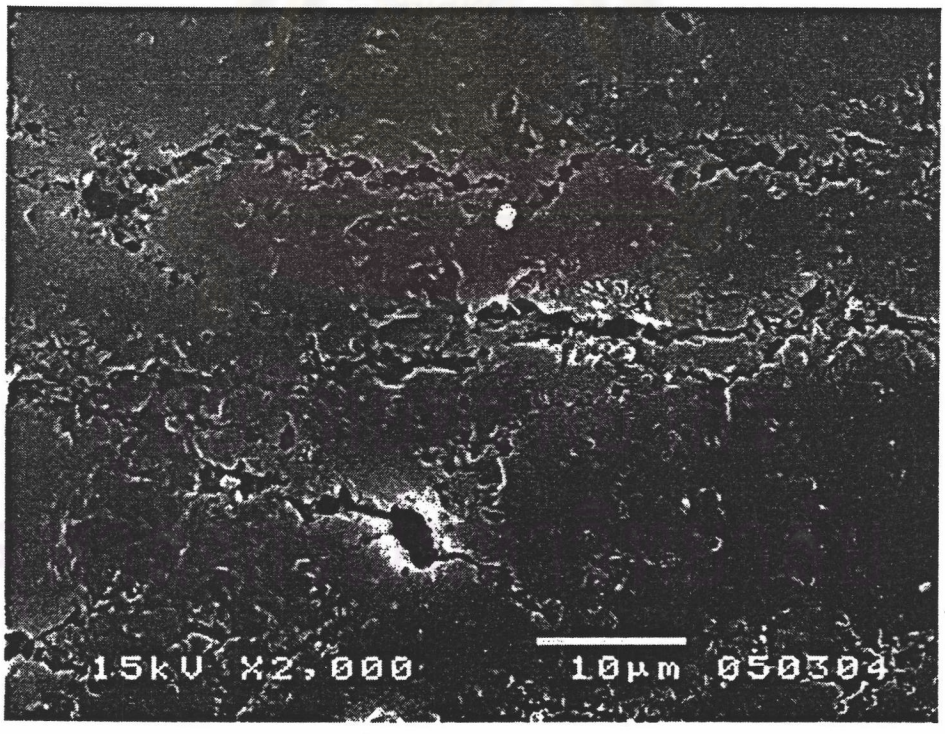

(b)

Figure 5.51 Morphology of the surface of the (a) Biomer/50%PPG blend and (b) f-PHB1/50%PPG blend

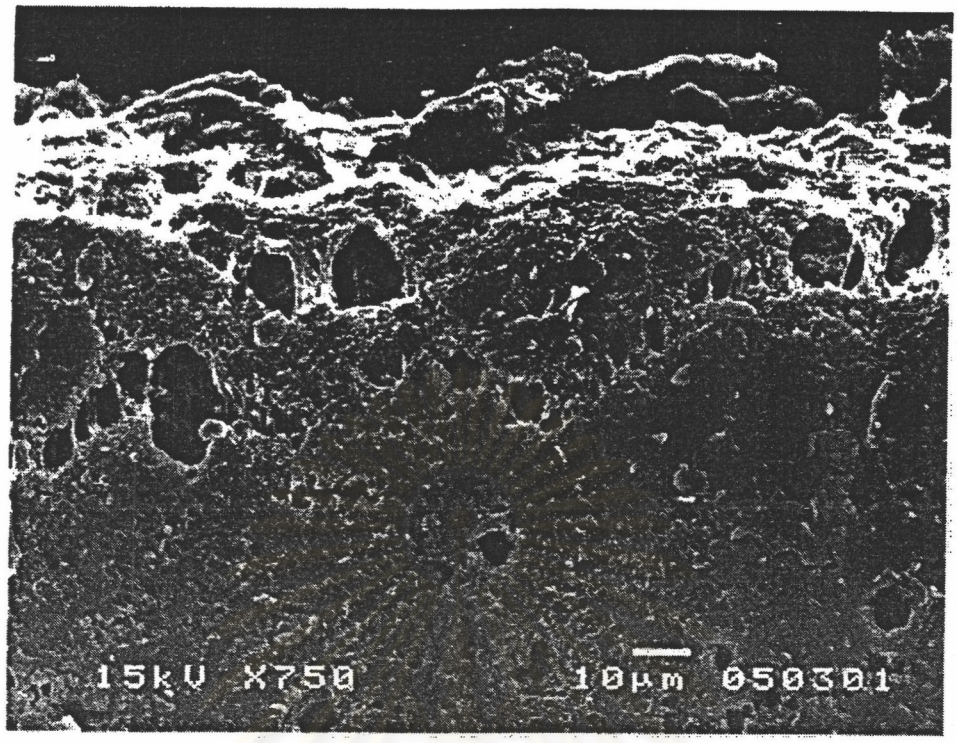

(a)

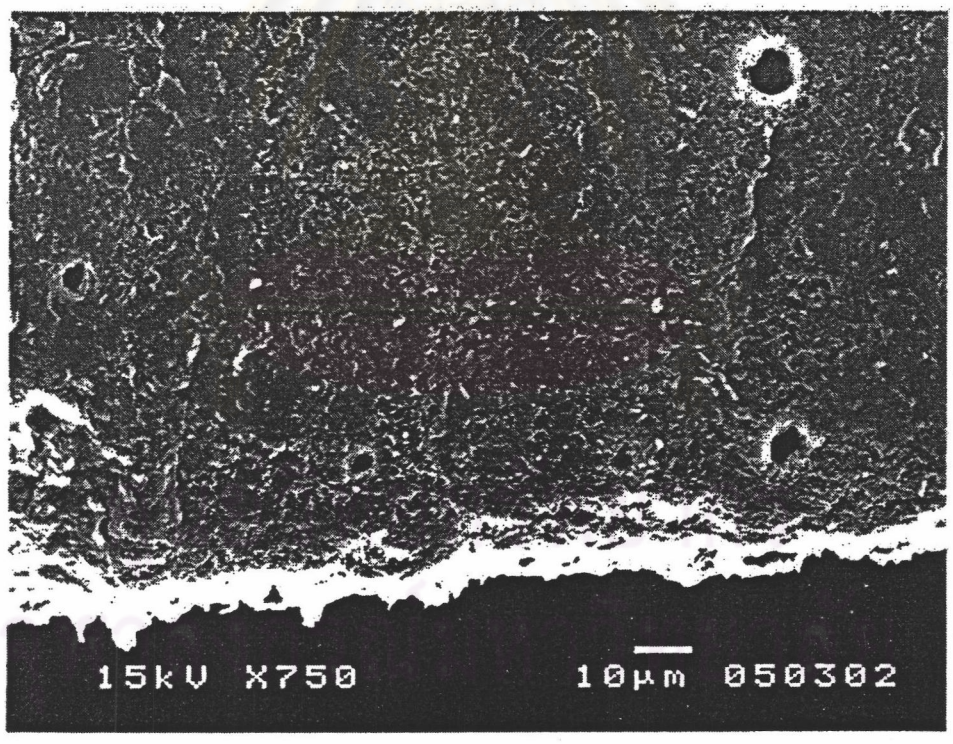

(b)

Figure 5.52 Surface morphology at the edge of the specimen of Biomer/50%PPG occurred (a) by tensile fracture and (b) by specimen cutting.

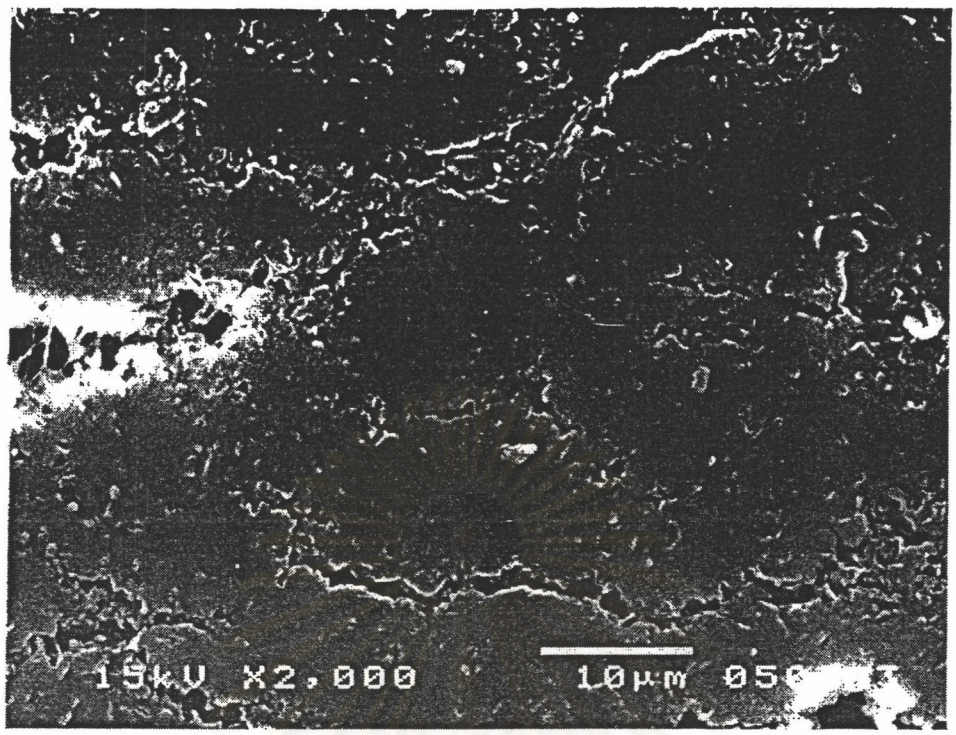

(a)

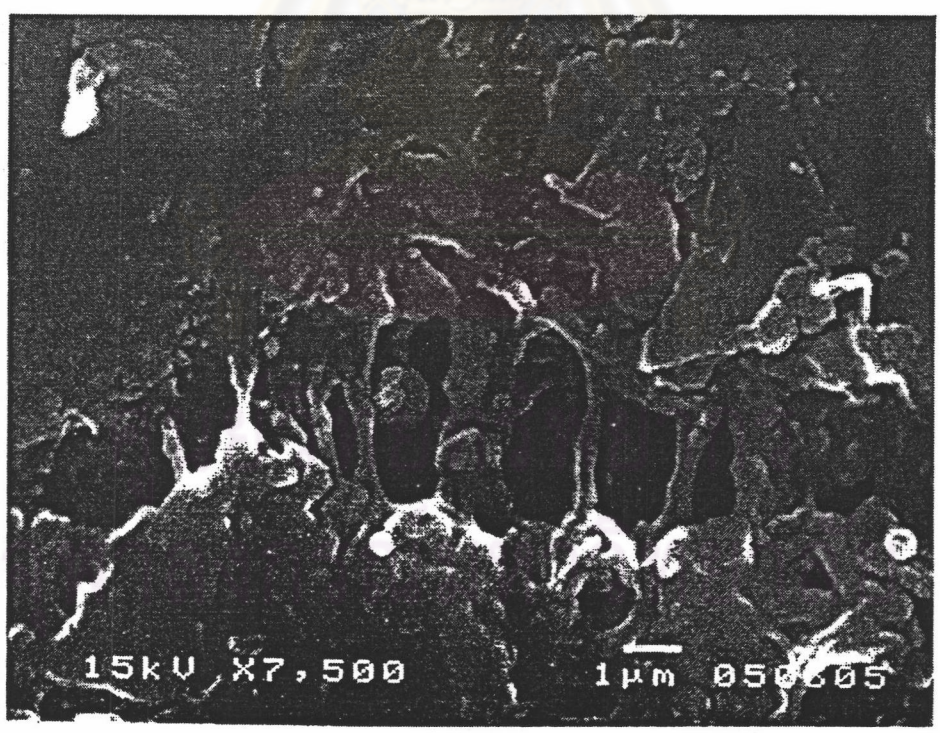

(b)

Figure 5.53 The cracks on the surface of the f-PHB1/50%PPG blend at two magnifications (a) x2000 and (b) x7500

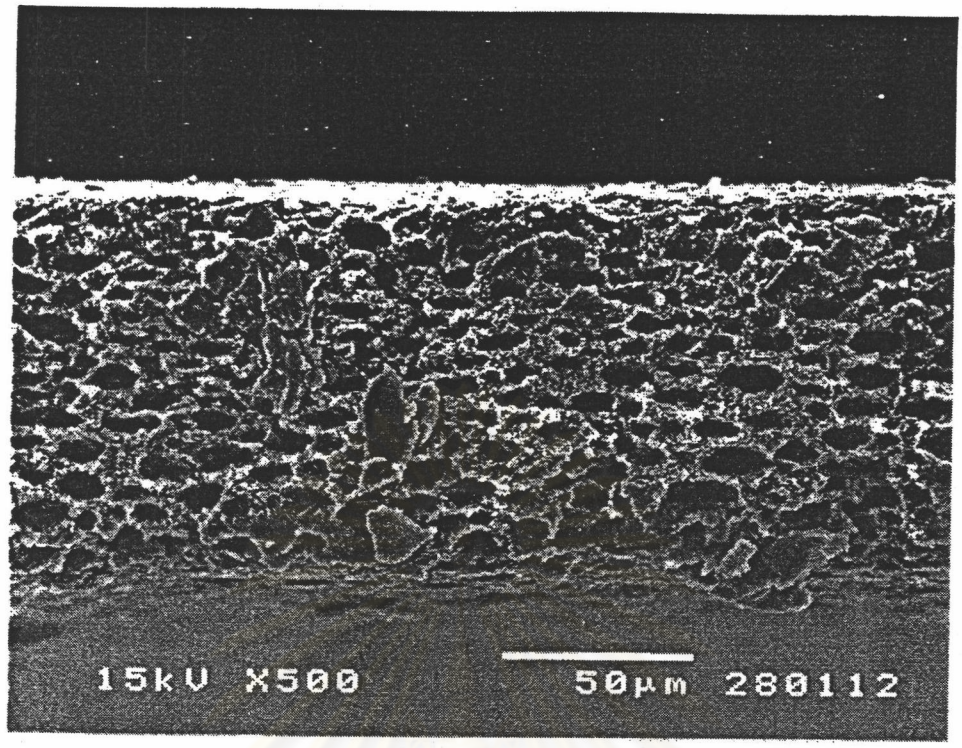

(a)

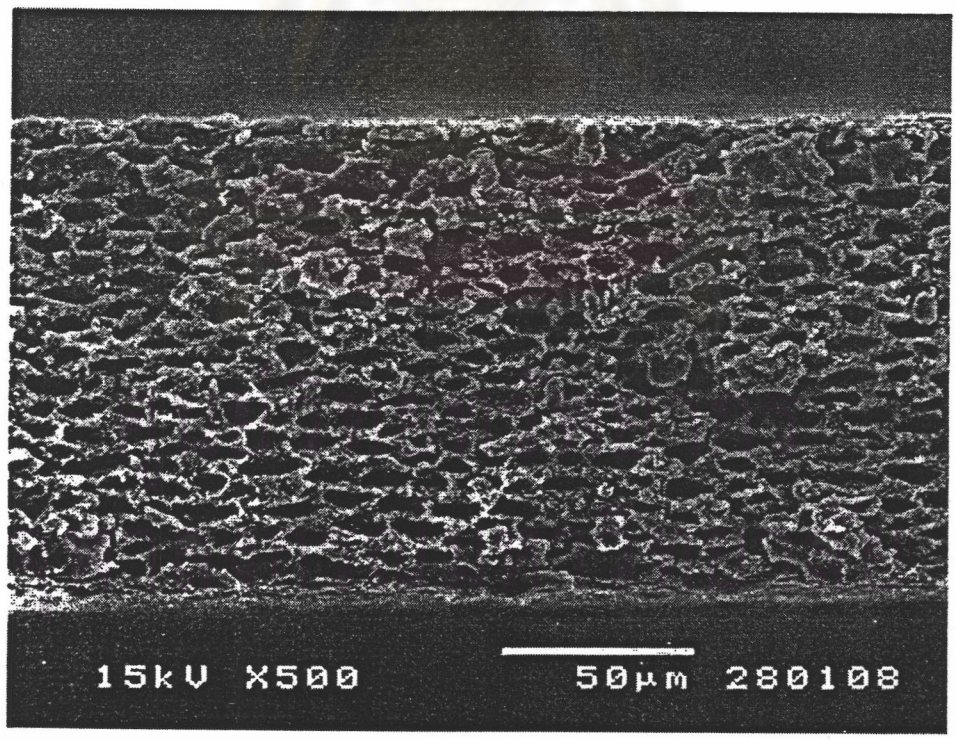

(b)

Figure 5.54 Fracture surface of the (a) Biomer/50%PPG blend and (b) f-PHB1/50%PPG blend at low magnification (x500)

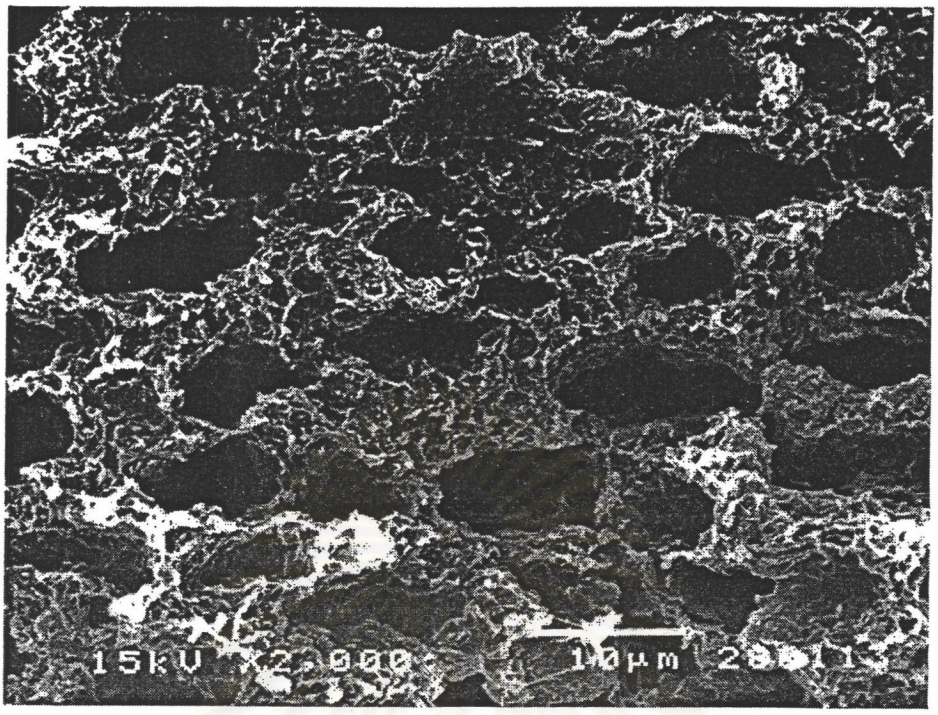

(a)

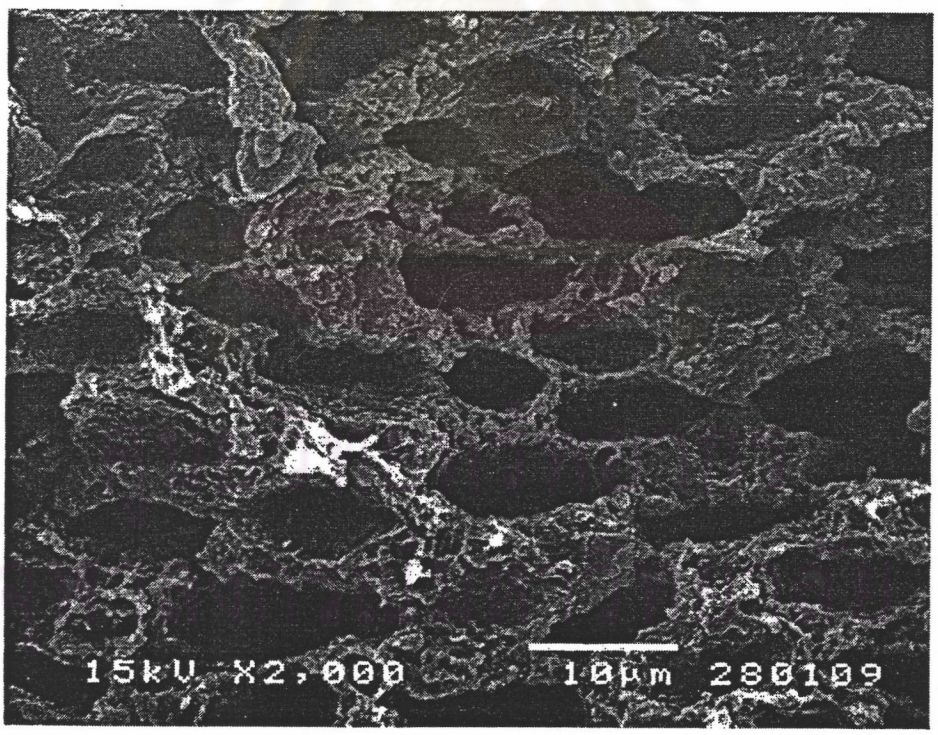

(b)

Figure 5.55 Fracture surface of the (a) Biomer/50%PPG blend and (b) f-PHB1/50%PPG blend at high magnification (x2000)